Universidade de Aveiro Departamento de Biologia
2009

MARIANA SANTOS MOREDA GRAÇA

VALIDAÇÃO DA LAP1B COMO NOVA PROTEÍNA REGULADORA DA PROTEÍNA FOSFATASE 1

VALIDATION OF LAP1B AS A NOVEL PROTEIN PHOSPHATASE 1 REGULATOR

Universidade de Aveiro Departamento Biologia
2009

MARIANA SANTOS MOREDA GRAÇA

VALIDAÇÃO DA LAP1B COMO NOVA PROTEÍNA REGULADORA DA PROTEÍNA FOSFATASE 1

VALIDATION OF LAP1B AS A NOVEL PROTEIN PHOSPHATASE 1 REGULATOR

Dissertação apresentada à Universidade de Aveiro para cumprimento dos requisitos necessários à obtenção do grau de Mestre em Biologia Molecular e Celular, realizada sob a orientação científica do Professor Doutor Edgar Cruz e Silva, Professor Associado do Departamento de Biologia da Universidade de Aveiro, e co-orientação da Professora Doutora Sandra Rebelo, Professora Auxiliar Convidada da Secção Autónoma de Ciências da Saúde da Universidade de Aveiro.

o júri

presidente

Professora Doutora Maria de Lourdes Gomes Pereira
Professora Associada com Agregação da Universidade de Aveiro

Professor Doutor Edgar Figueiredo da Cruz e Silva
Professor Associado da Universidade de Aveiro

Professora Doutora Sandra Maria Tavares da Costa Rebelo
Professora Auxiliar Convidada da Universidade de Aveiro

Doutor Michael Schrader
Investigador Principal do Centro de Biologia Celular da Universidade de Aveiro

agradecimentos

Ao Professor Edgar Cruz e Silva e à Professora Odete Cruz e Silva pela oportunidade trabalhar no Laboratório de Transdução de Sinais e no Laboratório de Neurociências, respectivamente.

Ao Professor Edgar Cruz e Silva pela orientação e pelos conhecimentos partilhados que permitiram o desenvolvimento da tese.

À Sandra Rebelo pela ajuda, disponibilidade e orientação da tese.

A todos os colegas do Laboratório de Neurociências e do Laboratório de Transdução de Sinais que sempre se disponibilizaram para ajudar.

Aos meus pais e à minha irmã por todo o apoio.

Aos meus amigos que estiveram sempre presentes.

palavras-chave

Fosforilação de proteínas, proteína fosfatase 1 (PP1), proteína 1B associada com a lâmina (LAP1B), torsinaA, distonia de torção de incidência precoce (DTIP).

resumo

A proteína fosfatase 1 (PP1) é uma proteína fosfatase específica para a desfosforilação de resíduos de serina e treonina que apresenta elevados níveis de expressão no cérebro. A PP1 participa na regulação de diversos processos celulares através da ligação a outras subunidades proteicas responsáveis pela sua especificidade e actividade. No rastreio de uma biblioteca de cDNA de cérebro humano, pelo método dois híbrido de levedura utilizando as isoformas da PP1 como isco, a proteína 1B associada com a lâmina (LAP1B) foi identificada como uma nova potencial proteína reguladora da PP1. A função da LAP1B não é totalmente conhecida, mas sabe-se que é uma proteína da membrana interna do núcleo que interage com as lâminas nucleares e com a proteína torsinaA, a qual está envolvida na distonia de torção de incidência precoce (DTIP). A LAP1B apresenta três motivos potenciais de ligação à PP1, um motivo SILK (um segundo motivo genérico de ligação à PP1) e diversos locais de fosforilação. Dado isto, a interacção entre a PP1 e a LAP1B foi confirmada por meio de várias técnicas. Por co-transformação em levedura, a interacção entre a LAP1B e as isoformas alfa (α), gama1 (γ1) e gama2 (γ2) da PP1 foi confirmada e, além disso, ficou demonstrado que a LAP1B interage com a PP1γ1 através do domínio de ligação 1 (BM1, REVRF). Este domínio está localizado na porção nucleoplásmica da LAP1B. O ensaio de *blot overlay,* utilizando a PP1γ1 purificada, permitiu comprovar *in vitro* a interacção entre a PP1 e a LAP1B através da porção nucleoplásmica da LAP1B. A interacção PP1/LAP1B foi comprovada *in vivo* por co-imunoprecipitação utilizando anticorpos específicos e por co-localização entre a LAP1B e a PP1γ e a PP1α, a qual foi verificada em estruturas subnucleares ainda não identificadas e em alguns pontos próximos do invólucro nuclear. O papel funcional do complexo PP1/LAP1B não foi determinado, mas pode ser importante na estrutura nuclear durante a mitose. Tendo em conta os elevados níveis de expressão da PP1 no estriado e a relação entre o sistema dopaminérgico dos núcleos basais e a DITC, a existência de um putativo tricomplexo PP1/LAP1B/torsinaA e a hipótese da PP1 e/ou a anormal fosforilação de proteínas ter um papel na DITC merece ser investigada.

keywords

Protein phosphorylation, protein phosphatase 1 (PP1), lamina associated polypeptide 1B (LAP1B), torsinA, early onset torsion dystonia (EOTD).

abstract

Protein phosphatase 1 (PP1) is a ubiquitously expressed serine/threonine protein phosphatase, with high expression levels in brain. PP1 regulates many cellular processes through interaction with different regulatory subunits that play regulatory and targeting roles. From yeast two-hybrid screens of a human brain cDNA library using PP1 isoforms as bait, lamina associated polypeptide 1B (LAP1B) was identified as a novel putative PP1 regulator. The functional role of LAP1B is poorly understood, but it is known that LAP1B is an inner nuclear membrane protein that interacts with lamins and torsinA, a protein involved in early onset torsion dystonia (EOTD). Furthermore, LAP1B has three potential PP1 binding motifs, a second generic PP1 binding motif named SILK and several phosphorylation sites. Thereby, we confirmed the PP1/LAP1B interaction by a variety of techniques. By yeast co-transformation we confirmed the interaction of LAP1B with PP1 isoforms alpha (α), gamma1 (γ1) and gamma2 (γ2) and demonstrated that LAP1B interacts with PP1γ1 through binding motif 1 (BM1, REVRF) that is located in the nucleoplasmic portion of LAP1B. The PP1/LAP1B interaction through the nucleoplasmic portion of LAP1B was also confirmed *in vitro* by blot overlay assay with purified PP1γ1 protein. The PP1/LAP1B interaction *in vivo* was evaluated by co-immunoprecipitation with specific antibodies and by co-localization between LAP1B and PP1α and PP1γ, ocurring at subnuclear structures and at locations near the nuclear envelope. The functional role of PP1/LAP1B complex was not determinated but it may be important in the maintenance of the nuclear architecture during mitosis. Given the high expression levels of PP1 within striatum and the relationship between basal ganglia dopaminergic signalling and EOTD, the existence of a putative tricomplex PP1/LAP1B/torsinA and the hypothesis that PP1 and/or abnormal protein phosphorylation may have a role in EOTD should be worthwhile exploring.

Abbreviations

aa	Amino acid
AAA^+ ATPases	ATPases associated with various cellular activities
AD	Alzheimer's disease
Ade	Adenine
ADP	Adenosine diphosphate
Ala	Alanine
APS	Ammonium persulfate
ATP	Adenosine triphosphate
AKAP-149	A-kinase-anchoring protein 149
APP	Amyloid precursor protein
Asn	Asparagine
BCA	Bicinchoninic acid
BM	Binding motif
BSA	Bovine serum albumin
cDNA	Complementary deoxyribonucleic acid
CK	Casein Kinase
DAPI	4',6-diamidino-2-phenylindole
DARPP-32	Dopamine and cAMP-regulated phosphoprotein
DAT	Dopamine transporter
DNA	Deoxyribonucleic acid
DOPAC	3,4-dihydroxyphenylacetic acid
ECL	Enhanced Chemiluminescence
ER	Endoplasmic reticulum
EOTD	Early onset torsion dystonia
FITC	Fluorescein isothiocyanate
GAL4	Gal4 transcription factor
GAL4-AD	Gal4 activation domain
GAL4-BD	Gal4 DNA binding domain
GSK3	Glycogen synthetase kinase 3
His	Histidine
HVA	Homovallinic acid
INM	Inner nuclear membrane

IP	Immunoprecipitation
IPTG	Isopropyl-β-D-thiogalactopyranoside
KLC	Kinesin light chain
LAP	Lamina associated protein
LB	Loading buffer
LB medium	Luria-Bertani medium
LBR	Lamin B receptor
LGB	Lower gel buffer
LiAc	Lithium acetate
Leu	Leucine
mRNA	Messenger ribonucleic acid
NE	Nuclear envelope
NIPP1	Nuclear inhibitor of PP1
NLS	Nuclear localization signal
NRBOX	Nuclear receptor box
OD	Optical density
ONM	Outer nuclear membrane
PBS	Phosphate buffered saline
PCR	Polymerase chain reaction
PEI	Polyethylenimine
PLK	Polo-like kinase
PP1	Protein phosphatase 1
PP2A	Protein phosphatase 2A
PP1c	Protein phosphatase 1 catalytic subunit
PPM	Metal ion dependent protein phosphatase
PPP	Phosphoprotein phosphatase
PTP	Tyrosine protein phosphatase
QDO	Quadruple dropout
RNA	Ribonucleic acid
rpm	Rotation per minute
SD	Supplement dropout medium
SDS	Sodium dodecyl sulphate
SDS-PAGE	Sodium dodecyl sulphate – polyacrylamide gel electrophoresis
SP	Signal peptide

SIPP1	Splicing factor that interacts with PQBP-1 and PP1
SUMO-1	Small ubiquitin-like modifier-1
TBS	Tris-buffered saline solution
TBST	TBS supplemented with Tween detergent
TDO	Triple dropout
TEMED	N,N,N',N'-Tetramethylethylenediamine
TM	Transmembrane domain
TOR1AIP1	TorsinA interacting protein 1
TPR	Tetratricopeptide repeat
Trp	Tryptophan
UAS	Upstream activating sequence
UGB	Upper gel buffer
ULM	UHM ligand motif
Val	Valine
VMAT2	Vesicular monoamine transporter 2
Wt	Wild type
YPD	Yeast Peptone Dextrose
YTH	Yeast two-hybrid

1. Introduction

1.1. Protein phosphorylation

Reversible protein phosphorylation is a major mechanism for controlling intracellular events in eukaryotic cells. Cellular health and vitality are dependent on the fine equilibrium of protein phosphorylation systems (1). Reversible protein phosphorylation involves either the addition of phosphate groups via the transference of the terminal phosphate from ATP to an amino acid residue by protein kinases or its removal by protein phosphatases (Fig. 1). This post-translational modification can have profound effects on the activities and properties of various proteins.

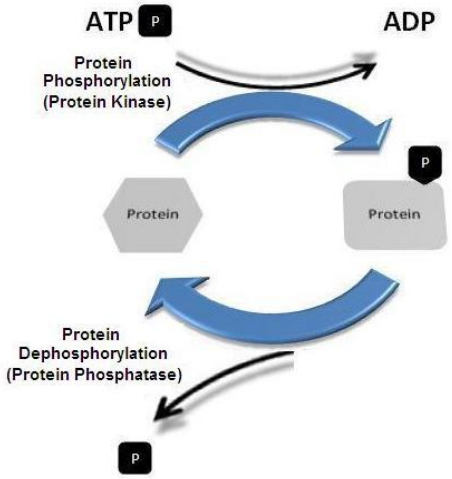

Figure 1. Schematic representation of reversible protein phosphorylation. Protein kinases transfer a phosphate group from ATP to a target protein (protein phosphorylation), while protein phosphatases catalyze the hydrolysis of the phosphate group from the target protein (protein dephosphorylation).

Protein phosphorylation regulates several processes like the metabolism, contractility, membrane transport and secretion, the transcription and translation of genes, cell division, fertilization and memory (reviewed in 1). Additionally, various diseases, like neurodegenerative diseases and diabetes, are associated with abnormal phosphorylation of specific proteins. In Alzheimer's disease (AD) there is evidence for abnormal regulation of protein phosphorylation. AD is characterized mainly by the presence of neuritic plaques and neurofibrillary tangles in the brains of affected individuals. Neurofibrillary tangles result from the aggregation of abnormally phosphorylated Tau protein into paired helical filaments. Glycogen synthase kinase 3 β and protein kinase A may be key kinases involved

in Tau phosphorylation (2), with protein phosphatase 2A (PP2A) and protein phosphatase 1 (PP1) being responsible for tau hyperphosphorylation (3, 4). Moreover, the inactivation of PP1 leads to a relative increase in the utilization of the non-amyloidogenic pathway for Alzheimer's amyloid precursor protein (APP) processing (5). Other neurodegenerative diseases associated with abnormal protein phosphorylation are Parkinson's disease and Huntington's disease. Lewy bodies (proteinaceous inclusions) are one of the pathological features of Parkinson's disease and the polypeptide α-synuclein was found to be a major constituent of Lewy bodies. Protein phosphorylation may have a role in the regulation of α-synuclein. It was demonstrated that α-synuclein is constitutively phosphorylated, predominantly on serine residues (6). Huntington's disease is characterized by motor and cognitive deficits probably caused by progressive and neuronal dysfunction preceding neuronal cell death. Synapsin I is considered one of the major phosphoproteins with importance in regulating of neurotransmitter release. Synapsin I is abnormally phosphorylated in mice expressing the Huntington's disease mutation and it has been suggested that an inbalance between kinase and phosphatase activities also occurs in Huntington's disease (7).

About one-third of all eukaryotic proteins are controlled by protein phosphorylation of specific tyrosine, serine and threonine residues. The protein phosphorylation (or dephosphorylation) of tyrosine, serine and threonine residues causes conformational changes in proteins modifying their biological properties. The reversible protein phosphorylation level of a protein reflects the balance between the activities of the protein kinases and phosphatases involved. Eukaryotic cells express various proteins kinases and phosphatases, which have specific substrates, cellular localizations and regulation mechanisms. Whereas the number of tyrosine phosphatases is approximately the same of tyrosine kinases, the number of serine/threonine kinases is much higher to that of serine/threonine phosphatases. However, the diversity of phosphatase interacting proteins is enormous, so the diversity of serine/threonine phosphatases is seen mainly at the holoenzyme level (8, 9). Therefore, protein phosphorylation systems represent attractive targets for diagnostics and therapeutics of several diseases, like neurodegenerative diseases and others (10).

1.2. Protein phosphatases

Protein phosphatases belong to three unrelated gene families: the PPM family (metal ion dependent protein phosphatases), the PTP family (tyrosine protein phosphatases) and the PPP family (phosphoprotein phosphatases). Members of PPP family are responsible for desphosphorylation of serine/threonine residues and are divided in the following subfamilies: PP1, PP2A, Protein Phosphatase 4 (PP4), Protein Phosphatase 6 (PP6), Protein Phosphatase 2B (PP2B), Protein Phosphatase 5 (PP5) and Protein Phosphatase 7 (PP7) (8, 11, 12). The remarkable degree of evolutionary conservation of these enzymes (Fig. 2) is related to their essential role in the regulation of fundamental cellular processes (13, 14). Among the serine/threonine protein phosphatases, PP1 forms a major class and is highly conserved among all eukaryotes examined to date (15).

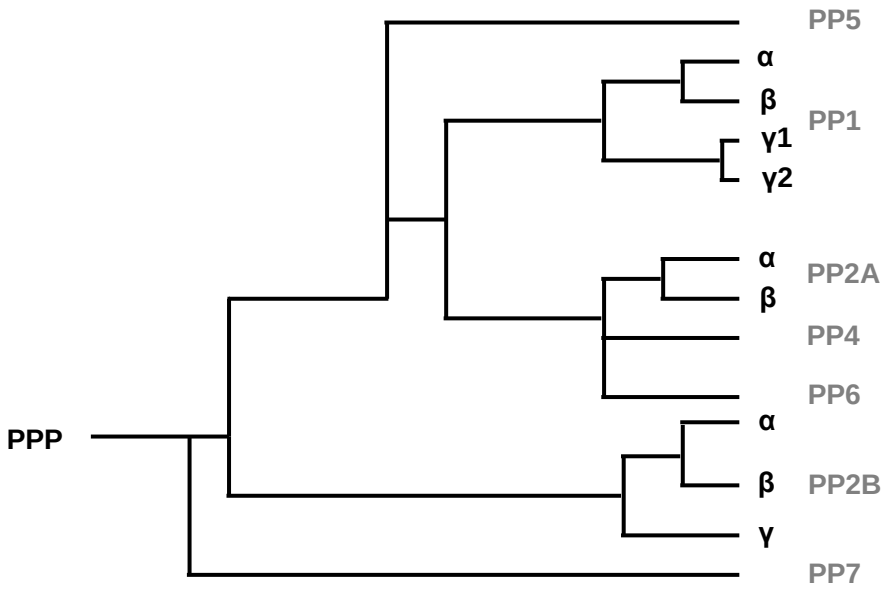

Figure 2. Phylogenic tree representing the similarity between the known members of the phosphoprotein phosphatase (PPP) family based on their primary amino acid sequence (adapted from 16).

1.2.1. Protein Phosphatase 1 (PP1)

PP1 is the most widely expressed and abundant protein serine/threonine phosphatase which regulates a variety of cellular functions (17). PP1 is involved in glycogen metabolism, transcription, protein synthesis, cellular division and meiosis, and apoptosis. When nutrients are abundant PP1 stimulates the synthesis of glycogen and also enables the return to the basal state of protein synthesis and the recycling of transcription and splicing factors. PP1 is required for anaphase progression, exit from mitosis and is also responsible for maintenance of the cells in G_1 or G_2 cell cycle phases. In addition, PP1 can also promote apoptosis when cells are damaged (reviewed in 8).

PP1 holoenzymes are composed by a highly conserved catalytic subunit called protein phosphatase 1 catalytic subunit (PP1c) and one or two variable regulatory subunits. Interestingly, the catalytic subunit of PP1 has multiple points of interaction with a regulatory subunit (Fig. 3), with the latter being responsible for the targeting of PP1 to a particular subcellular compartment and also determining its substrate specificity and activity. These regulatory subunits can be substrates that directly associate with PP1c, substrate specifiers and/or targeting proteins (9, 17). The inhibitors like inhibitor-1 (18), for example, in their phosphorylated form, block the activity of PP1c towards all substrates. I_1^{PP2A}/PHAP-II (19), is a substrate specifier that promotes the dephosphorylation of specific substrates by PP1c. Spinophilin is a targeting subunit for PP1 (20), which directs PP1 to dendritic spines in brain. PP1 regulates several cellular functions through the interaction of its catalytic subunit with the different regulatory subunits (14).

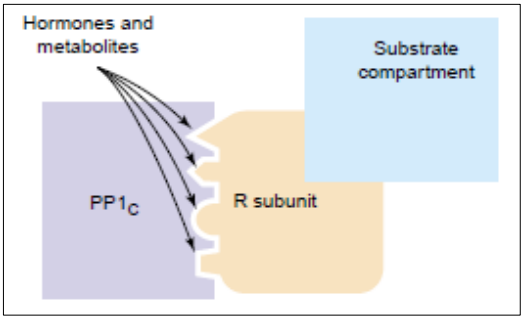

Figure 3. Schematic representation of the PP1 holoenzyme structure. The protein phosphatase 1 catalytic subunit (PP1c) interacts with a regulatory subunit (R subunit) which often brings the holoenzyme to proximity of its substrates. Hormones and metabolites can modulate PP1 interactions (adapted from 9).

Most PP1 binding proteins interact with the PP1 catalytic subunit through a conserved PP1 binding motif termed the RVxF motif which have the consensus (R/K) $X_{A(0-1)}$ (V/I) X_B (F/W) sequence, where X_a is any amino acid and X_B is any amino acid except proline (9, 21). The binding of the RVxF motif to PP1c does not cause major conformational changes of PP1, and no significant effect on its catalytic activity (22). However, the RVxF motif mediate the initial anchoring of regulatory subunits to PP1 and thereby promotes the occupation of secondary and lower affinity binding sites, and this often does affect the activity and/or substrate specificity of PP1 (9, 21). Recently, a second generic PP1-binding motif was identified and is called the SILK-motif: [GS]-IL-[KR] (23). The SILK motif was first described for inhibitor-2 (24), a specific PP1 inhibitor, and can functionally replace the RVxF motif in NIPP1 (21). The existence of these conserved binding sites within regulatory subunits explains why a relatively small protein such as PP1c can interact with numerous different regulatory proteins and why the binding of most regulatory subunits is mutually exclusive (9). Since the regulatory subunits are responsible for controlling PP1 activity, the key to understanding PP1 function lies in studying the cellular functions of these subunits (25).

PP1 is expressed in mammalian cells in three isoforms: PP1alpha (α), PP1gamma (γ) and PP1Beta/Delta (β/δ), which are encoded by distinct genes (26-28). These isoforms are about 90% identical in amino acid sequence; most of the differences are located on the N and C terminals (Fig. 4). The gene encoding PP1γ undergoes alternative splicing to originate a ubiquitous PP1gamma 1 (PP1γ1) variant and a PP1gamma 2 (PP1γ2) variant enriched in testis (26, 29).

```
PP1gamma1       MADLDKLNIDSIIQRLLEVRGSKPGKNVQLQENEIRGLCLKSREIFLSQPILLELEAPLK 60
PP1gamma2       MADLDKLNIDSIIQRLLEVRGSKPGKNVQLQENEIRGLCLKSREIFLSQPILLELEAPLK 60
PP1alpha        MSDSEKLNLDSIIGRLLEVQGSRPGKNVQLTENEIRGLCLKSREIFLSQPILLELEAPLK 60
PP1beta         MADG-ELNVDSLITRLLEVRGCRPGKIVQMTEAEVRGLCIKSREIFLSQPILLELEAPLK 59
                *:*  :**:**:* *****:*.:*** **: * *:****:********************

PP1gamma1       ICGDIHGQYYDLLRLFEYGGFPPESNYLFLGDYVDRGKQSLETICLLLAYKIKYPENFFL 120
PP1gamma2       ICGDIHGQYYDLLRLFEYGGFPPESNYLFLGDYVDRGKQSLETICLLLAYKIKYPENFFL 120
PP1alpha        ICGDIHGQYYDLLRLFEYGGFPPESNYLFLGDYVDRGKQSLETICLLLAYKIKYPENFFL 120
PP1beta         ICGDIHGQYTDLLRLFEYGGFPPEANYLFLGDYVDRGKQSLETICLLLAYKIKYPENFFL 119
                ********* **************:************************************

PP1gamma1       LRGNHECASINRIYGFYDECKRRYNIKLWKTFTDCFNCLPIAAIVDEKIFCCHGGLSPDL 180
PP1gamma2       LRGNHECASINRIYGFYDECKRRYNIKLWKTFTDCFNCLPIAAIVDEKIFCCHGGLSPDL 180
PP1alpha        LRGNHECASINRIYGFYDECKRRYNIKLWKTFTDCFNCLPIAAIVDEKIFCCHGGLSPDL 180
PP1beta         LRGNHECASINRIYGFYDECKRRFNIKLWKTFTDCFNCLPIAAIVDEKIFCCHGGLSPDL 179
                ***********************:************************************

PP1gamma1       QSMEQIRRIMRPTDVPDQGLLCDLLWSDPDKDVLGWGENDRGVSFTFGAEVVAKFLHKHD 240
PP1gamma2       QSMEQIRRIMRPTDVPDQGLLCDLLWSDPDKDVLGWGENDRGVSFTFGAEVVAKFLHKHD 240
PP1alpha        QSMEQIRRIMRPTDVPDQGLLCDLLWSDPDKDVQGWGENDRGVSFTFGAEVVAKFLHKHD 240
PP1beta         QSMEQIRRIMRPTDVPDTGLLCDLLWSDPDKDVQGWGENDRGVSFTFGADVVSKFLNRHD 239
                ***************** *************** ***************:**:***::**

PP1gamma1       LDLICRAHQVVEDGYEFFAKRQLVTLFSAPNYCGEFDNAGAMMSVDETLMCSFQILKPAE 300
PP1gamma2       LDLICRAHQVVEDGYEFFAKRQLVTLFSAPNYCGEFDNAGAMMSVDETLMCSFQILKPAE 300
PP1alpha        LDLICRAHQVVEDGYEFFAKRQLVTLFSAPNYCGEFDNAGAMMSVDETLMCSFQILKPAD 300
PP1beta         LDLICRAHQVVEDGYEFFAKRQLVTLFSAPNYCGEFDNAGGMMSVDETLMCSFQILKPSE 299
                ************************************.*****************::

PP1gamma1       KKK---------PNATRPVTPPRG------MITKQAKK-------- 323
PP1gamma2       KKK---------PNATRPVTPPRVGSGLNPSIQKASNYRNNTVLYE 337
PP1alpha        KNKGKYGQFSGLNPGGRPITPPRN-------SAKAKK--------- 330
PP1beta         KKAKYQYG---GLNSGRPVTPPRT--------ANPPKKR------- 327
```

Figure 4. Analysis of homology of PP1 isoforms using a CLUSTAL W multiple sequence alignment.

The subcellular localization of endogenous PP1 isoforms is not entirely clear. Although the three isoforms can be found in the nucleus and cytoplasm, they exhibit some differences in intranuclear distribution. PP1α is diffusely distributed in the cytoplasm and in the nucleoplasm and is excluded from the nucleolus. PP1γ has diffuse distribution in the cytoplasm and nucleoplasm and accumulates in nucleoli with a pattern corresponding to the granular compartment that contains ribosomal RNA. PP1β/δ is also diffuse in cytoplasm and nuclei and localizes in nucleoli, but not to the same extent as PP1γ. Different subcellular localization of PP1 isoforms can be due to different affinities for regulatory subunits which have distinct subcellular distribution themselves. Localization of a particular PP1 isoform can also change according to the level of expression of interacting subunits (30, 31).

PP1α and PP1γ1 are ubiquitously expressed in mammalian tissues, with higher expression in brain. In brain, the mRNA for PP1α, PP1γ1 and also for PP1β/δ was found to be particularly abundant in hippocampus and cerebellum. At the protein level PP1α and

PP1γ1 have highest levels of expression in the striatum, where they were shown to be relatively enriched in the medium-sized spiny neurons. These neurons are also known to contain DARPP-32 (29) which is a PP1 inhibitor. In the neostriatum PP1 is involved in the action of several neurotransmitters, like dopamine and glutamate, via regulation by DARPP-32 (dopamine and cAMP-regulated phosphoprotein, Mr 32000 Da). Dopamine causes the phosphorylation and activation of DARP-32 by the increase of intracellular cAMP and by activation of protein kinase A (32). Glutamate causes the dephosphorylation and inactivation of DARPP-32 by increasing calcium levels and activating protein phosphatase 2B (33). Dopamine and the dopamine D_1 receptor are also highly enriched in the neostriatum. Thus, it is believed that PP1 may play a role in dopaminergic signal transduction (34). Modifications of the normal action of these neurotransmitters contribute to the etiology of several neuropsychiatric disorders. At the ultrastructural level, PP1α and PP1γ1 immunoreactivity was demonstrated in dendritic spine heads and spine necks (34). PP1γ1 is highly and specifically concentrated in the post-synaptic density of these spines. Dendritic spines are the principal sites for excitatory synapses in the central nervous system, so neuronal signalling study focus on PP1α and PP1γ1 (35). Furthermore, spinophilin is a PP1 binding protein that is highly expressed in brain and within neurons and is enriched in dendritic spines (20). Another PP1 binding protein enriched in brain and particularly in dendritic spines is neurabin (36). Both spinophilin and neurabin bind actin (20, 37), and it was also demonstrated that PP1γ1 associates with actin. PP1α and PP1γ1 bind to spinophilin and actin more avidly than PP1β (38, 39). These findings suggest that the dendritic spine localization of PP1γ1 (and PP1α) may result from binding of these phosphatases to neurabin and/or spinophilin (39).

The higher expression levels of PP1 in brain indicate that possibly it has an important role in the control of several brain functions. For instance, a role for PP1 in memory and learning has been outlined. Inhibition of PP1 *in vivo* induces deficits in memory retention and a role in age-related cognitive decline was proposed for PP1 (40). Additionally, PP1 is involved in AD. AD is characterized clinically by a progressive and irreversible decline of cognitive functions, and pathologically by the presence of neuritic plaques and neurofibrillary tangles. The cognitive decline seen in AD is thought to be related mainly with a decrease in synaptic contacts (41), where PP1 has an important role since it is enriched in dendritic spines.

PP1 is also involved in the maintenance of microtubule stability (42). Microtubules are a major cytoskeleton element in eukaryotic cells and have a crucial role in cell motility, division and differentiation. The microtubule motor protein kinesin plays an important role in intracellular mobility. Phosphorylation of kinesin light chain (KLC) is regulated by a kinase and by PP1, and the level of KLC phosphorylation is directly correlated with activation of kinesin motor activity (43). Tau is responsible for PP1 binding to microtubules, suggesting that tau is a PP1 targeting subunit. The association of PP1 with microtubules may lead to dephosphorylation of microtubule-associated proteins, like tau, which enhances their association with microtubules and promotes microtubule stability (42).

1.3. TorsinA

TorsinA and its related family members belong to the AAA^+ superfamily of ATPases associated with several subcellular activities (44). Members of AAA^+ ATPases are typically chaperone proteins that mediate conformational changes in target proteins. AAA^+ ATPases use the energy of ATP binding and hydrolysis to induce conformational changes in their substrates. These proteins are involved in several functions: protein folding and degradation, membrane trafficking, DNA replication and repair and cytoskeletal regulation (45). The high conservation of the AAA^+ ATPase family among species suggests an important role for torsinA in cell biology (46). TorsinA knockout mices die 48 hours after birth, indicating that torsinA plays an essential role on cellular function (47).

A mutation in *DYT1* (*TOR1A*) gene, which encodes human torsinA, is responsible for the movement disorder termed early onset torsion dystonia (EOTD) (44). Dystonias are a relatively rare class of neurologic disease. The term dystonia refers to pathological involuntary muscle contractions that induce repetitive and twisting movements, and abnormal posture. Early onset torsion dystonia (or Oppheim's disease or DYT1 dystonia) is the most common and severe form of hereditary primary dystonia, and develops in childhood or adolescence. EOTD is an autosomal dominant disease with a penetrance of

30-40% (reviewed in 48). Most cases of this disease are associated with an in-frame 3bp deletion (ΔGAG) in torsinA that removes one glutamic acid residue at position 302 or 303 (ΔE302/303), close to the C terminal of torsinA (44).

Despite the absence of neuronal neurodegeneration in other organisms down-regulation of torp4a, encoding the *Drosophila* homologue TorsinA, was shown to enhance neurodegeneration in retina of the flies (49).

TorsinA is expressed in many tissues, with highest levels in liver, muscle, pancreas and brain (44). In brain, torsinA mRNA is expressed in all brain regions with higher levels in cerebral cortex, thalamus, hippocampus, striatum, substantia nigra pars compacta, cerebellum, midbrain pons and spinal cord (50-52). The highest expression was detected in the dopaminergic neurons of substantia nigra pars compacta (50, 51), suggesting a link between the basal ganglia dopaminergic system and EOTD (52-54).

As a primary neurological characteristic, dystonia can be associated with neurodegenerative diseases like Parkinson disease. Parkinson disease is associated with progressive loss of dopaminergic neurons from the substantia nigra pars compacta. TorsinA is highly expressed in dopaminergic neurons and is a component of Lewy bodies (pathological feature of Parkinson disease), where it is associated with α-synuclein (55). In mice overexpressing mutant torsinA (ΔGAG), dopamine and its metabolites, 3,4-dihydroxyphenylacetic acid (DOPAC) and homovallinic acid (HVA) levels were altered (56). Coexpression of torsinA with DAT (dopamine transporter) in HEK293 cells decreased dopamine uptake as compared with cells expressing only DAT. Thus torsinA overexpression did not alter significantly the affinity of dopamine for DAT but it may interfere with DAT delivery to plasma membrane. As a consequence, it was observed that DAT levels at the plasma membrane are reduced in the presence of torsinA and it colocalizes with torsinA in intracellular compartments (57). Overexpression of torsinA and TOR-2 (TorsinA *Caenorhabditis elegans* homolog) in *C. elegans* dopaminergic neurons can lead to the suppression of neurodegeneration induced by 6-OHDA treatment. Animals expressing mutant torsinA (ΔGAG) demonstrated reduced protection from 6-OHDA. Therefore, it was demonstrated that torsinA and TOR-2 may protect dopaminergic neurons from 6-OHDA through downregulating the expression of the dopamine transporter DAT-1 *in vivo*. Additionally, it was demonstrated that torsinA and TOR-2 also protected dopaminergic neurodegeneration caused by overexpression of α-synuclein (58).

TorsinA is a 332 amino acid protein with potential sites of glycosylation and phosphorylation, as well as a putative membrane spanning domain (44) and a putative bipartite nuclear localization sequence (54). This protein contains a single ATP-binding AAA^+ module, including Walker A and Walker B nucleotide binding motifs and α-helical domains, sensor 1 and sensor 2 (Fig. 5), which have been proposed to mediate substrate interactions and are critical for ATP hydrolysis. In the C-terminal region there is poor similarity between torsinA and other AAA^+ proteins (59). This C-terminal region of torsinA (where ΔGAG deletion occurs) may contain a supposed binding domain, which determines the role of the protein (60).

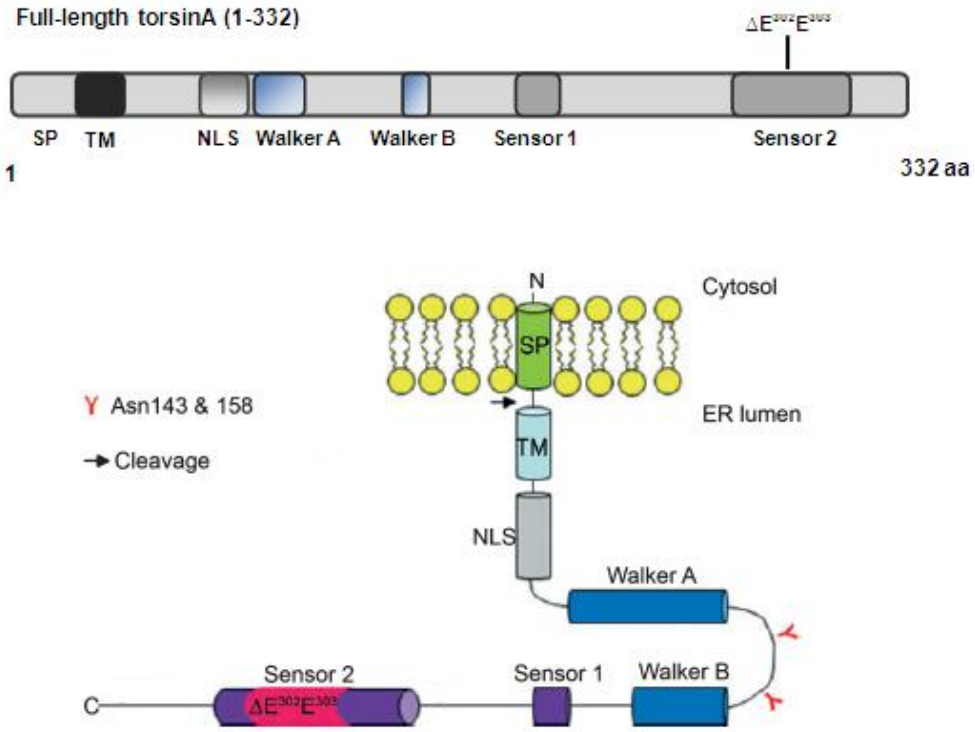

Figure 5. Schematic representation of torsinA protein and its characteristic domains. TorsinA is a 332 amino acid (aa) protein. The structure of torsinA was predicted to contain an amino-terminal signal peptide (SP) sequence which is removed from the mature protein, a putative transmembrane domain (TM) and a putative bipartite nuclear localization signal (NLS). Arrow indicates the signal peptide cleavage, which results in translocation of torsinA into the lumen of the endoplasmatic reticulum (ER). Walker A and Walker B are ATP binding sites and Sensor 1 and Sensor 2 are configurational domains of AAA^+ ATPases. The ΔGAG mutation ($\Delta E^{302}E^{303}$) is located in sensor 2 region. TorsinA contains two sites for potential glycosylation (Asn 143 and 158) (adapted from 61).

Some studies established that torsinA is a membrane-associated protein that faces the lumen of the endoplasmic reticulum (ER) (60, 62). In contrast Callan *et al* (63) demonstrated that torsinA does not behave as a typical integral membrane protein, since extraction at pH 11.3 is sufficient to completely remove torsinA from the ER membrane, but at pH 9.5 half of the protein remains associated with the membrane. Furthermore, it was suggested that signal peptidase complex cleaves the N-terminal signal peptide (Fig. 5) leading to full translocation of torsinA into de lumen of the ER. Consequently they conclude that torsinA is peripherally associated with the inner face of the ER membrane and this may be the result of binding to an integral membrane protein. ATP-free TorsinA is diffusely distributed throughout the ER, but if ATP is bound to torsinA, it is recruited to the nuclear envelope (NE) (64). Upon over-expression, wild type (Wt) torsinA was also found to be localized in the NE (64, 65) and mutant torsinA (ΔGAG) showed redistribution to the NE. Furthermore, mutant torsinA colocalized with lamin B1 in the NE of neurons and there was almost no expression in the ER (65). Another study (66), which provides a quantitative analysis of the relative NE/ER distribution, demonstrated that dystonia-associated mutations do not influence the localization of torsinA in non-neuronal cells (HeLa cells) in contrast with previous studies. However, dystonia-associated mutations were shown to induce translocation of torsinA from de ER to NE in neuronal cells (66). Abnormal accumulation of mutant torsinA (ΔGAG) in the NE suggests that a NE dysfunction may contribute to EOTD pathogenesis (67). Interestingly, two torsinA binding proteins identified to date are integral membrane proteins: LULL1 in the ER and lamina associated polypeptide 1 (LAP1) in the nuclear envelope. Like torsinA, LAP1 and LULL1 mRNAs are widely expressed in both neuronal and non-neuronal tissues (67). Increased expression of LULL1 was also found to change the localization of Wt torsinA and mutant torsinA from the ER to the nuclear envelope, suggesting a role for LULL1 in the distribution and activity of torsinA. Alterations in the activity of LAP1 or LULL1 may play a role in the pathogenesis of EOTD (68). Accumulation of mutant torsinA in the NE may alter the functions of NE interacting proteins, such as LAP1 and cause abnormality of the NE, including formation of blebs and herniations into the perinuclear space, which have been observed in cultured primary neurons from homozygous knock-out and knock-in mice (47).

AAA^+ ATPases frequently act as molecular chaperones and modulate protein-protein interactions (45), so it was proposed that torsinA could modulate these interactions in the lumen of the perinuclear space. The interaction between transmembrane proteins of the inner and outer nuclear membrane can also be fundamental to the connection of nuclei with the cytoplasmic cytoskeleton (Fig. 6). TorsinA may regulate lumenal interactions between inner nuclear membrane (INM) and outer nuclear membrane (ONM) proteins (69).

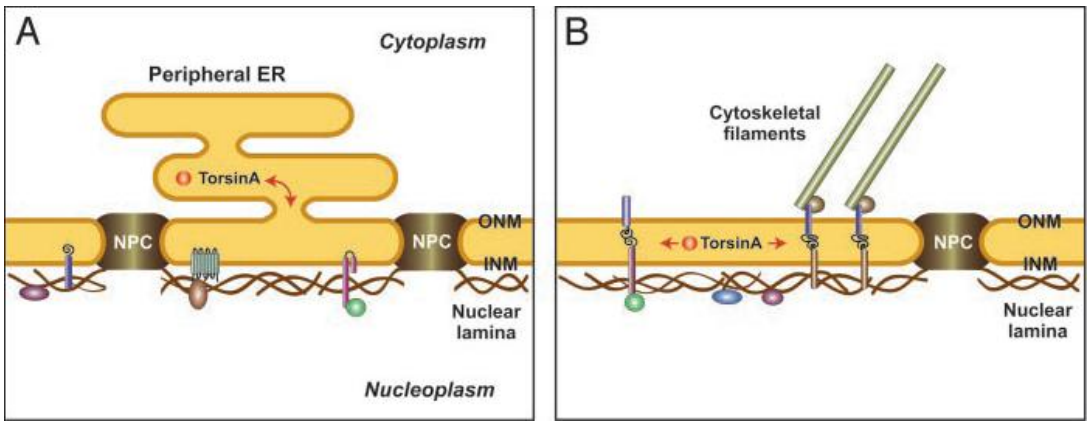

Figure 6. Schematic representation of the nuclear envelope (NE) and potential functions of torsinA. A- Schematic model of NE. The outer nuclear membrane (ONM) is morphologically continuous with the peripheral endoplasmatic reticulum (ER) and torsinA is relocalized from the (ER) to the NE. B- Model for association of cytoskeletal filaments with the NE. Cytoskeletal filaments may interact with the transmembrane proteins of the ONM and may associate with lamina associated polypeptides (LAPs) of the inner nuclear membrane (INM) via the lumenal domains. TorsinA may regulate lumenal interactions between the INM and the ONM proteins. NPC- Nuclear pore complex (69).

TorsinA was also found associated with cytoskeletal elements like kinesin (70) and vimentin (71) (Fig. 7). The TPR (tetratricopeptide repeat) domain of the light chain subunit (KLC1) of kinesin-I interacts directly with the C-terminal region of torsinA. Wt torsinA and KLC1 have the same distribution in cytoplasm and processes of neural cells with enrichment at distal ends. Mutant torsinA was localized in cells bodies, in inclusions and often altered the distribution of kinesin that was then localized in these inclusions. This data support a possible role of torsinA in intracellular trafficking mediated by kinesin microtubules and possible etiology of EOTD (70). EOTD patients that do not develop

dystonic symptoms by age 28 are very unlikely to develop dystonia later. The age of vulnerability is associated with the period of motor learning in humans and with the developmental stage of high synaptic plasticity of neostriatum in primates (72) and rodents (73). An enrichment of kinesin and torsinA was found in growth cones of cultured rat cortical neurons. The interaction of kinesin and torsinA and their functional integrity could be required for active neurite outgrowth and/or synaptic plasticity, possibly associated with motor learning in the brain (70). Vimentin is an intermediate filament protein that associates with other cytoskeletal proteins such as kinesin, tubulin, actin and myosin. TorsinA was also found to associate with vimentin in fibroblasts. However, EOTD patient cells showed a decrease in the association of torsinA with the cytoskeletal elements. Immunoprecipitation of vimentin brings torsinA and other cytoskeletal proteins including kinesin and actin, suggesting a role for torsinA in their collective interaction (71). Additionally, another vimentin binding partner is LAP1B that interacts with torsinA at NE (67) and with vimentin and microtubules during mitosis (74). Nesprin-3, a protein of the outer nuclear membrane implicated in connecting the nucleus and cytoskeleton, is another NE protein that interacts with torsinA (75).

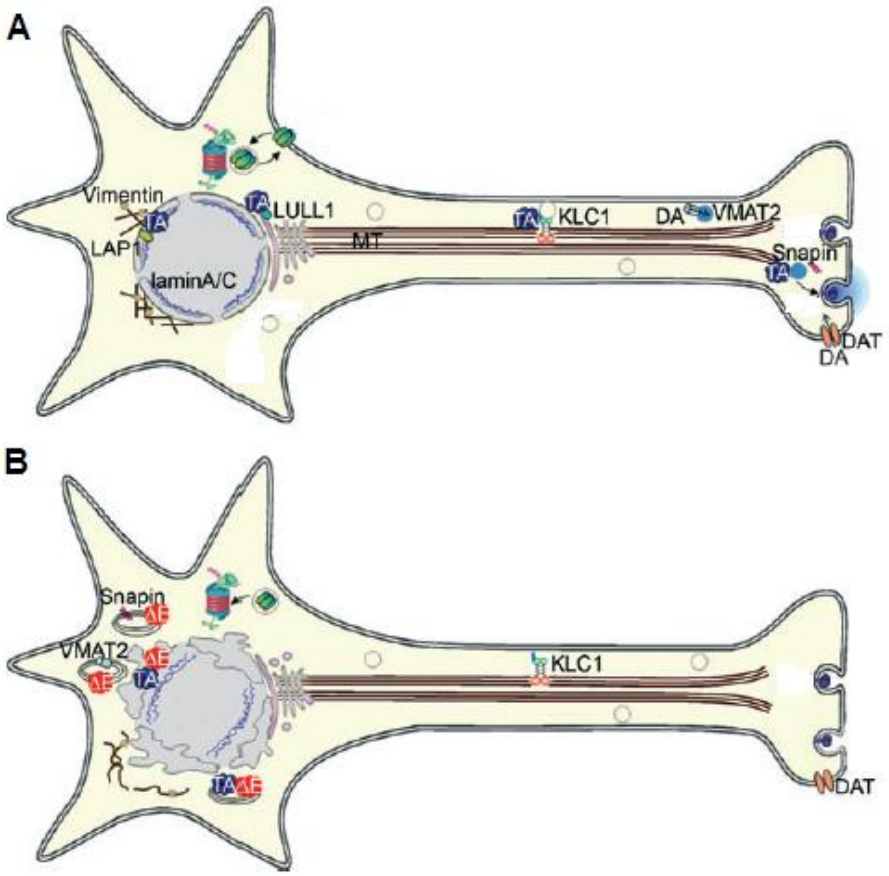

Figure 7. Schematic illustration of torsinA (TA) and mutant torsinA (ΔGAG, ΔE) subcellular localization and potential roles. A- TorsinA is found in the endoplasmatic reticulum (ER) and nuclear envelope (NE), where its interacting proteins are shown. TorsinA is also associated with kinesin light chain 1 (KLC1) and binds snapin at the synapse. TorsinA may be involved in the localization of dopamine transporter (DAT) and may play a role in the correct function of vesicular monoamine transporter 2 (VMAT2). B- Cellular alterations caused by mutant torsinA (ΔGAG). TorsinA and some factors controlling synaptic vesicles, including snapin and VMAT2, are recruited in perinuclear inclusions. The NE structure is abnormal and KLC1 function may be also affected. DA, dopamine; LAP1, lamina associated polypeptide 1; MT, microtubules (adapted from 61).

Association of torsinA with the microtubule cytoskeleton was proposed to result from an indirect interaction through a protein partner. Additionally, torsinA was found to co-immunoprecipitate with the principal isoforms of tau in differentiated SH-SY5Y neuroblastoma cells. This association suggests that torsinA may modulate the interaction between tau and microtubules. SH-SY5Y cells express torsinA in both the cytoplasm and the perinuclear space. TorsinA distribution presents a punctate pattern, typical of

membrane associated proteins, and also a particular concentration at synaptic varicosities. Colocalization of torsinA and an integral vesicular protein synaptobrevin (VAMP), a marker of synaptic vesicles, was also demonstrated. Based on the localization of torsinA in the ER and colocalization of torsinA with synaptic vesicles markers, it was proposed that torsinA has a role in tubular-vesicular membrane trafficking along the neuronal processes. The association between torsinA, tau and microtubules is in apparent contrast with ER localization of torsinA. Nevertheless torsinA could be processed in the ER and then exported along the processes (76). More recently it was suggested that torsinA has a role in synaptic vesicle recycling. Snapin, a protein involved in vesicle exocytosis, and endogenous torsinA colocalize in dense core granules in PC12 cells, and was recruited to perinuclear inclusions (Fig. 7) containing mutant torsinA (ΔGAG) in SH-SY5Y cells (77). Overexpression of mutant torsinA (ΔGAG) also causes the entrapment of vesicular monoamine transporter 2 (VMAT2), a crucial regulator for dopamine levels, in membranous inclusions (78) (Fig. 7).

1.4.Lamins and lamina associated polypeptides (LAPs)

The NE is composed of an inner and outer nuclear membrane, the nuclear lamina and nuclear pore complexes. The ONM is continuous with the peripheral ER. The INM contains specific proteins that are not detected in the peripheral membrane and it is lined by the nuclear lamina (Fig. 8). The nuclear lamina is composed mainly by nuclear lamins that are proteins of the intermediate filament family. The nuclear lamina also contains peripheral and integral membrane proteins of the inner nuclear membrane (79, 80). The nuclear pore complexes are responsible for protein and nucleic acid movement to and from the nucleus. The perinuclear space is located between the INM and the ONM (Fig. 8) and is continuous with the ER (80).

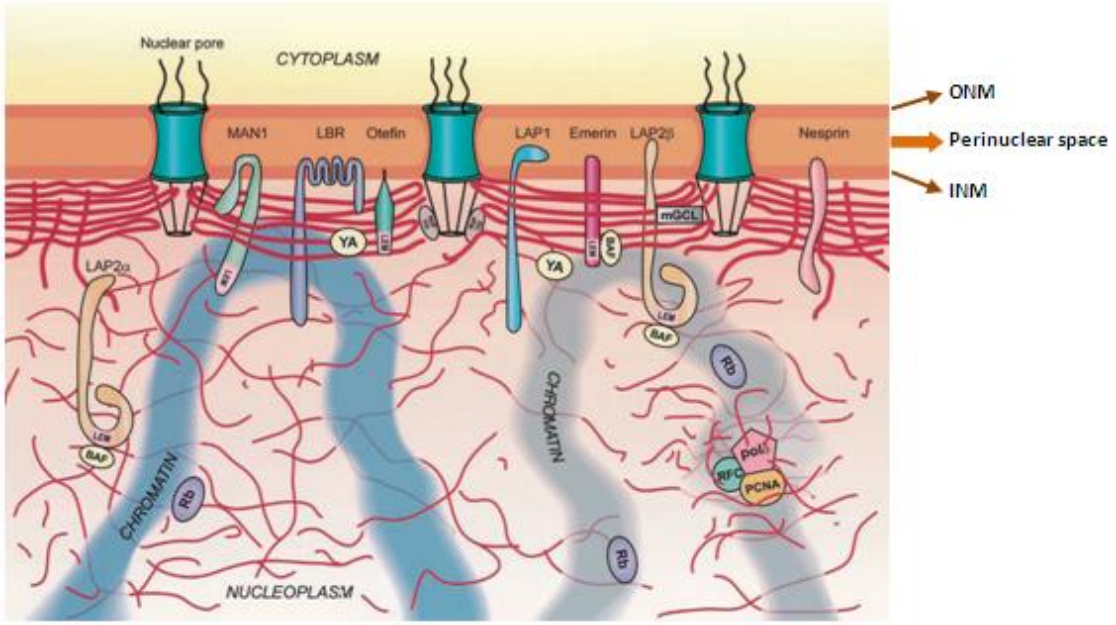

Figure 8. Illustration of the nuclear membrane and proposed interactions between the nuclear lamina with inner nuclear membrane (INM) proteins, nuclear pores and other nucleoplasmic factors. The lamins are concentrated in the lamina and are also present in the nucleoplasm (red lines). The INM proteins include MAN1, lamin B receptor (LBR), ofetin, lamina associated polypeptide 1 and 2 (LAP1 and LAP2), emerin and nesprin. INM, inner nuclear membrane; ONM, outer nuclear membrane (adapted from 79).

Lamins are classified as A-type or B-type lamins. The A-type lamins include lamin A, AΔ10, C and C2; they are all encoded by the *LMNA* gene and are expressed in differentiated cells (81). The B-type lamins include lamin B, which is encoded by the *LMNB1* gene, and lamin B2-B3 derived from the *LMNB2* gene (82). These lamins are expressed in embryonic and somatic tissues. Originally, nuclear lamins were proposed to have a role in supporting the nuclear envelope and providing anchorage sites for chromatin, due to their position at the periphery of the inner nuclear membrane. More recently lamins were found in the nucleoplasm (Fig. 8), suggesting their involvement in nuclear envelope assembly, DNA synthesis, transcription and apoptosis. Thereby the nuclear lamina is disassembled during prophase/metaphase and this event is regulated by lamin phosphorylation. At telophase the lamins are dephosphorylated and the nuclear lamina is reassembled, approximately at the same time of nuclear envelope formation. The regulation of the lamin structures formed during nuclear envelope assembly may be

determined by the association of lamins with other proteins. These proteins can be integral proteins of the inner nuclear membrane or proteins that are not integral membrane components but are localized mostly in the region of the nuclear lamina. The first group, the INM proteins, include lamina associated proteins (LAPs), emerin, A-kinase-anchoring protein 149 (AKAP-149), lamin B receptor (LBR), MAN1, nesprin, otefin and others (79). INM proteins interact directly with nuclear lamina *in vitro* and remain associated with the nuclear lamina after extraction of the nuclei with non-ionic detergents, nucleases and/or high-salt buffers (83). The second group, proteins that are not integral INM proteins but are concentrated in the region of the nuclear lamina, include among others PP1 (84). PP1 has been implicated in lamin B dephosphorylation in late mitotic cells. It was proposed that PP1 mediates nuclear lamina reassembly, in part by dephosphorylation of lamin B (85). More recently, AKAP-149, identified as a component of the ER-nuclear system, was found to contain an RVxF motif that mediates interaction with PP1 (84). AKAP-149 recruits PP1 to the NE upon NE assembly *in vitro* and promotes lamin B dephosphorylation and polymerization. At G_1 phase, AKAP-149 anchors PP1 in the NE in proximity to lamin B and this complex is dissociated at the G_1/S phase transition when serine phosphorylation of AKAP-149 occurs. Reassembly of the NE at the end of mitosis requires this association of PP1/lamin B to the nuclear envelope by AKAP-149 (86).

1.4.1. Lamina associated polypeptide 1 (LAP1)

Lamina associated polypeptides (LAPs) are type two INM proteins stably associated with the nuclear lamina. Lamina associated polypeptide 1 (LAP1) and lamina associated polypeptide 2 (LAP2) were identified by monoclonal antibodies generated against lamina-enriched fractions of rat liver nuclei (83, 87). LAP2 proteins are expressed in several isoforms that are derived from alternative splicing of the same gene and they are associated with type B lamins and mitotic chromosomes. LAP1 is expressed in three isoforms: LAP1A, LAP1B and LAP1C, which are, probably, splice products of one gene. Only the cDNA for LAP1C has been completely sequenced in rat, but partial characterization of other cDNAs suggested that the three LAP1 isoforms arise from

alternative splicing, since LAP1A and LAP1B cDNAs were identical to the LAP1C sequence with the addition of two insertions (88). In human, the sequences of LAP1A and LAP1C are only partially known and the full-length cDNA of human LAP1B was reported by Kondo *et al* (2002) (89). LAP1C was the most abundant LAP1 isoform found in a variety of cultured cells (87, 88).

LAP1 isoforms have a large lumenal domain (Fig. 9) that has no homology with other type two proteins of the inner nuclear membrane (89). The transmembrane and the lumenal domains (Fig. 9) of LAP1 isoforms are encoded by a single exon, in rat, mouse and human. So, it is believed that LAP1 isoforms are different only in their nucleoplasmic portion (67).

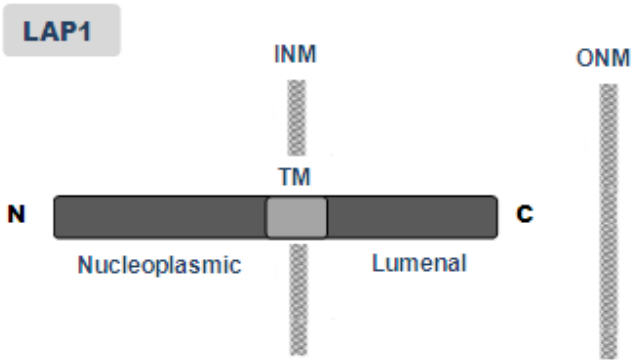

Figure 9. Schematic representation of LAP1 protein. Predicted nucleoplasmic and lumenal portions are represented as well the transmembrane domain (TM). INM- Inner nuclear membrane; ONM- Outer nuclear membrane (adapted from 67).

LAPs are normally associated with type A and type B lamins, as well as mitotic chromosomes (83). During mitosis, LAP1C and lamin B colocalize in mitotic vesicles which associate transiently with the mitotic spindle (74). The function of LAP1 is poorly understood, but the interactions of LAPs with lamins and chromosomes may be important for maintenance of the nuclear architecture during interphase and mitosis (89). During mitosis, the ER undergoes disassembly to allow the partitioning of ER membranes to the daughter cells. In interphase LAP1 is localized in a nuclear rim, but during prometaphase LAP1 seems to be localized throughout the entire ER. In late anaphase, when nuclear envelope reassembles, LAP1 appeared to be concentrated in certain ER elements and is associated with chromosomes. Nuclear envelope membranes lose their identity as a distinct

subcompartment of the ER during mitosis and integral membrane proteins become dispersed throughout ER membranes. NE reassembly in late anaphase results from cooperative interactions between lamins, integral membrane proteins and chromossomes (90). LAP1 and LAP2 dissociate from the lamins at the onset of mitosis and associate before the reassembly of the nuclear lamin (83).

Several INM proteins are involved in human diseases. Emerin mutations cause the X-linked form of Emery-Dreifuss Muscular Dystrophy, characterized by progressive weakness of the upper arms and lower limbs, and contractures of the elbows, Achilles tendon, neck and spine (91). LAP2α is associated with familial dilated cardiomyopathy and loss of LAP2α-lamin A binding was observed for the mutated protein *in vitro* (92). LBR mutations are associated with Pelget-Huet anomaly, characterized by abnormal nuclear shape and chromatin organization in blood granulocytes, and Greenberg's skeletal dysplasia (93). MAN1 mutations cause Buschke-Ollendorff syndrome characterized by increased bone density (94). LAP1 has been identified as a torsinA interacting protein (67). As described previously, a mutation in torsinA is responsible for the autosomal movement disorder EOTD (44). TorsinA may interact with the conserved lumenal domain of LAP1. It was demonstrated that LAP1 recruits Wt torsinA to the NE in a perinuclear localization. These findings suggest that alterations in torsinA function may influence the nuclear lamina properties and that EOTD may cover abnormal molecular properties similar to that seen in diseases resulting from lamin mutations (67).

1.5. Yeast two-hybrid system

The yeast two-hybrid system is a method capable of detecting the interaction between two proteins via transcriptional activation of one or several reporter genes and is also used for searching for unknown partners (the prey) of a given protein (the bait) (Fig. 10). This method is based on the properties of the yeast GAL4 protein, which has two separable domains, one responsible for DNA binding and another for transcriptional activation. The yeast two-hybrid assay is performed by expressing two fusion proteins in yeast. The first contains the GAL4 DNA binding domain (GAL4-BD) fused to a bait

protein and the other contain the GAL4 activation domain (GAL-AD) fused to a targeted protein (the prey) (95). The prey and bait constructs are introduced, by co-transformation or mating, into yeast strains containing the appropriate "Upstream Activating Sequence" (UAS) proximal to a reporter gene. When the bait and the target protein interact, the binding domain and the activation domain are brought together forming a functional transcriptional activator which leads to the transcriptional activation of the reporter gene (Fig. 10). Each Gal4 responsive gene contains a UAS target site. When Gal4 binds the UAS, transcription is activated from a downstream promoter. By linking the Gal4 UAS with other metabolic genes (e.g. *ADE2*, *HIS3*, *MEL1* and *lacZ*) and by eliminating the wild type *GAL4* gene, researchers have developed yeast strains that change phenotype when Gal4 is activated. Although the Gal4-BD can bind the UAS, it cannot activate transcription by itself. Transcription is activated only when the other half of the protein, Gal4-AD, joins the binding domain at the UAS. When performing a large scale screen, a plasmid library expressing cDNA-encoded GAL4-AD fusion proteins can be screened by introduction into a yeast strain. These larger scale yeast two-hybrid approaches typically rely on interaction by yeast mating (96, 97).

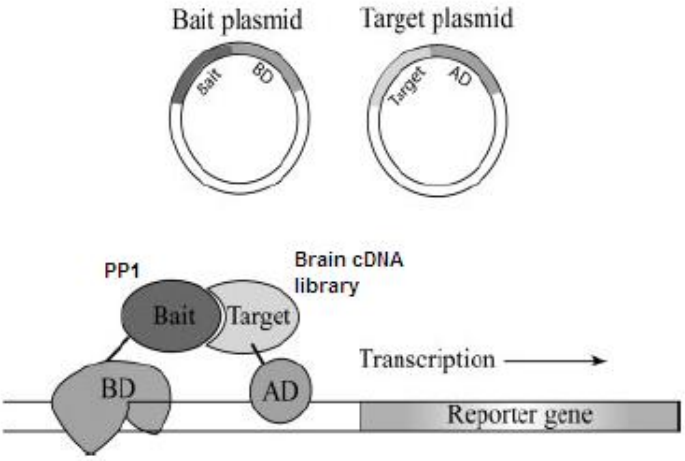

Figure 10. General overview of the yeast two-hybrid system. The bait (PP1 in our experiments) is fused to the GAL4 DNA binding domain and the target protein (sequence from brain cDNA library) is fused to the activation domain. If the bait and prey interact, the GAL4 binding domain (BD) and the GAL4 activation domain (AD) are brought together forming a functional transcriptional activator which leads to the transcriptional activation of a downstream reporter gene (adapted from 98).

The advantages of this method are that it is simple, requires little optimization, is relatively inexpensive and is able to detect protein interactions *in vivo*. This method can generate false positives, however, high stringency media is used to prevent it. Even though two proteins can interact, it is not certain that they will also interact under physiological conditions. Therefore, the biological relevance of the proteins identified must always be confirmed using alternative methodology (98).

In order to identify potential PP1 interacting and regulating proteins, and to characterize the PP1 human brain interactome, a large scale screen for PP1 binding proteins was performed, using the yeast two-hybrid system. The PP1γ1, PP1γ2 and PP1α were used as baits and this methodology was used to screen a human brain cDNA library. The binding domain plasmid carries the yeast *TRP1* gene and, for example, the PP1γ1 sequence (the bait) fused to GAL4-BD. The activation domain plasmid carries the yeast *LEU2* gene and a sequence from the cDNA library (the prey) fused to GAL4-AD. The reporter genes used were the *MEL-1* gene, which encodes α-Galactosidase, and *HIS3* and *ADE4*. The plasmids were transformed into yeast strain which requires tryptophan (Trp), leucine (Leu), histidine (His) and adenine (Ade). If the two proteins (the bait and the prey) interact the reporter genes will be activated and the yeast will grow on synthetic complex medium lacking the amino acids Trp, Leu, His and Ade. The α-Galactosidase activity is detected by the formation of blue yeast colonies on medium with the cromogenic substrate X-α-Gal (5-bromo-4-chloro-3-indolyl alpha-D-galactopyranoside).

The brain cDNA library screen, using PP1γ1 as bait identified 300 positives clones, four of which were identified as torsinA interacting protein 1 (TOR1AIP1), or lamina associated protein 1B (LAP1B). A total of 298 positive clones were obtained in the yeast-two hybrid (YTH) screen using PP1α as bait, and 14 were identified as LAP1B. Using PP1γ2 as bait 298 positive clones were obtained and 2 were identified as LAP1B protein. Given that LAP1B was detected with all the PP1 isoforms tested, and since LAP1B is known to interact with torsinA, a protein involved in the incurable neurologic disease termed early onset torsion dystonia (EOTD), it seemed important to validate the PP1/LAP1B interaction. This decision was also supported by the well known involvement of PP1 in dopaminergic signalling, thus raising the possibility that PP1 and/or abnormal protein phosphorylation may have an important role in EOTD.

1.6.Aims of the thesis

Given the various different roles that have been proposed for PP1, concomitant with different binding and regulatory subunits, it is important to identify novel PP1 binding proteins. Thus a yeast two-hybrid screen of a human brain cDNA library was performed using various PP1 isoforms as baits. Among several interesting proteins, LAP1B was identified as a novel putative PP1 regulator. The function of LAP1B is poorly understood but it is known to interact with torsinA, which is involved in EOTD. Therefore, the main goal of this thesis was to validate the interaction of LAP1B with PP1 using a variety of methodologies. The specific aims of this thesis were:

- To validate the interaction between LAP1B and different PP1 isoforms by yeast co-transformation.

- To determine the likely physiological relevance of the various putative PP1 binding motifs of LAP1B, using deletion mutants and yeast co-transformation.

- To express LAP1B protein in bacteria.

- To validate the PP1/LAP1B interaction *in vitro* by blot overlay using purified recombinant PP1γ1 protein.

- To determine the subcellular localization of the PP1/LAP1B complex in mammalian cells.

- To validate the physiological PP1/LAP1B interaction *in vivo* by co-immunoprecipitation.

2. Bioinformatics analysis of LAP1B

YTH screenning of a human brain cDNA library using various PP1 isoforms as bait identified a novel putative PP1 interactor: torsinA interacting protein 1 (TOR1AIP1) or lamina associated protein 1B (LAP1B). Overall, fourteen, four and two positive clones encoding LAP1B were identified using PP1α, PP1γ1 and PP1γ2 as baits, respectively (Table 1). Sequencing analysis of all LAP1B clones isolated led us to determine that all of them represent an alternative splice variant of LAP1B reported in the NCBI database (NM_015602), with the only difference being an additional CAG insertion which results in the addition of one alanine (Fig. 11). This sequence is identical to that previously reported by Kondo *et al* (2002) (89). For further studies, we choose clone 135 (interaction with PP1γ1) which has an insert of 2.0 Kb and encodes the full-length LAP1B (Table 1).

Table 1. Summary of LAP1B clones isolated from the yeast-two hybrid (YTH) screens.

Bait	Clone ID	Number of clones	YTH clone ID	Insert (Kb)	Start position
PP1α	TOR1AIP1 (NM_015602)	14	12	2.0	140
			31	1.75	138
			36	2.25	24
			45	2.15	138
			50	2.75	30
			61	3.85	21
			76	3.5	18
			96	2.2	139
			184	4.3	21
			192	3.75	30
			261	4.0	21
			262	2.1	138
			271	2.2	138
			273	3.75	21
PP1γ1	TOR1AIP1 (NM_015602)	4	120	2.4	17
			124	1.5	22
			135	2.0	138
			164	1.6	24
PP1γ2	TOR1AIP1 (NM_015602)	2	124	1.8	18
			164	0.3	26

Clone 135 (interaction with PP1γ1) was selected for further study. The start position indicated is relative to the GenBank sequence NM_015602.

The alternatively spliced isoform of LAP1B (LAP1B') includes 3 more nucleotides (CAG) and results in the inclusion of a single amino acid (alanine) at position 185 of LAP1B amino acid sequence (Fig. 11).

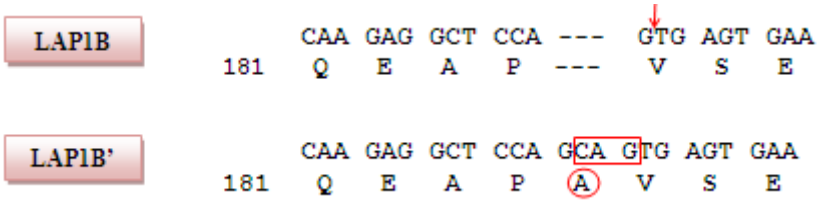

Figure 11. Analysis of homology between LAP1B sequence in NCBI database (NM_015602) and the sequence of the alternatively spliced LAP1B' isoform isolated in this study. The arrow indicates the site of a CAG insertion which results in the insertion of alanine (A) in LAP1B'.

The *LAP1B* gene is localized on chromosome 1 (1q24.2). Alignment of the LAP1B cDNA with the corresponding genomic sequence identifies the exon-intron boundaries. LAP1B is encoded by 10 exons and the alternative splicing occurs at exon 3 (Fig. 12).

A

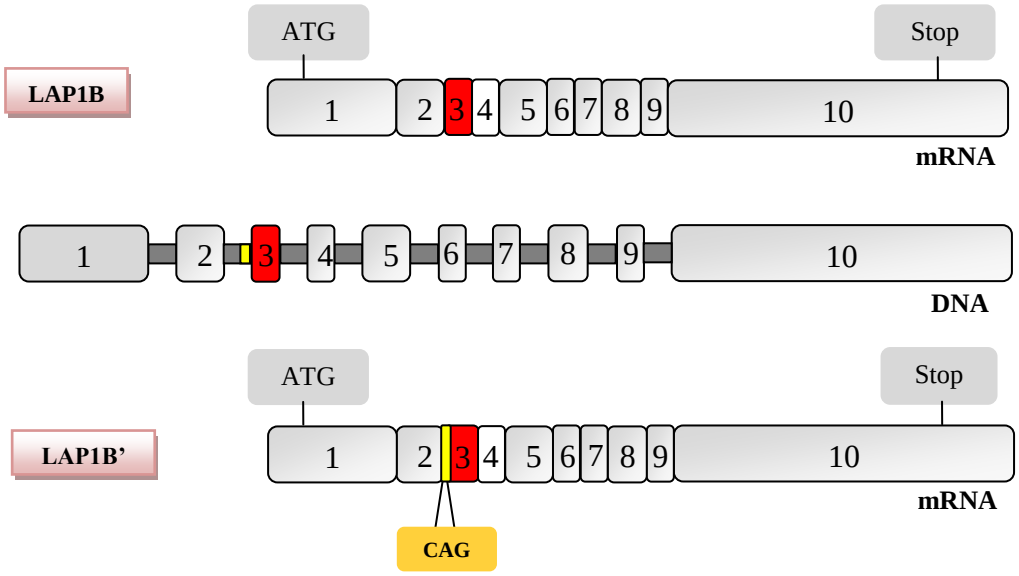

B

Intron **5' Splice donor site**	**Exon** **3' Splice acceptor site**	**Amino acid change**
cctatattagcag	cagtgagtgaagatc	Val/AlaVal

Figure 12. Shematic representation of the genomic structure of the LAP1B gene, showing the exon-intron organization. **A-** Exons are represented as numbered boxes and introns as gray lines (not to scale). The alternative splicing occurs at exon 3 and isoform LAP1B' includes three more nucleotides (CAG). **B-** Exon and intron boundaries of the isoform LAP1B'. Val- valine; Ala- alanine.

Despite the inclusion of the extra CAG in the coding sequence of our clone we will refer it here as LAP1B. LAP1B is a type two INM protein with 584 amino acids. LAP1B has an N-terminal nucleoplasmic domain, a putative transmembrane domain and a C-terminal lumenal domain. In order to obtain an overview of the most important domains and motifs present in the LAP1B sequence, a detailed bioinformatic analysis was performed. Several interesting putative domains and motifs were identified, including three well conserved PP1 binding motifs (BM) (Figs. 13A and 14). BM1, comprising amino acids 55-59 (REVRF), and BM2, comprising aa 212-215 (KVNF), are localized in the nucleoplasm. BM3 comprises aa 538-541 (KVKF) and is localized in the lumen of the perinuclear space. A second generic PP1 binding motif (SILK, aa 306-309) was also identified (Figs. 13A and 14). Additionally, the transmembrane domain (aa 339-359) was predicted by Goldman and Engelman Steitz hydrophobicity analysis (Fig. 13B).

The amino acid sequence was obtained using the Expasy Translate tool (http://www.expasy.org/tools/dna.html). Various LAP1B putative domains were predicted using ELM server (http://elm.eu.org/) and the SILK domain was predicted on ExPASy ScanProsite tool (http://www.expasy.ch/tools/scanprosite). The hydrophobicity analysis was performed using TopPred (http://mobyle.pasteur.fr/cgi-bin/portal.py?form=toppred).

A

```
       agaagccatcgccaccaccgg
       caggagaacctagggtccataaagccatcttcgcgatcgactaaagctacgtcaacaact
  82   atggcgggcgacgggcggcgggcagaggcggtgcgggaaggatggggtgtgtacgtcacc
        M  A  G  D  G  R  R  A  E  A  V  R  E  G  W  G  V  Y  V  T  20
 142   cccagggcccccatccgagagggaaggggccggctcgcccctcaaaatggcggcagcagc
        P  R  A  P  I  R  E  G  R  G  R  L  A  P  Q  N  G  G  S  S  40
 202   gatgcgcctgcgtacagaactcctccgtcgcgccagggccggcgggaagtgaggttctcg
        D  A  P  A  Y  R  T  P  P  S  R  Q  G  R  R  E  V  R  F  S  60
 262   gacgagccgccagaagtgtacggcgacttcgagcccctggtggccaaagaaaggtccccg
        D  E  P  P  E  V  Y  G  D  F  E  P  L  V  A  K  E  R  S  P  80
 322   gtgggaaaacgaacccggctagaagagttccggtccgattctgcgaaagaggaagtgaga
        V  G  K  R  T  R  L  E  E  F  R  S  D  S  A  K  E  E  V  R  100
 382   gaaagcgcgtactaccttcggtctaggcagcggaggcagccgcgaccccaggaaaccgag
        E  S  A  Y  Y  L  R  S  R  Q  R  R  Q  P  R  P  Q  E  T  E  120
 442   gaaatgaagacgcgaaggactacccgccttcagcagcagcactcagagcagcctccgcta
        E  M  K  T  R  R  T  T  R  L  Q  Q  Q  H  S  E  Q  P  P  L  140
 502   cagccgtctcctgttatgaccaggagagggctgcgggactctcattcctctgaagaggat
        Q  P  S  P  V  M  T  R  R  G  L  R  D  S  H  S  S  E  E  D  160
 562   gaagcatcttcccaaactgatttaagccaaacgatctcaaagaaaactgtcaggagcata
        E  A  S  S  Q  T  D  L  S  Q  T  I  S  K  K  T  V  R  S  I  180
 622   caagaggctccagcagtgagtgaagatcttgtaatcaggttacgtcgacccccctctaaga
        Q  E  A  P  A  V  S  E  D  L  V  I  R  L  R  R  P  P  L  R  200
 682   tacccaagatatgaagccaccagtgtccaacagaaggtcaatttctctgaagaaggagaa
        Y  P  R  Y  E  A  T  S  V  Q  Q  K  V  N  F  S  E  E  G  E  220
 742   actgaagaagatgatcaagacagctctcacagcagtgtcactactgttaaggccagatcc
        T  E  E  D  D  Q  D  S  S  H  S  S  V  T  T  V  K  A  R  S  240
 802   agggattctgatgaatctggagataaaaccaccagatcatctagtcaatatatagaatca
        R  D  S  D  E  S  G  D  K  T  T  R  S  S  S  Q  Y  I  E  S  260
 862   ttttggcagtcatcacaaagtcaaaacttcacagctcatgataagcaaccttcagtgcta
        F  W  Q  S  S  Q  S  Q  N  F  T  A  H  D  K  Q  P  S  V  L  280
 922   agctcaggatatcaaaaaactccccaggaatgggccccacaaactgcaagaataaggacc
        S  S  G  Y  Q  K  T  P  Q  E  W  A  P  Q  T  A  R  I  R  T  300
 982   aggatgcaaaatgacagcattctgaaatcagagcttggaaaccagtcaccatcaacctcc
        R  M  Q  N  D  S  I  L  K  S  E  L  G  N  Q  S  P  S  T  S  320
1042   agccgacaagtgactggacaaccccaaaatgcatcttttgtcaagaggaaccggtggtgg
        S  R  Q  V  T  G  Q  P  Q  N  A  S  F  V  K  R  N  R  W  W  340
1102   ctacttcctctgatagctgctcttgcctctgggagttttggttctttagtactcctgag
        L  L  P  L  I  A  A  L  A  S  G  S  F  W  F  F  S  T  P  E  360
1162   gtagaaaccactgctgttcaagagttccagaaccagatgaatcaacttaagaataagtac
        V  E  T  T  A  V  Q  E  F  Q  N  Q  M  N  Q  L  K  N  K  Y  380
1222   caaggtcaagatgagaagctgtggaaaaggagccaaacattcctggaaaaacatcttaat
        Q  G  Q  D  E  K  L  W  K  R  S  Q  T  F  L  E  K  H  L  N  400
1282   agctcccatcctcggtctcagcctgctatcttactgctcactgctgcccgagatgctgaa
        S  S  H  P  R  S  Q  P  A  I  L  L  L  T  A  A  R  D  A  E  420
1342   gaagcacttaggtgtctgagtgaacaaattgctgatgcctattcttcttttcgtagtgtc
        E  A  L  R  C  L  S  E  Q  I  A  D  A  Y  S  S  F  R  S  V  440
1402   cgtgccatccggattgatgggacagataaagctactcaagacagtgatactgtcaaacta
        R  A  I  R  I  D  G  T  D  K  A  T  Q  D  S  D  T  V  K  L  460
1462   gaggtagaccaagaactgagcaatggatttaagaatggccagaatgcagctgtggtacac
        E  V  D  Q  E  L  S  N  G  F  K  N  G  Q  N  A  A  V  V  H  480
1522   cgctttgagtcatttcccgcaggctctactttgatcttctacaaatattgtgaccatgaa
        R  F  E  S  F  P  A  G  S  T  L  I  F  Y  K  Y  C  D  H  E  500
1582   aacgcggccttcaaagatgtagccttagtcctgactgtcttattggaggaagagacactt
        N  A  A  F  K  D  V  A  L  V  L  T  V  L  L  E  E  E  T  L  520
1642   ggaacaagtctaggcctaaaggaagttgaagaaaaagtaagagattttcttaaagtcaag
        G  T  S  L  G  L  K  E  V  E  E  K  V  R  D  F  L  K  V  K  540
1702   ttcaccaattctaacacacccaactcctacaatcatatggacccagacaaactgaatggc
        F  T  N  S  N  T  P  N  S  Y  N  H  M  D  P  D  K  L  N  G  560
1762   ctctggagccgtatttctcacttagttctgcctgtgcaacctgaaaatgccctgaaaagg
        L  W  S  R  I  S  H  L  V  L  P  V  Q  P  E  N  A  L  K  R  580
1822   ggcatctgctta
        G  I  C  L                                                  584
1882   taagaagtgagagagaagaaaaatcatgtcccaagttctgagaattgttcacactttcta
1942   accagagacagaattcagagctctttttgaaagaactagtttcttttaaagaagttaag
2002   tgcttacataaacatggaacatataaatcattcattcaacct
```

B

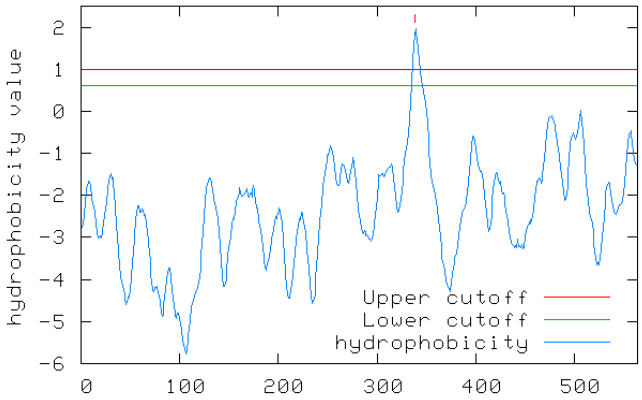

Figure 13. A- Nucleotide and corresponding amino acid sequence of human LAP1B encoded by clone 135. Stop and start codons are coloured blue. The three well conserved PP1 binding motifs (RVxF) are highlighted in red (positions 55-59, 212-215 and 538-541 in aa sequence) and a second generic PP1binding motif (SILK) is coloured green (position 306-309 in aa sequence). The putative transmembrane domain is highlighted in orange (position 339-359 in aa sequence). **B-** Goldman and Engelman Steitz hydrophobicity highlighting the occurrence of a single transmembrane domain.

Furthermore, LAP1B possesses several potential phosphorylation sites for casein kinase 1 (CK1) and casein kinase 2 (CK2), glycogen synthase kinase 3 (GSK3) and polo-like kinase (PLK) (Fig. 14). A nuclear receptor box (NRBOX) motif that confers binding to nuclear receptor was also predicted. Additionally, LAP1B also contains a motif recognized for modification by the small ubiquitin-like modifier-1 (SUMO-1) and a UHM ligand motif (ULM) found in splicing factors SF1 and SAP155 (Fig. 14). These LAP1B putative domains were predicted using ELM (http://elm.eu.org/).

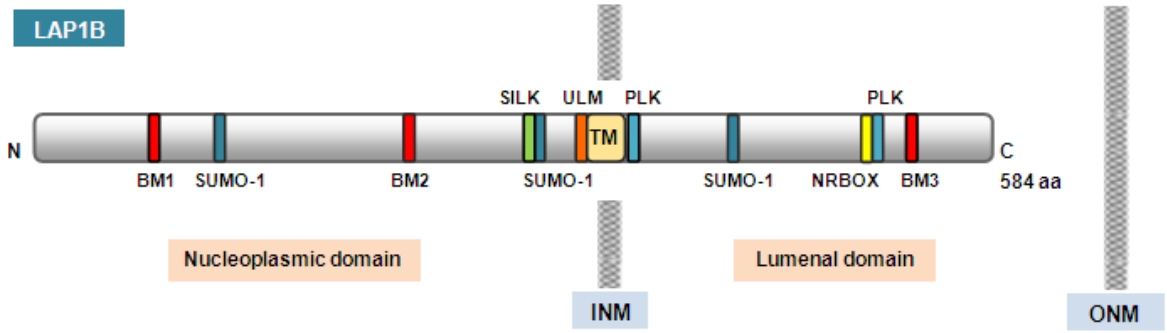

Figure 14. Schematic illustration of LAP1B protein and its putative domains. BM1, PP1 binding motif 1; SUMO-1, motif recognized for modification by small ubiquitin-like modifier-1 (SUMO-1); BM2, PP1 binding motif 2; SILK, a second generic PP1binding motif; ULM, pattern encompassing the ULMs (UHM ligand motifs) in SF1 and SAP155; TM, transmembrane domain; PLK, site phosphorylated by the polo-like-kinase (PLK), NRBOX, nuclear receptor box motif; BM3, PP1 binding motif 3; INM, inner nuclear membrane; ONM, Outer nuclear membrane.

3. Validation of the PP1/LAP1B interaction

3.1.Validation of the PP1/LAP1B interaction by yeast co-transformation

3.1.1. Introduction

The yeast two-hybrid system is a method enabling the detection of the interactions between proteins and is also used to search for unknown partners (the prey) of a given protein (the bait). This method is based on the properties of the yeast GAL4 protein, which possesses two separable domains, one responsible for DNA binding and the other for transcriptional activation. To identify proteins expressed in human brain that interact with different PP1 isoforms, this methodology was used with PP1α, PP1γ1 and PP1γ2 as bait (previous work from our laboratory). The cDNAs encoding those PP1 isoforms were transferred into the GAL4-BD pAS2-1 expression vector (Appendix II), which carries the yeast *TRP1* gene. The brain cDNA library was cloned into the pACT2 vector, which contains the yeast *LEU2* gene (Appendix II), in frame with GAL4-AD. As described previously among the positives identified was LAP1B. In order to confirm the interaction between LAP1B and all PP1 isoforms a yeast co-transformation assay was performed, combining the bait plasmids pAS2-1-PP1α, pAS2-1-PP1γ1, pAS2-1-PP1γ2 or pAS2-1-PP1γ2end (carrying the specific C-terminus of the protein) with the prey plasmid pACT2-LAP1B (clone 135 from the PP1γ1 YTH screen, encoding the full-length LAP1B). Additionally, in order to determine the PP1 binding motif (BM) of LAP1B responsible for the interaction with PP1γ1, several deletion mutants (Fig. 15) were produced and co-transformed with PP1γ1. These constructs were cloned into the pACT2 vector and fused with GAL4-AD. Each construct contained one of the three well conserved PP1 binding motifs (BM1, BM2 or BM3) and one construct included both BM1 and BM2 (Fig. 15). All constructs were fully verified by DNA sequencing.

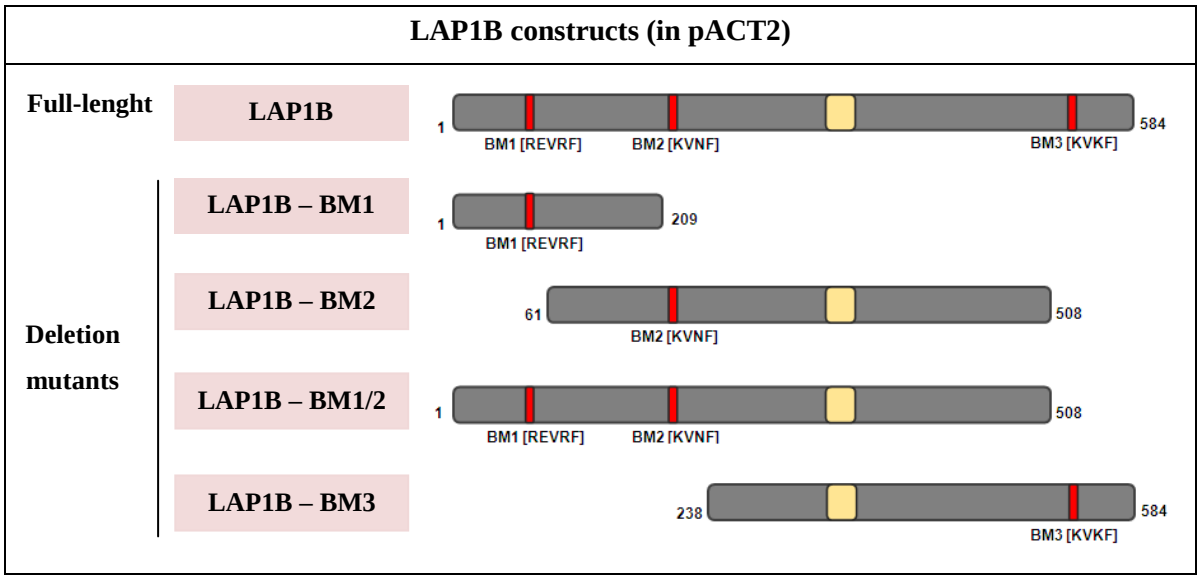

Figure 15. Schematic illustration of the LAP1B and LAP1B deletion mutants used. The red boxes represent the three well conserved putative PP1 binding motifs (BMs) present in the constructs and the yellow boxes represent the transmembrane domain.

In order to validate the PP1/LAP1B interaction and to determine the PP1 binding motif of LAP1B responsible for this interaction, full-length LAP1B or LAP1B deletion mutants and PP1 were co-transformed in the AH109 yeast strain. The reporter genes used were *MEL-1* which encodes α-Galactosidase and *HIS3* and *ADE4*. If the two proteins (the bait and the prey) interact, the reporter genes will be activated and the yeast will grow on synthetic complex medium lacking the amino acids Trp, Leu, His and Ade. The α-Galactosidase activity is detected by the formation of blue yeast colonies on medium with the chromogenic substrate X-α-Gal (5-bromo-4-chloro-3-indolyl alpha-D-galactopyranoside).

3.1.2. Materials and methods

3.1.2.1. Bacterial transformation

Preparation of *E. coli* XL1-Blue competent cells

A single colony of *E. coli* XL1-Blue was incubated in 10 mL of SOB medium (Appendix I) at 37ºC overnight. Then, 1 mL of this culture was used to inoculate 50 mL of SOB and the culture was incubated at 37ºC with shaking at 180 rpm for 1-2 hr, until OD_{550nm}=0.3. The culture was cooled on ice for 15 min and centrifuged at 4000 rpm at 4ºC for 5 min. The supernatant was discarded and the pellet resuspended in 15 mL of Solution I (Appendix I). After standing on ice for 15 min, the cells were centrifuged at 4000 rpm for 5 min at 4ºC and 3 mL of Solution II (Appendix I) were added to resuspend the cell pellet. The cells were immediately divided in 100 µL aliquots and stored at -80ºC.

E. coli XL1-Blue transformation

Competent cells (50 µL) were thawn on ice and 5 ng of DNA were added to the cells and gently swirled. The microtube was incubated on ice for 20 min and heat shocked at 42ºC for 70 sec. The microtubes were then incubated on ice for 2 min before adding 450 µL of SOC medium (Appendix I). The tubes were subsequently incubated at 37ºC for 60 min with shaking at 190 rpm. The culture was centrifuged at 14000 rpm during 1 min and the supernatant was discarded. The cells were then resuspended in the remaining supernatant and spread on the appropriate agar medium. The plates were incubated at 37ºC for 16 hr until colonies appeared. Control transformations were also performed in parallel. These included a negative control transformation without DNA and a positive control transformation with 1 ng of a control plasmid, such as pAS2-1.

3.1.2.2. Isolation and purification of plasmid DNA

A single bacterial colony was transferred into 50 mL of LB medium (Appendix I) containing ampicillin (100 µg/mL) and incubated overnight at 37ºC with shaking (190

rpm). The bacterial culture was poured into a 50 mL tube and centrifuged at 4000 g for 10 min. The supernatant was discarded and the pellet was ressuspended in 3 mL of Cell Resuspension Solution (Appendix I). Next, 3 mL of Cell Lysis Solution (Appendix I) was added to the cells, mixed by gently inverting the tube 5 times and left to incubate for 3 min. Then, 5 mL of Neutralization Solution (Appendix I) were added and immediately mixed by gentle tube inversion; the lysate was allowed to sit for 3 min. After this initial procedure DNA Purification by Centrifugation (Promega) was carried out according to the manufactures protocol. A blue PureYield^{TM}Clearing Column (Promega) was placed in a 50 mL plastic tube, the lysate was transferred to the column and allowed to incubate for 2 min. The column assembly to the tube was then centrifuged at 1500 g for 5 min. A white PureYield^{TM} Binding Column (Promega) was assembled in a new 50 mL tube and the filtered lysate was transferred to this column and centrifuged at 1500 g for 3 min. The column was washed by adding 5 mL of Endotoxin Removal Wash solution (Appendix I) and centrifugating at 1500 g for 3 min. After that, 20 mL of Column Wash solution (Appendix I) were added and the column centrifuged at 1500 g for 5 min. The flowthrough was discarded and an additional 10 min, 1500 g centrifugation was performed. Afterwards, the column was placed in a new 50 mL disposable plastic tube and 600 μL of Nuclease-Free Water were added to the column. After 1 min standing, the DNA was eluted by centrifugation at 1500 g for 5 min.

3.1.2.3. Ethanol precipitation

Approximately 1/10 volume of sodium acetate (3M) and 2.5 volumes of 100% ethanol were added to the DNA samples. The samples were vortexed and incubated for 20 min at -20°C. Then the samples were centrifuged for 20 min at 14000 rpm and 4°C. The supernatants were discarded and the pellets rinsed with 250 μL of 70% ethanol, and then the samples were incubated for 5 minutes at -20°C before new centrifugation for 5 minutes at 14000 rpm and 4°C. After discarding the supernatant, the pellet was dried in a Speedvac. The pellet was resuspended in 50 μL of water and the DNA concentration and 260/280 nm purity ratio was calculated by absorbance measurements.

3.1.2.4. Restriction fragment analysis of DNA

Plasmid DNAs were analysed by digestion with two convenient restriction endonucleases, namely *EcoRI* and *XhoI* (New England Biolabs). For plasmid DNA digestion the manufacturer's instructions were followed. In a microtube the following components were added: 500 ng DNA; 1x reaction buffer (Neb 2); 0.1 µg/µl BSA and 1 U/µg DNA of restriction enzyme. The volume was made up to 20 µl with distilled H_20 and the mixture was incubated at the appropriate temperature (37ºC) for 4 hr before further analysis.

3.1.2.5. Electrophoretic analysis of DNA

The electrophoresis apparatus was prepared and the electrophoresis tank was filled with enough 1x TAE (Appendix I) to cover the agarose gel. The appropriate amount of agarose was transferred to an Erlenmeyer with 100 mL 1x TAE. The slurry was heated until the agarose was dissolved and allowed to cool to 60ºC before adding ethidium bromide to a final concentration of 0.5 µg/mL. The agarose solution was poured into the mold and the comb was positioned. After the gel became solid the comb was carefully removed and the gel mounted in the tank. The DNA samples were mixed with the 6x loading buffer (LB) and the mixture was loaded into the wells of the submerged gel using a micropipette. Marker DNA (1 Kb ladder) of known size was also loaded onto the gel. The lid of the gel tank was closed and the electrical cables were attached so that the DNA migrated towards the anode. The gel was run until the bromophenol blue had migrated the appropriate distance through the gel. At the end, the gel was examined under UV light and photographed or otherwise analysed on a Molecular Imager (Biorad).

3.1.2.6. DNA sequencing

All the DNA samples to be sequenced were purified using the Promega Pure Yield^{TM} Plasmid Midiprep System, as described above in section 3.1.2.2. Sequencing reactions were performed as follows:

Sequencing PCR reaction

The following components were mixed in a 0.2 mL microtube:

500 ng dsDNA

4 µL Ready Reaction Mix*

10 pmol primer

H_2O to a final volume of 20 µL

* Ready Reaction Mix is composed of dye terminators, deoxynucleoside triphosphates, AmpliTaq DNA polymerase, FS, rTth pyrophosphatase, magnesium chloride and buffer (Applied Biosystems).

This reaction mixture was vortexed and span down for a few seconds. The PCR was then performed using the following conditions:

96ºC 1 min

96ºC 30 sec
42ºC 15 sec | 25 cycles
60ºC 4 min

The samples were purified after PCR by ethanol precipitation, as described above. Finally the DNA was sent to the sequencing facility for analysis using an automated DNA sequencer (ABIPRISM 310, Applied Biosystems).

3.1.2.7. Verifying protein interactions by yeast co-transformation

In order to verify protein interactions, a small-scale LiAc yeast co-transformation procedure was performed, combining one of the bait plasmids (pAS2-1-PP1α, pAS2-1-PP1γ1, pAS2-1-PP1γ2 or pAS2-1-PP1γ2end) with one of the specific target proteins [full-length LAP1B or its deletions mutants (BM1, BM2, BM1/2 and BM3)]. In parallel, co-transformation of the vectors pAS2-1 and pACT2 and transformation with LAP1B were performed as a negative control. The association of murine p53 (encoded by plasmid pVA3) and SV40 large T antigen (plasmid pTD1) was used as a positive control.

Preparation of competent yeast cells

One yeast colony was inoculated into 1 mL of YPD medium (Appendix I) in a 1.5 mL microtube and vortexed vigorously to disperse cell clumps. The culture was transferred into a 250 mL flask containing 50 mL of YPD and incubated at 30ºC with shaking at 230 rpm overnight, until it reached stationary phase with OD_{600nm} > 1.5. Enough of this culture (30 mL) was transferred into 300 mL YPD in a 2 L flask to yield an OD_{600nm}= 0.2-0.3. The culture was incubated at 30ºC with shaking at 230 rpm, until OD_{600nm} = 0.4-0.6, and then centrifuged at 2200 rpm for 5 min, and the supernatant was discarded and the cells resuspended in 25 mL H_2O. The cells were recentrifuged and the pellet was resuspended in 1.5 mL of freshly prepared, sterile 1x TE/LiAc (Appendix I).

Yeast transformation by the lithium acetate (LiAc)-mediated method

In a microtube 0.1 µg of plasmid DNA were added to 0.1 mg of salmon testis carrier DNA. Then, 100 µL of freshly prepared competent cells were added to the microtube, followed by 600 µL of sterile PEG/LiAc (40% PEG 4000/ 1X TE/ 1X LiAc). The mixture was incubated at 30ºC for 30 min with shaking (200 rpm). After adding 70 µL of DMSO the solution was mixed gently and then heat-shocked for 15 min in a 42ºC water bath. The cells were chilled on ice for 1-2 min and pelleted by centrifugation for 5 sec at 14000 rpm and resuspended in 0.5 mL of 1x TE buffer. The cells (100 µL) were then plated in SD/-Trp-Leu plates and in SD/-Leu plate for LAP1B (negative control) and incubated at 30ºC for 2-4 days, until colonies appeared. To confirm protein-protein interactions a colony was picked and transferred to a SD/TDO (-Trp-Leu-His) plate and a SD/QDO (-Trp-Leu-His-Ade) plate, and latter to a SD/TDO/X-α-Gal plate and a SD/QDO/X-α-Gal plate.

3.1.3. Results

3.1.3.1. Electrophoretic analysis of the constructs

All constructs (full-length LAP1B and LAP1B deletion mutants) used for yeast co-transformation analysis, were first verified by restriction analysis to confirm the correct insertion into the pACT2 vector. The constructs were transformed into *E. coli* XL1-Blue and the DNA isolated was analysed by restriction digestion with the endonucleases *EcoRI* and *XhoI*. The restriction fragments were then separated by 1.3% agarose gel electrophoresis to confirm the correct size of the insert (Fig. 16).

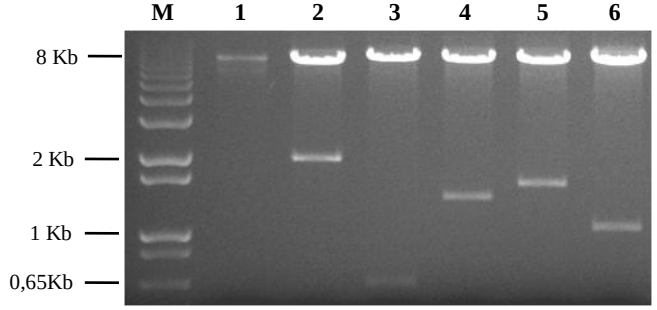

Figure 16. Restriction analysis of LAP1B constructs. Lane M, 1 Kb Plus DNA ladder marker; Lane 1, pACT2 vector (8.1 Kb); Lane 2, pACT2 + full-length LAP1B insert (8.1 + 2.0 Kb); Lane 3, pACT2 + BM1 insert (8.1 + 0.6 Kb); Lane 4, pACT2 + BM2 insert (8.1 + 1.3 Kb); Lane 5, pACT2 + BM1/2 insert (8.1 + 1.5 Kb); Lane 6, pACT2 + BM3 insert (8.1 + 1.0 Kb).

3.1.3.2. DNA sequence analysis

All LAP1B constructs were further analysed by DNA sequencing to confirm the absence of mutations and to validate the correct insertion into the pACT2 vector and reading frame of the fusion proteins. All constructs were sequenced with the appropriate primers (Appendix III). Figure 17 shows an example of a sequencing result obtained using the Chromas program.

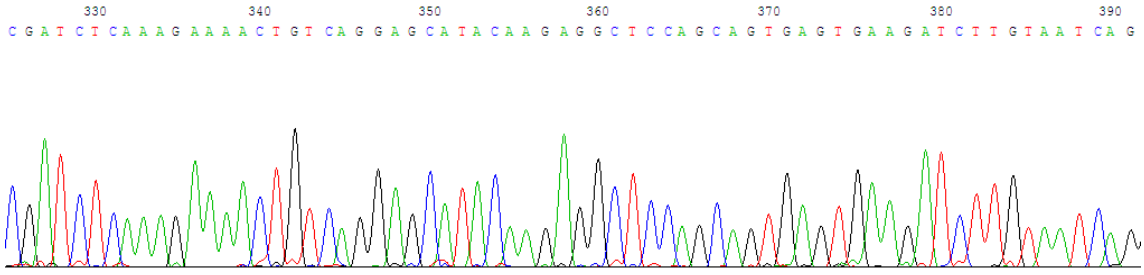

Figure 17. Partial nucleotide sequence obtained for full-length LAP1B, visualized using the Chromas program.

The nucleotide sequence of each construct was converted to FASTA format and then copied to the BLAST window (www.ncbi.nlm.nih.gov/BLAST/) to be compared with the GenBank Database of human nucleotide sequences. The sequence alignment with the LAP1B sequence present in the GenBank Database was obtained and one example is presented in Figure 18.

```
>ref|NM_015602.2| GM Homo sapiens torsin A interacting protein 1 (TOR1AIP1), mRNA
Length=3824

 GENE ID: 26092 TOR1AIP1 | torsin A interacting protein 1 [Homo sapiens]
(10 or fewer PubMed links)


 Score =  780 bits (422),  Expect = 0.0
 Identities = 450/473 (95%), Gaps = 2/473 (0%)
 Strand=Plus/Plus

Query  1    AGAAGCCATCGCCACCACCGGCAGGAGAACCTAGGGTCCATAAAGCCATCTTCGCGATCG  60
            ||||||||||||||||||||||||||||||||||||||||||||||||||||||||||||
Sbjct  138  AGAAGCCATCGCCACCACCGGCAGGAGAACCTAGGGTCCATAAAGCCATCTTCGCGATCG  197

Query  61   ACTAAAGCTACGTCAACAACTATGGCGGGCGACGGGCGGCGGGCAGAGGCGGTGCGGGAA  120
            ||||||||||||||||||||||||||||||||||||||||||||||||||||||||||||
Sbjct  198  ACTAAAGCTACGTCAACAACTATGGCGGGCGACGGGCGGCGGGCAGAGGCGGTGCGGGAA  257

Query  121  GGATGGGGTGTGTACGTCACCCCCAGGGCCCCCATCCGAGAGGGAAGGGGCCGGCTCGCC  180
            ||||||||||||||||||||||||||||||||||||||||||||||||||||||||||||
Sbjct  258  GGATGGGGTGTGTACGTCACCCCCAGGGCCCCCATCCGAGAGGGAAGGGGCCGGCTCGCC  317

Query  181  CCTCAAAATGGCGGCAGCAGCGATGCGCCTGCGTACNNAANTCCTCCGTCGCGCCAGGGC  240
            ||||||||||||||||||||||||||||||||||||  || ||||||||||||||||||||
Sbjct  318  CCTCAAAATGGCGGCAGCAGCGATGCGCCTGCGTACAGAACTCCTCCGTCGCGCCAGGGC  377

Query  241  CGGCGGGAAGTGAGGTTCTCGGACGAGCCGCCAGAAGTGTACGGCGACTTCGAGCCCCTG  300
            ||||||||||||||||||||||||||||||||||||||||||||||||||||||||||||
Sbjct  378  CGGCGGGAAGTGAGGTTCTCGGACGAGCCGCCAGAAGTGTACGGCGACTTCGAGCCCCTG  437

Query  301  GTGGCCAAAGAAAGGTCCCCGGTGGGAAAACGAACCCGGCTAGAANAGTTCCGGTCCGAT  360
            ||||||||||||||||||||||||||||||||||||||||||||| ||||||||||||||
Sbjct  438  GTGGCCAAAGAAAGGTCCCCGGTGGGAAAACGAACCCGGCTAGAAGAGTTCCGGTCCGAT  497

Query  361  TCTGCGAAAGANGAAGTGANANAAAGCGCGTACTACCTTCGGTCTANGCAGCGNAGGCAN  420
            |||||||||||| ||||||| | |||||||||||||||||||||||| |||||| |||||
Sbjct  498  TCTGCGAAAGAGGAAGTGAGAGAAAGCGCGTACTACCTTCGGTCTAGGCAGCGGAGGCAG  557
```

Figure 18. Blast results for alignment of LAP1B construct sequence obtained with the LAP1B sequence present in the GenBank database. Ambiguities present in the query sequence were further validated by visual verification of the sequencing results.

3.1.3.3. Validation of the PP1/LAP1B interaction by yeast co-transformation

In order to confirm the interaction between LAP1B with various PP1 isoforms, a yeast co-transformation assay was performed. Interaction of LAP1B with the specific C-terminus of PP1γ2, named PP1γ2end, was also tested. The mapping of the LAP1B domain responsible for the interaction with PP1γ1 was performed using LAP1B deletion mutants. Constructs corresponding to full-length LAP1B and LAP1B deletions (the prey in the pACT2 vector) and the various PP1 isoforms (the bait in the pAS2-1 vector) were co-transformed in yeast strain AH109 and tested in SD/TDO, SD/QDO, SD/TDO/X-α-gal and SD/QDO/X-α-gal medium. If interaction occurs the colonies will grow and in the X-α-gal plates they will appear blue. The results obtained showed that LAP1B interacts with the three PP1 isoforms tested (PP1α, PP1γ1 and PP1γ2) but does not interact with the C-terminus of PP1γ2 (PP1γ2 end) (Fig 19A). Moreover, the assay was positive for PP1γ1/LAP1B interaction through BM1 (Fig. 19B), but was negative for interaction through BM2 and BM3 (Fig. 19B). The construct with both BM1 and BM2 (BM1/2) also yielded a positive result with PP1γ1 (Fig. 19B).

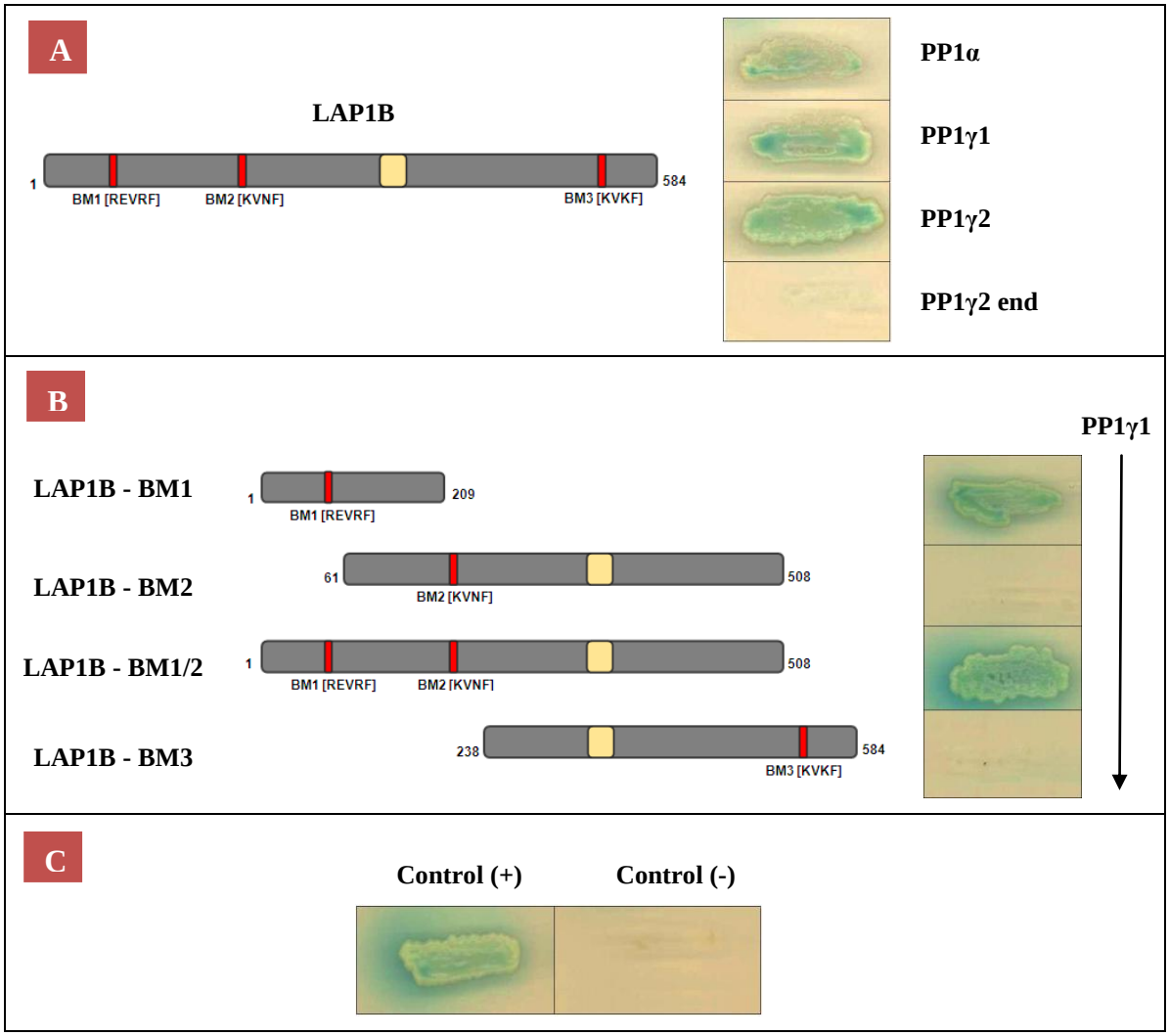

Figura 19. Yeast co-transformation assay in SD/QDO/X-α-gal medium. **A-** Positive interactions were observed between LAP1B and PP1α, PP1γ1 and PP1γ2. **B-** PP1γ1 interacted with LAP1B-BM1 and BM1/2 but not with LAP1B-BM2 and BM3. **C-** Positive (+) and negative (-) controls were also included as described in the methods. In the schematic representations, the red boxes represent the BMs present in the constructs and the yellow boxes represent the transmembrane domains of LAP1B.

3.1.4. Discussion

From the yeast-two hybrid screens of a human brain cDNA library using various PP1 isoforms as bait, a novel PP1 interactor was identified: LAP1B or TOR1AIP1. Confirmation of the interaction in yeast was performed by co-transformation of strain AH109 and assaying for X-α-Gal activity resulting from expression of the *MEL-1* reporter gene. Interaction of LAP1B with PP1 α, γ1 and γ2 isoforms was tested and the results were positive for all isoforms. However, LAP1B does not interact with the specific C-terminus of PP1γ2, demonstrating that this region is not responsible for the interaction. LAP1B has three putative PP1 binding motifs: BM1 and BM2 located in the nucleoplasm, and BM3 in the lumenal space. Using LAP1B deletion mutants, the mapping of the LAP1B domain responsible for the interaction with PP1γ1 was performed. Our results indicated that LAP1B interacts with PP1γ1 through BM1. A positive result was also obtained with LAP1B-BM1/2 construct. However, negative results were observed for LAP1B-BM2 and LAP1B-BM3. These results thus indicate that it is the BM1 of LAP1B which mediates the primary interaction between PP1 and LAP1B. Since BM1 is located in the nucleoplasmic domain of LAP1B, these results are consistent with the high abundance of PP1 in the nucleus.

3.2. Validation of the PP1/LAP1B interaction using an *in vitro* blot overlay assay

3.2.1. Introduction

The pET system is arguably the most powerful system developed for cloning and expression of recombinant proteins in *Escherichia coli*. Target genes are cloned in pET plasmids under the control of bacteriophage T7 transcription and (optionally) translational signals and expression is induced by providing a source of T7 RNA polymerase. Addition of isopropyl-β-D-thiogalactopyranoside (IPTG) to a growing culture induces T7 RNA polymerase production, which will transcribe the target DNA of the plasmid. Various constructs expressing either full-lenght LAP1B or different fragments comprising the nucleoplasmic or lumenal domains of LAP1B (with or without the transmembrane domain) were generated in pET-28c (Fig. 20).

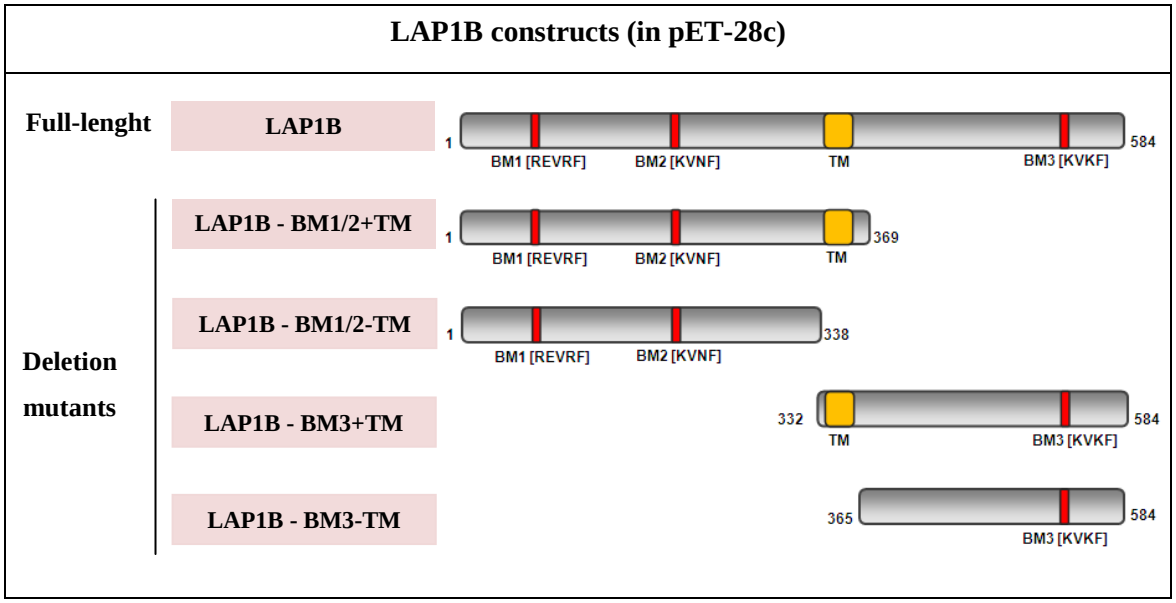

Figure 20. Schematic representation of full-length LAP1B and LAP1B deletion mutants expressed in *E. coli*. The red boxes represent the PP1 binding motifs (BMs) present in the constructs. TM, transmembrane domain, +TM, with transmembrane domain; -TM, without transmembrane domain.

pET-28 is a translation vector with an N-terminal 6xHis-tag and possesses the Kanamycin resistance gene (Appendix II). The His-tag allows easy detection of the fusion

protein by Western blotting and is very useful for protein purification, especially for those proteins initially expressed as inclusion bodies. The *E. coli* Rosetta strains used in this study are designed to enhance expression of eukaryotic proteins that contain codons rarely used in *E. coli* and that would otherwise hamper translation.

A time course, after IPTG induction, was performed in order to determine the optimal time of expression of recombinant full-length LAP1B and LAP1B deletion mutants. The soluble and insoluble fractions were recovered and tested. To confirm the interaction of LAP1B with PP1γ1 and to determine the LAP1B domain responsible for the interaction with PP1γ1, an *in vitro* blot overlay assay was performed using purified PP1γ1 protein (readily available in our laboratory).

3.2.2. Materials and methods

Isolation and purification of recombinant plasmids was performed using the Promega Pure Yield Plasmid Midiprep System. The plasmid DNA was further analysed by digestion with the restriction enzymes *EcoRI* and *XhoI*. The restriction fragments were then separated by agarose gel electrophoresis and the plasmid DNA was sequenced to confirm the nucleotide sequence, as previously described in sections 3.1.2.1 - 3.1.2.6.

3.2.2.1. Expression of recombinant proteins in *E. coli*

Transformation of the Rosetta (DE3) *E. coli* strain with recombinant plasmid DNA was performed as described for *E. coli* XL1 Blue cells. A single bacterial colony was transferred into 5 mL of LB medium containing Kanamycin (30 μg/mL) and incubated overnight at 37ºC with shaking (190 rpm). After incubation 500 μL of the overnight culture was added to 50 ml of LB with Kanamycin, until the OD_{600} was around 0.5-0.6. Then 10 ml of the culture were transferred into a new tube (non-induced, control). Induction was started by adding 1 mM IPTG to the remaining culture. The samples were placed back in the incubator (37˚C, 190 rpm) and 10 mL of the culture were harvested after 1, 3 and 5 hr, and all samples including the control at 5 hr were centrifuged at 4000 rpm for 10 min. The pellets were stored at -20°C. The cells were thawed and resuspended in 500 μL of 1x PBS and transferred to microtubes. Then the cells were lysed by sonication, with pulses of 10 sec, 3 times. After sonication the cells were centrifuged for 30 min at 13200 rpm at 4˚C. The supernatant was transferred to a new microtube (soluble fraction). The pellet was resuspended in 500 μL of 1x PBS and centrifuged for 10 min at 13200 rpm at 4°C. The supernatant was discarded and the pellets resuspended in 500 μL of boiling 1% SDS (insoluble fraction). The samples were loaded onto two identical gels, one was stained with Coomassie blue and the other was used for immunoblotting analysis. The negative controls used include the pET-28c vector without an insert or with an insert but non-induced. As a positive control the pET28c-Nek2A was used, given that Nek2A is a well known protein that strongly interacts with PP1.

3.2.2.2. BCA protein assay

Measurements of total protein concentration were carried out using Pierce's BCA protein assay kit, following the manufacturer's instructions. This method combines the reduction of Cu^{2+} to Cu^{+} by proteins in an alkaline medium (the biuret reaction), with a sensitive colorimetric detection of the Cu^{+} cation using a reagent containing bicinchoninic acid (BCA). The purple-coloured reaction product of this assay is formed by the chelation of two molecules of BCA with one Cu^{+} ion. This water-soluble complex exhibits a strong absorbance at 562 nm that is linear with increasing protein concentration over a working range of 20 μg/mL to 2000 μg/mL. At least duplicates of all samples were assayed by this method, as well as the appropriate protein standards as described below (Table 2).

Table 2. Standard curve used in the BCA protein assay.

Standard	BSA (μL)	10% SDS (μL)	H_20 (μL)	Protein mass (μg)	W.R. (mL)
P_0	0	5	45	0	1
P_1	1	5	44	2	1
P_2	2	5	43	4	1
P_3	5	5	40	10	1
P_4	10	5	35	20	1
P_5	20	5	25	40	1
P_6	40	5	5	80	1

W.R. - Working reagent.

The Working Reagent was prepared by mixing BCA reagent A with BCA reagent B in the proportion of 50:1. Then, 1 mL of WR was added to each microtube (standards and samples) and the microtubes were incubated at 37ºC for 30 min. Once the tubes cooled to room temperature the absorbance was measured at 562 nm. A standard curve was obtained by plotting BSA standard absorbance *vs* BSA concentration, and it was then used to determine the total protein concentration of each sample.

3.2.2.3. SDS-PAGE

Samples were subjected to SDS polyacrylamide gel electrophoresis (SDS-PAGE). In SDS-PAGE the migration of the proteins is determined by their molecular weight. For the time course analysis and to visualize the full-length LAP1B protein, with a molecular weight around 65 kDa, a 7.5% polyacrylamide gel was used (Table 3). To visualize LAP1B deletion mutants BM1/2+TM and BM1/2-TM, with a calculated molecular weight of 41 and 38 kDa, respectively, a 10% polyacrylamide gel was used and for BM3+TM and BM3-TM, with 28 and 24 kDa, respectively, a 12% polyacrylamide gel was used (Table 3). For the blot overlay analysis a 10% polyacrylamide gel was used.

Table 3. Composition of the running and stacking gels for SDS-PAGE.

Components	Running gel (7.5%)	Running gel (10%)	Running gel (12%)	Stacking gel (3.5%)
Water	4.9 mL	4.2 mL	3.45 mL	3.3 mL
30%Acryl/8%Bisacryl.	2.5 mL	3.3 mL	4 mL	0.6 mL
4x LGB	2.5 mL	2.5 mL	2.5 mL	---
5x UGB	---	---	---	1.0 mL
SDS 10%	---	---	---	50 µL
10% APS	50 µL	50 µL	50 µL	50 µL
TEMED	5 µL	5 µL	5 µL	5 µL

APS, Ammonium Persulfate; LGB, Lower Gel Buffer; SDS, Sodium Dodecyl Sulphate; UGB, Uper gel Buffer.

The running and the stacking gels were prepared as indicated in Table 3. The samples were prepared by the addition of ¼ volume of loading gel (LB) buffer and run at 100 V for approximately 2 hours.

3.2.2.4. Coomassie blue staining

After running, gels were transferred into Coomassie blue staining solution and left for 30 min. After staining, gels were washed with water and destained using destain buffer

for 1 hr. After the first hour of destaining, fresh destaining buffer was added and the gel was destained overnight.

3.2.2.5. Immunoblotting

In our experimental system, after electrophoresis, proteins were transferred to nitrocellulose membranes for 2 hours at 200 mA and then visualised with specific antibodies.

Immunodetection by enhanced chemiluminescence (ECL)

ECL™ is a light emitting non-radioactive method for the detection of immobilized antigens, conjugated directly or indirectly with horseradish peroxidase-labelled antibodies. In order to visualize the proteins the blots were probed with an anti-His primary antibody, which recognizes the His-tag of the fusion protein. Briefly, the membranes were soaked in 1x TBS (5 min). Non-specific binding sites were blocked by incubating the membrane in 5% low fat milk in 1x TBST (3 hr). The membrane was further incubated with the primary antibody (1:1000 dilution) diluted in 3% low fat milk in 1x TBST (2 hr with shaking). After three washes of 10 min each in 1x TBST the membrane was incubated with an anti-mouse horseradish peroxidase conjugated secondary antibody (1:5000 dilution) in 3% low fat milk in 1x TBST (2 hr with shaking). The membrane was then washed 3 times with 1x TBST for 10 min. Subsequently, the membrane was incubated for 1 min with the ECL detection solution (a mixture of equal volumes of solution 1 and solution 2 from the ECL kit (Amersham)). After exposure to X-ray film (Kodak), immunoblots were scanned and quantited using Quantity One densitometry software (Bio-Rad).

3.2.2.6. Blot overlay assay

The nitrocellulose membranes were soaked in 1x TBS for 5 min. Non-specific binding sites were blocked by immersing the membrane in 3% BSA in 1x TBST for 3 hr. Then membranes were overlaid with purified PP1γ1 protein (1 μg/mL, purified in our laboratory) in 3% BSA in 1x TBST for 2 hr. After washing three times with 1x TBST, to

remove excess protein, the bound PP1γ1 was detected by incubating the membrane with polyclonal anti-PP1γ antibody (CBC3C; 1:5000 dilution in 1x TBST/3% non-fat milk) for 2 hr. After three washes of 10 min each in 1x TBST the membrane was incubated with a solution of an anti-rabbit secondary antibody (1:5000 dilution) in 3% low fat milk in 1x TBST for 2 hr with shaking. The membrane was then washed 3 times with 1x TBST for 10 min and further developed using the ECL kit.

3.2.3. Results

3.2.3.1. Restriction analysis

All constructs (full-length LAP1B and LAP1B deletion mutants) were first analysed by restriction digestion with the endonucleases *EcoRI* and *XhoI,* to confirm the correct insertion into the pET-28c vector (Appendix II). The restriction fragments were separated by 1.4% agarose gel electrophoresis and their size was confirmed (Fig. 21).

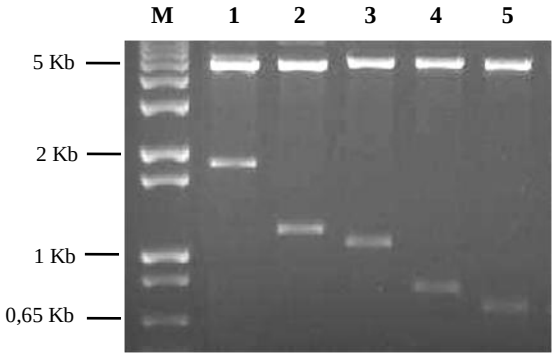

Figure 21. Restriction analysis of LAP1B recombinant plasmids. Lane M, 1 Kb Plus DNA ladder marker; Lane 1, pET-28c + full-length LAP1B insert (5.4 + 1.75 Kb); Lane 2, pET-28c + BM1/2+TM (5.4 + 1.11 Kb); Lane 3, pET-28c + BM1/2-TM (5.4 + 1.02 Kb); Lane 4, pET-28c + BM3+TM (5.4 + 0.76 Kb); Lane 5, pET-28c + BM3-TM (5.4 + 0.66 Kb).

The size of the fragments observed was in agreement with the expected size.

3.2.3.2. DNA sequencing analysis

All constructs (full-length LAP1B and deletion mutants) cloned into the pET-28c vector were sequenced with the appropriate primers (Appendix III) as previously described (section 3.1.3.2). The sequence was verified and the insert orientation and the correct reading frame were confirmed.

3.2.3.3. Expression of recombinant LAP1B protein in bacteria

The cDNAs encoding full-length LAP1B protein and its deletion mutants (BM1/2+TM, BM1/2-TM, BM3+TM, BM3-TM) were inserted into pET-28c vector (Appendix II) and transformed in Rosetta (DE3) *E. coli* strain. The pET-28c vector inserts an N-terminal 6xHis-tag into the recombinant proteins which allows the detection of the fusion proteins using an anti-His antibody. Expression of the recombinant proteins was induced by adding 1 mM IPTG to the growing cultures at 37°C. The optimal time course of expression was determined for recombinant LAP1B protein and its deletions mutants by taking aliquots at 1, 3, and 5 hours after induction and then analysing the soluble and insoluble fractions. Non-induced samples were used as negative controls. The samples were analysed by SDS-PAGE, and one gel was stained with Coomassie blue (data not shown) and another gel analysed by immunoblotting using the anti-His antibody.

Recombinant full-length LAP1B protein was mainly found in the insoluble fraction (Fig. 22). The observed higher molecular mass protein (approximately 75 kDa) represents the full-length fusion protein that seems to achieve maximal expression levels 1 hr after induction. However, a smaller band, of approximately 50 kDa (Fig. 22), was also detected and may result from proteolytic cleavage of the higher molecular mass protein. Smaller proteolytic fragments were also detected in the soluble fraction.

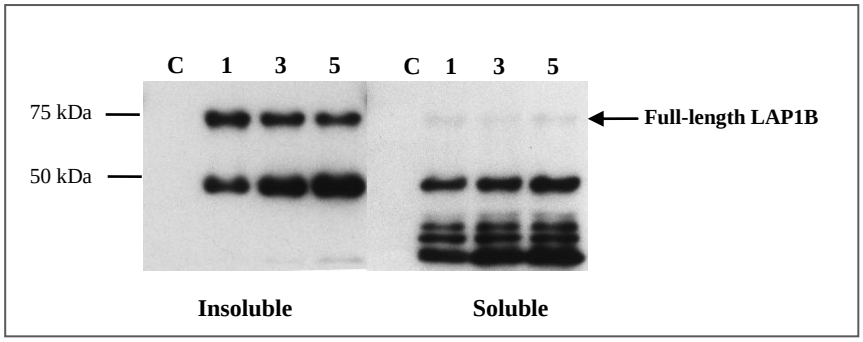

Figure 22. Immunoblot analysis of full-length LAP1B fused with 6xHis-tag in bacterial extracts using an anti-His antibody. Bacterial cultures were collected 1, 3 and 5 hours (indicated on top) after IPTG (1mM) induction at 37°C. Insoluble and soluble fractions were collected. C, non-induced control.

Recombinant BM1/2+TM and BM1/2-TM proteins were found both in the insoluble and soluble fractions (Fig. 23A and B). However, the recombinant protein levels were higher in the insoluble fraction. The BM1/2+TM protein exhibited maximal expression levels at 3 hr after IPTG induction (Fig. 23A), while for BM1/2-TM maximal expression was seen 5 hr after induction (Fig. 23B). Lower molecular weight bands that propably represent proteolytic fragments were also detected. Recombinant BM3+TM protein was detected almost exclusively in the insoluble fraction and maximal expression occurs 1 hr after induction (Fig. 23C). Recombinant BM3-TM protein was mainly found in the insoluble fraction and highest expression levels were observed 5 hr after induction (Fig. 23D). Nonetheless, at 3 and 5 hr after induction BM3-TM was also detected in the soluble form (Fig. 23D).

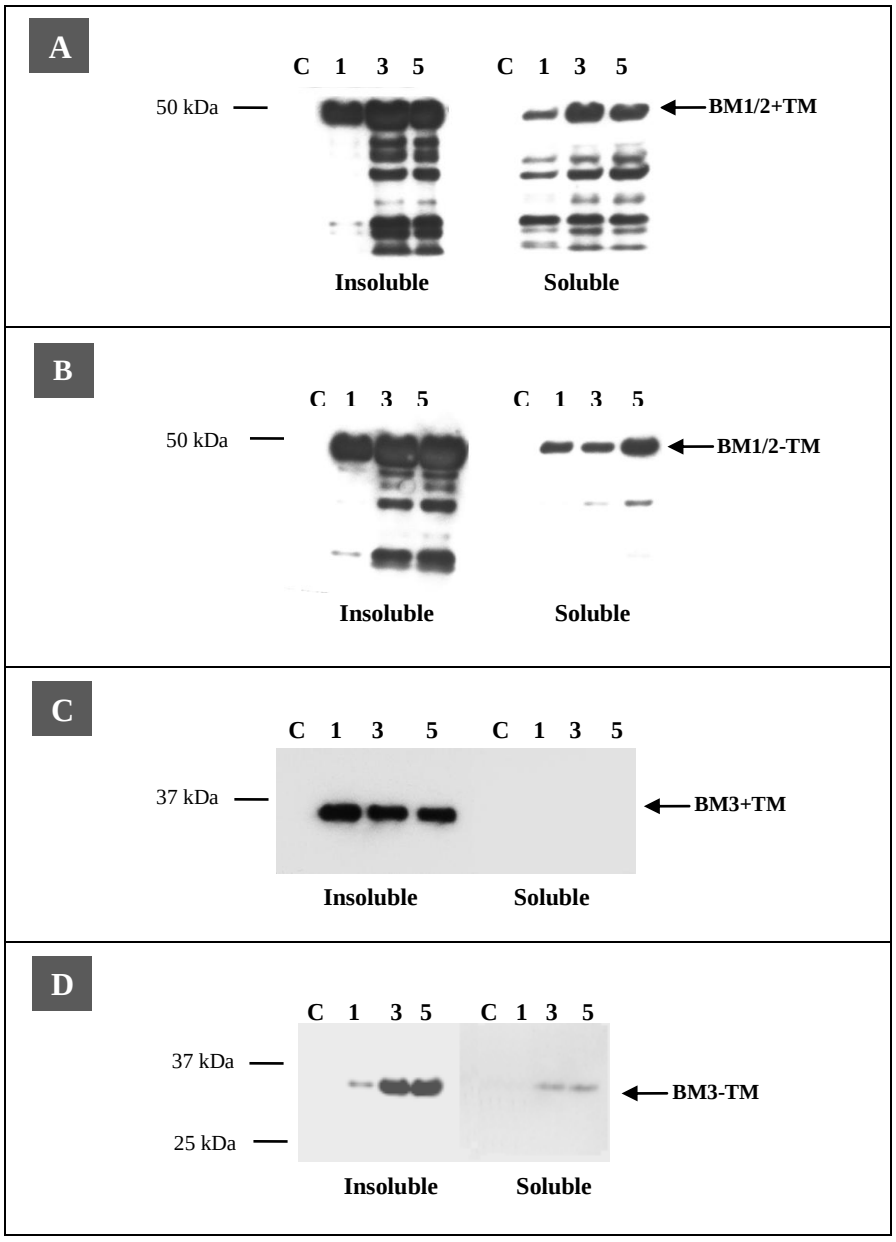

Figure 23. Immunoblot analysis of LAP1B deletion mutants fused with 6xHis-tag in bacterial extracts using an anti-His antibody. Immunoblot detection of BM1/2+TM expression (A); BM1/2-TM expression (B); BM3+TM expression (C); and BM3-TM expression (D). Bacterial cultures were collected 1, 3 and 5 hours (indicated on top) after IPTG (1 mM) induction at 37°C. Insoluble and soluble fractions were collected. C, non-induced control.

3.2.3.4. Blot overlay assay

In order to confirm the interaction of LAP1B with PP1γ1, a blot overlay assay was used. For this purpose, bacterial extracts from pET-28c-LAP1B transformed Rosetta cells were loaded on a 10% SDS-PAGE gel and transferred to a nitrocellulose membrane. As negative controls the bacterial extracts of pET-28c and non-induced pET-28c-LAP1B were used. As positive control, purified Nek2A protein was used. The membrane was first incubated with PP1γ1 protein (purified in our laboratory) and then incubated with the anti-PP1γ antibody, and finally developed by ECL. Immunoblot of increasing amounts of LAP1B protein were also detected using an anti-His antibody (Fig. 24A) in parallel with the overlay assay (Fig. 24B). For these assays the insoluble fraction of bacterial extract collected 3 hr after induction was used. Since most of the recombinant proteins were found in the insoluble fraction, at this time point a reasonable level of expression was observed. As expected, increasing amounts of recombinant LAP1B were detected concomitant with increasing binding of PP1γ1 (Figure 24B), demonstrating its interaction with LAP1B.

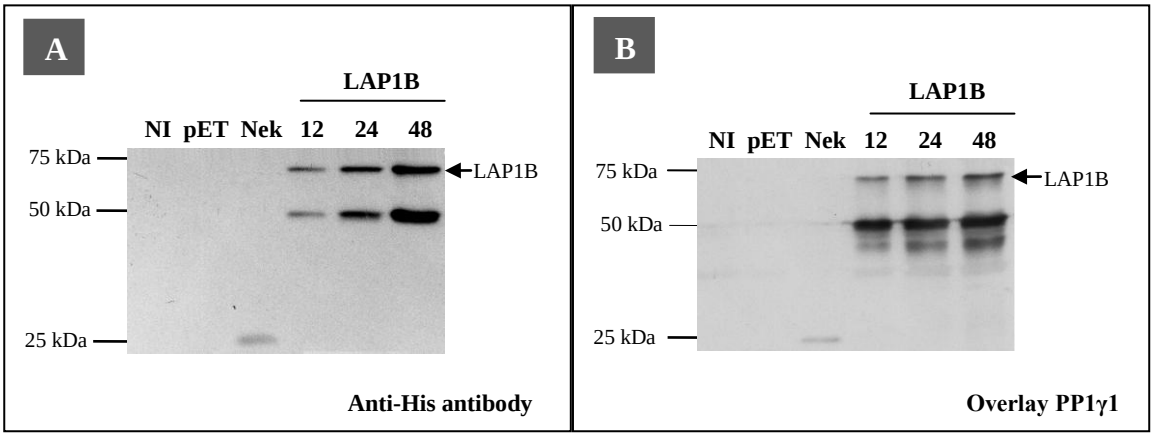

Figure 24. A- Immunoblot analysis of expressed LAP1B using an anti-His antibody. **B-** Blot overlay of LAP1B with PP1γ1 protein. The amount of LAP1B bacterial extract (μL) loaded on each well is indicated. NI, non-induced control; pET, pET-28c vector without an insert (negative control); Nek, Nek2A (positive control). The insoluble fraction of expressed recombinant LAP1B was collected 3 hours after IPTG (1 mM) induction at 37°C.

In order to evaluate which domain in LAP1B is responsible for the interaction with PP1γ1, a blot overlay assay of LAP1B deletion mutants with PP1γ1 was performed. Immunoblot analysis of the same LAP1B deletion mutants using an anti-His antibody was also performed (Fig. 25A). For these assays equal amounts of protein from the insoluble fraction of bacterial extracts collected 3 hr after induction were separated by SDS-PAGE. The results showed that PP1γ1 binds to full-length LAP1B (Fig. 25B) and to BM1/2 with or without the presence of the transmembrane domain (Fig. 25B). However, PP1γ1 does not interact with the BM3+TM or BM3-TM (Fig. 25B). These results are in agreement with the co-transformation results previously described.

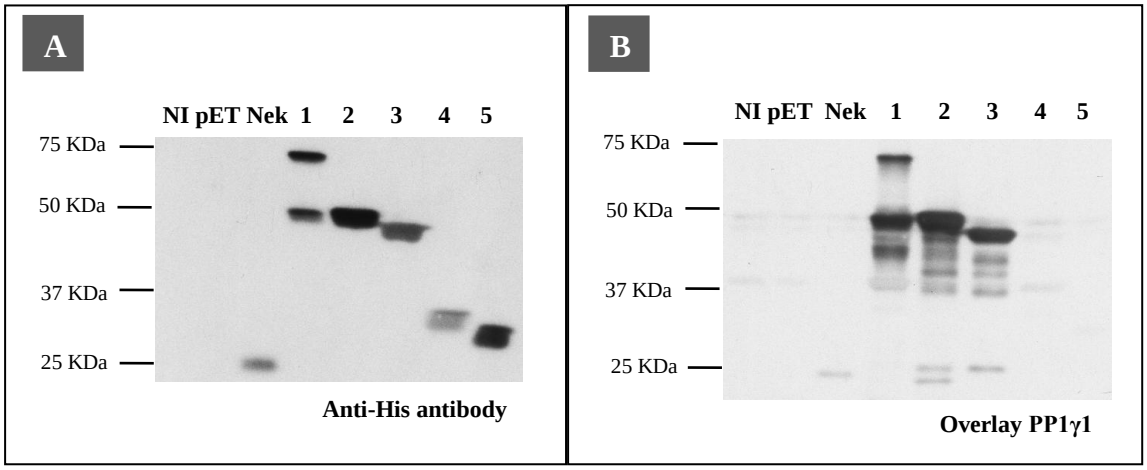

Figure 25. A- Immunoblot analysis of LAP1B (1) and LAP1B deletion mutants (2-5) using an anti-His antibody. **B-** Blot overlay assay of LAP1B (1) and LAP1B deletion mutants (2-5) with PP1γ1. NI, non-induced control; pET, pET-28c vector without an insert (negative control); Nek, Nek2A (positive control); 1, LAP1B; 2, LAP1B – BM1/2+TM; 3, LAP1B – BM1/2-TM; 4, LAP1B – BM3+TM; 5, LAP1B – BM3-TM. The insoluble fractions were collected 3 hours after IPTG (1 mM) induction at 37°C and equal amounts of protein were separated by SDS-PAGE and transferred to nitrocellulose.

3.2.4. Discussion

LAP1B expression was induced in bacteria [Rosetta (DE3) *E. coli* strain] and aliquots were taken at 1, 3 and 5 hr after induction of recombinant protein expression. A temperature of 37°C for bacterial growth and a concentration of 1 mM IPTG for induction allowed the abundant production of recombinant full-length LAP1B and LAP1B deletion proteins. However, most of the recombinant protein expressed was found in the insoluble fraction, which may be the result of protein accumulation in inclusion bodies. Since LAP1B is an integral membrane protein, that may explain why LAP1B was mainly found in an insoluble form. Further, a smaller protein, which may result from proteolytic cleavage of the full-length LAP1B protein, was found both in the insoluble and soluble fractions. This can be explained by the fact that small proteins are more easily soluble in bacteria. Therefore, the LAP1B deletion mutants BM1/2+TM and BM1/2-TM, which possess only the nucleoplasmic portion of LAP1B, and the transmembrane domain for BM1/2+TM, were found both in the insoluble and soluble fractions. BM3+TM, comprising the lumenal and the transmembrane domains, was mostly expressed in the insoluble form. However, BM3-TM, lacking the transmembrane domain, had some expression in the soluble fraction. In order to optimaize soluble protein expression new conditions of expression need to be tested, such as lower temperature for growth and varying the IPTG concentration and time of induction.

PP1 interaction with LAP1B *in vitro* was demonstrated by blot overlay assay using PP1γ1 purified protein. The results obtained confirmed that the interaction of the LAP1B with PP1γ1 must be direct (without the need for a bridging protein). The LAP1B domain responsible for the interaction with PP1γ1 was assessed by using a blot overlay assay of LAP1B deletion proteins with purified PP1γ1 protein. As expected, PP1γ1 binds BM1/2+TM and BM1/2-TM which comprise the nucleoplasmic portion of LAP1B. These results are in agreement with yeast-co-transformation results demonstrating that PP1γ1 interacts with LAP1B through BM1 in the nucleoplasm.

3.3. Validation of the PP1/LAP1B interaction by co-immunoprecipitation

3.3.1. Introduction

Several procedures may be used to validate a novel putative protein-protein interaction. Co-immunoprecipitation is most commonly used to prove that two proteins of interest are associated *in vivo*, but it can also be used to identify novel interacting partners of a target protein. Co-immunoprecipitation is based on the formation of antigen-antibody complex. Briefly, the target protein is specifically immunoprecipitated from cellular extracts using specific antibodies and the immunoprecipitates are then separated by SDS-PAGE. Co-immunoprecipated proteins are detected by immunoblotting with an antibody directed against the protein being evaluated.

The cDNA encoding LAP1B was transferred into a mammalian expression vector with an N-terminal Myc-tag (pCMV-Myc, Appendix II). With the purpose of confirming *in vivo* the interaction of LAP1B with PP1, COS-7 cells were transfected with Myc-LAP1B and analysed using specific anti-PP1γ, anti-PP1α and anti-Myc antibodies. The COS-7 cell line is a mammalian cell line derived from kidney cells of the African green monkey and is used for transfection experiments because it yields different expression of recombinant proteins. Transfection of COS-7 cells with Myc-LAP1B was performed using Lipofectamine 2000 (Invitrogen). Lipofectamine 2000 is a cationic liposome formulation that functions by complexing with nucleic acid molecules, allowing them to overcome the electrostatic repulsion of the cell membrane and to be taken up by the cell (99).

3.3.2. Materials and methods

The Myc-LAP1B construct was amplified and recovered from *E. coli* XL1-Blue. Isolation and purification of plasmid DNA was performed using the Promega Pure Yield Plasmid Midiprep System. The Myc-LAP1B construct was further analysed by restriction digestion with the endonucleases *EcoRI* and *XhoI* and the restriction fragments were separated by agarose gel electrophoresis. The Myc-LAP1B construct was fully sequenced to confirm the correct insertion of the LAP1B cDNA. These procedures were previously described in sections 3.1.2.1 - 3.1.2.6.

3.3.2.1. Cell culture

COS-7 cells were grown in Dulbecco's modified Eagle's medium (DMEM) supplemented with 10% fetal bovine serum, 100 U/mL penicillin, 100 mg/mL streptomycin and 3.7 g/L $NaHCO_3$ (Complete DMEM). Cultures were maintained at 37ºC and 5% CO_2. Cells were subcultured whenever approximately 90-95% confluency was reached.

3.3.2.2. Transfection with Lipofectamine

COS-7 cells were grown in complete DMEM until 90% confluency was reached and on the transfection day the culture medium was replaced with serum and antibiotic/antimycotic-free medium. 8 μg of DNA on each plate was diluted in DMEM (serum- and antibiotic/antimycotic-free). The Lipofectamine 2000 reagent was diluted in the same medium, and the tubes were left for 5 min. The DNA solution was added to the Lipofectamine solution drop by drop, and the solution was mixed by gentle bubbling with the pipette. In order to form the DNA-lipid complexes, the tube was allowed to rest for 25-30 min at room temperature. Then, the solution was directly added into the cell medium, drop by drop and with gentle rocking of the plate. The cells were then incubated at 37º C/5% CO_2 for 18 h. After that period cells were collected and further analysed.

3.3.2.3. Co-immunoprecipitation procedure

After transfection, COS-7 cells were washed in 1x PBS and collected with 1.2 mL of lysis buffer (50 mM Tris-HCl pH 8, 120 mM NaCl, 4% CHAPS) containing a protease inhibitor cocktail. The samples were sonicated for 5 seconds three times, intercalating the samples in order not to over-heat them. After BCA protein quantification described before (in section 3.2.2.2) mass normalized lysates were precleared with 25 μL Protein A-Sepharose beads (Pharmacia), for anti-PP1γ antibody and anti-PP1α antibody, or Protein G-Sepahrose beads (Pharmacia), for anti-Myc antibody, for 1 hr at 4ºC with agitation. After centrifuging for 5 min at 10000 g at 4ºC, the supernatant was transferred to a new microtube and 50 μL of Sepharose A plus the primary antibody [polyclonal anti-PP1γ (CBC3C) at 1:5000 dilution or polyclonal anti-PP1α (CBC2C) at 1:2500 dilution] or 50 μL of Sepharose G plus the primary antibody (monoclonal anti-Myc at 1:5000 dilution) was added and incubated overnight with shaking at 4º C. The mixture was then centrifuged for 3 min at 4ºC at 10000 g and the pellet washed four times with 500 μL of washing solution for 15 min with agitation at 4ºC. After the last wash, the tubes were centrifuged for 10 min at 10000 g and 4ºC, and the supernatant was fully discarded. The beads were then resuspended in 80 μL of Loading Buffer/1% SDS and boiled for 10 min.

Lysates of the same transfected cells were also collected and the appropriate volume of 10% SDS was added in order to obtain a final concentration of 1% SDS. Afterwards, they were boiled for 10 min and frozen.

Immunoprecipitates and lysates were separated by 10% SDS-PAGE and transferred to a nitrocellulose membrane that was then incubated with an anti-Myc antibody (1:5000 dilution) or an anti-PP1γ antibody (CBC3C, 1:5000 dilution) and developed using ECL, as previously described.

3.3.3. Results

3.3.3.1. Restriction analysis

The Myc-LAP1B construct was analysed by restriction digestion with the endonucleases *EcoRI* and *XhoI* to confirm the correct insertion into the pCMV-Myc vector (Appendix II). The restriction fragments were separated by 1% agarose gel electrophoresis and their size was confirmed (Fig. 26).

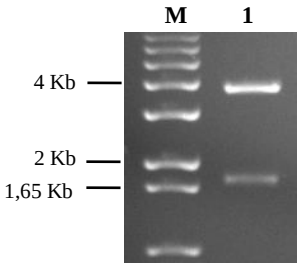

Figure 26. Analysis of the Myc-LAP1B construct by restriction analysis with *EcoRI* and *XhoI*. Lane M, 1 Kb Plus DNA ladder marker; Lane 1, pCMV-Myc + full-length LAP1B insert (3.8 + 1.75 Kb).

The fragments observed corresponded to the expected results.

3.3.3.2. DNA sequence analysis

The Myc-LAP1B construct in the pCMV-Myc vector was fully sequenced with the appropriate primers (Appendix III), as described in section 3.1.3.2. The LAP1B sequence obtained was analysed and the insert orientation into the pCMV-Myc vector and the reading frame confirmed.

3.3.3.3. Validation of PP1/LAP1B interaction by co-immunoprecipitation

In order to confirm the interaction of LAP1B with PP1 *in vivo*, co-immunoprecipitation assays were carried out using cellular extracts obtained from COS-7 cells transfected with Myc-LAP1B. Co-immunoprecipitations were performed using anti-PP1γ, anti-PP1α or anti-Myc antibodies. Cells lysates and immunoprecipitates were separated by 10% SDS-PAGE and transferred to a nitrocellulose membrane,

immunoblotted with anti-Myc or anti-PP1γ antibodies and developed by ECL. Upon immunoprecipitation with PP1γ (Fig. 27A) and PP1α (Fig. 27A), a strong band below 75 KDa, corresponding to Myc-LAP1B protein, could be detected by immunoblotting with anti-Myc antibody. This result indicates and confirms that Myc-LAP1B interacts with PP1 isoforms α and γ. A non specific Protein A band of approximately 50 kDa was also detected in immunoprecipitates (Fig. 27A). Immunoblot analysis of COS-7 cell extracts immunoprecipitated with the anti-Myc antibody also demonstrated that LAP1B co-immunoprecipitate with PP1γ (Fig. 27B), since a strong band at 37 kDa can be observed.

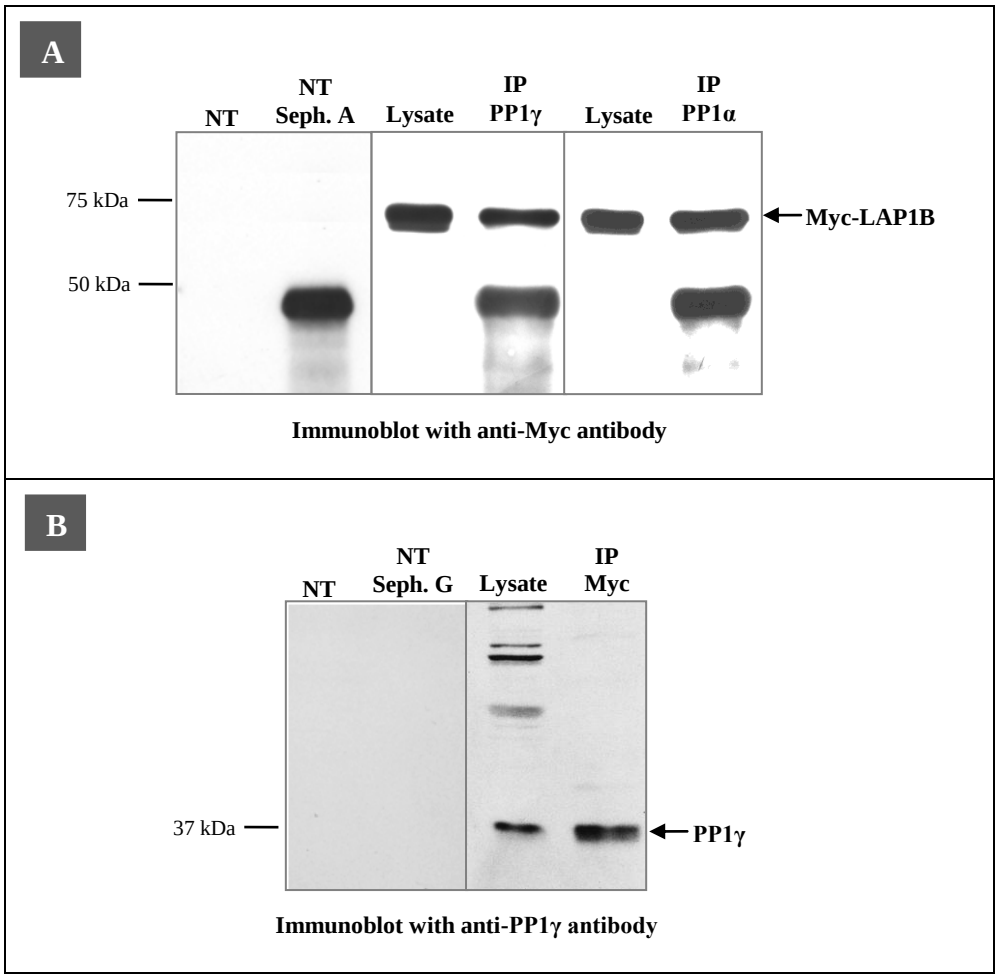

Figure 27. Validation of PP1/LAP1B interaction *in vivo* by co-immunoprecipitation. **A-** Immunoblot analysis of COS-7 cells immunoprecipitated with anti-PP1γ or anti-PP1α antibody and immunoblotted with anti-Myc antibody. Non-transfected (NT) cells and NT cells with Sepharose A (Seph. A) beads were used as controls. **B-** Immunoblot analysis of COS-7 cells immunoprecipitated with anti-Myc antibody and immunoblotted with anti-PP1γ antibody. NT cells and NT cells with Sepharose G (Seph. G) beads were used as controls. IP, immunoprecipitation.

3.3.4. Discussion

Co-immunoprecipitation is a reliable technique used to validate *in vivo* protein interactions that works by formation of antigen-antibody complexes. To address the physiological relevance of PP1/LAP1B interaction we attempted to demonstrate complex formation between Myc-LAP1B and endogenous PP1γ and α isoforms in a mammalian cell line. Immunoprecipitations were performed from COS-7 cellular extracts transfected with Myc-LAP1B, using specific antibodies: anti-PP1γ, anti-PP1α or anti-Myc. Immunoprecipitation with both anti-PP1γ and anti-PP1α antibodies followed by immunoblot analysis using an antibody (anti-Myc) that recognizes the Myc-tag of the Myc-LAP1B fusion protein, showed that LAP1B interacts with both PP1 isoforms. Furthermore, immunoblot analysis using anti-PP1γ antibody after immunoprecipitation with anti-Myc antibody also demonstrated that LAP1B interacts with PP1γ. These results clearly show that LAP1B interacts *in vivo* with both PP1γ and α isoforms. These results are in agreement and further extend the results obtained in the previous sections, thus validating the physiological relevance of PP1/LAP1B interaction.

3.4. Co-localization of LAP1B with PP1 isoforms α and γ

3.4.1. Introduction

In order to evaluate if and where PP1 and LAP1B co-localize in mammalian cells, subcellular localization studies were carried out using HeLa cells. HeLa cells are an immortal cell line derived from human cervical cancer cells, and they are often used for co-localization studies. The expression of the recombinant LAP1B fusion protein allows the analysis of its subcellular distribution and its co-localization with endogenous PP1 isoforms by immunocytochemistry using specific antibodies. Transfection was carried out with polyethylenimine (PEI) that is a class of cationic polymers proven to be effective for gene delivery into a variety of cells. PEI is one of the most densely charged polymers and has the function of condensing DNA into small particles, which facilitates DNA cellular uptake via endocytosis (100).

3.4.2. Materials and methods

3.4.2.1. Cell culture

HeLa cells were grown in Minimal Essential Medium with Earle's salts and GlutaMAX (MEM, Gibco), supplemented with 10% fetal bovine serum (FBS; Gibco), 1% MEM Non-Essential amino acids (Gibco, Invitrogen) and 100 U/mL penicillin and 100 mg/mL streptomycin (Gibco). Cultures were maintained at 37ºC and 5% CO_2. Cells were subcultured whenever 90-95% confluency was reached.

3.4.2.2. Transfection with polyethylenimine (PEI)

HeLa Cells were grown in complete MEM until 90% confluency was reached and 10 μg of recombinant plasmid DNA were diluted in 750 μL of NaCl (150 mM). The PEI solution (100 μL) was diluted in 650 μL of NaCl (150 mM) and the tubes were left for 15 min at room temperature. The PEI solution was added to the DNA drop by drop. In order to form the DNA-PEI complexes, the tube was left for 15 min at room temperature. During this time the medium of the cells was removed and 2.5 ml of fresh complete MEM was added. The complexes were added to this medium, drop by drop and with gentle rocking of the plate. The cells were then incubated at 37ºC/5% CO_2 for 5 hr. After that period the medium was replaced with fresh complete MEM and the cells were left to recover for 20 hr.

3.4.2.3. Immunocytochemistry procedure

HeLa cells were grown in glass coverslips pre-coated with 100 μg/mL poly-L-ornithine. HeLa cells were cultured until 90% confluency was reached and transfected as described above. Each well was washed three times with 1mL serum-free MEM medium and then 1 mL of 1:1 MEM/4% paraformaldehyde fixative solution was gently added and left to stand for 2 min. Subsequently, 1 mL of fixative solution was gently added and left for 25 min. Finally, cells were washed three times with 1 mL 1x PBS for 10 min. For cell permeabilization, 1 mL of methanol was added for 2 min and then washed 5 times with 1

mL 1x PBS for 10 min. The coverslips were blocked for 1 hr with 3% BSA in 1x PBS, and then incubated with primary antibody for 2 hours at room temperature. After three washes with 1x PBS, the secondary antibody was added and the coverslips incubated for 2 hr. The antibodies were diluted in 3% BSA in 1x PBS. Finally, three washes with 1x PBS were performed and coverslips were mounted on microscope glass slides with 1 drop of anti-fading reagent containing DAPI for nucleic acid staining (Vectashield, Vector Laboratories). Photographs were acquired using a LSM 510-Meta confocal microscope equipped with appropriate software (Zeiss).

3.4.2.3.1. Antibodies

The primary antibodies used were a monoclonal anti-Myc antibody (Cell Signaling, 1:5000 dilution), a polyclonal anti-PP1α antibody (CBC2C, 1:5000 dilution), a polyclonal anti-PP1γ antibody (CBC3C, 1:1000 dilution) and a polyclonal anti-lamin A/C antibody (1:50 dilution). The secondary antibodies used were an anti-mouse fluorescein isothiocyanate (FITC) conjugated antibody (Molecular Probes, 1:50 dilution) and the anti-rabbit Alexa Fluor 594 conjugated antibody (Molecular Probes, 1:300 dilution). The antibodies were diluted in 3% BSA in 1x PBS.

3.4.3. Results

In order to address the physiological relevance of PP1/LAP1B interaction, we evaluated the subcellular distribution and co-localization of both proteins in HeLa cells. Hela cells were transfected with the Myc-LAP1B construct and the expression of the fusion protein allowed the analysis of its subcellular distribution and its co-localization with endogenous PP1 isoforms (α and γ) and also with lamin A/C. Myc-LAP1B expression was detected with anti-Myc antibody and an anti-mouse FITC conjugated secondary antibody. Confocal fluorescence microscopy analysis revealed that Myc-LAP1B was almost exclusively localized at the nuclear envelope (Fig. 28A and B). Figure 28A shows two examples of cells transfected with Myc-LAP1B and two non transfected cells, the latter can be clearly differentiated from the transfected cells by the lower background staining of the cytoplasm and the absence of nuclear envelope staining. Myc-LAP1B immunoreactivity was also detected in some type of subnuclear structures (Fig. 28A and B, arrows).

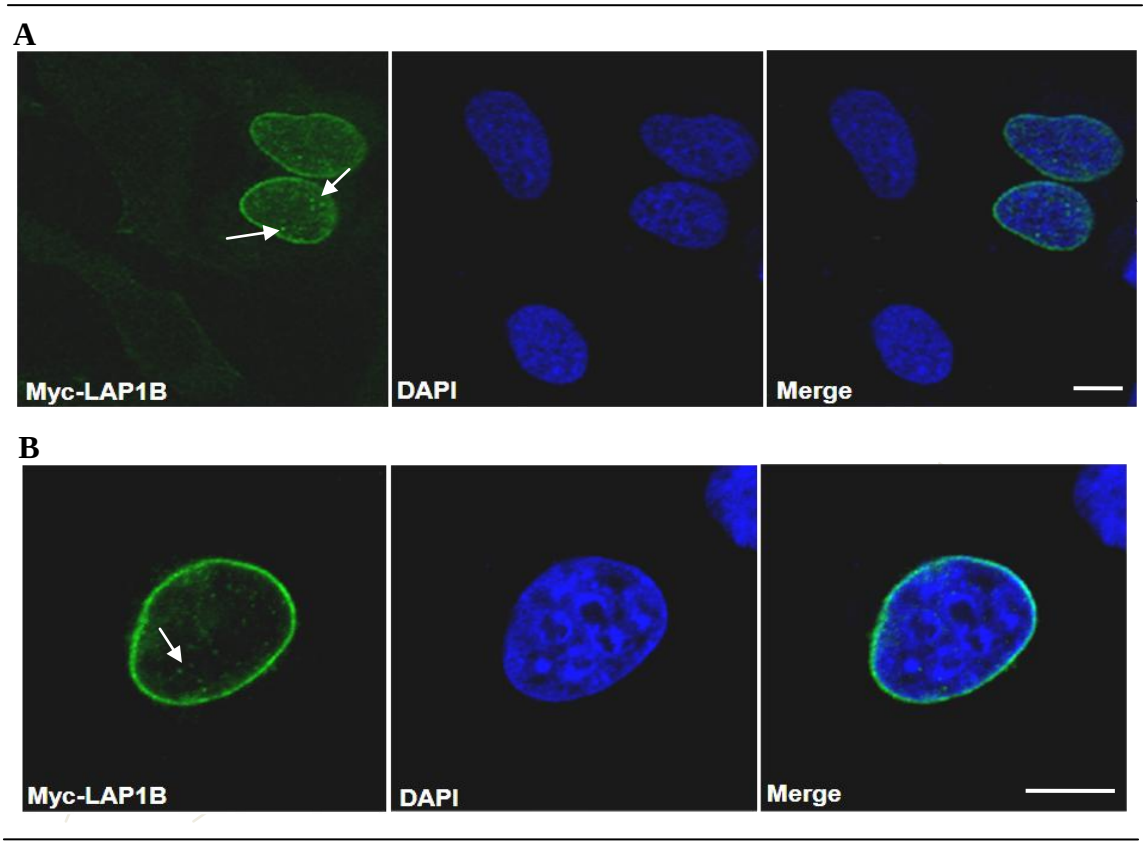

Figure 28. Subcellular distribution of Myc-LAP1B in HeLa cells. Myc-LAP1B was detected using an anti-mouse FITC conjugated secondary antibody (green). Nucleic acids were stained using DAPI (blue). Co-localization of Myc-LAP1B and DAPI staining can be observed in the merge figure. **A**- Two HeLa cells transfected with the Myc-LAP1B construct showing nuclear envelope immunoreactivity. Two non transfected cells are also observed. **B-** Nuclear envelope distribution of exogenous Myc-LAP1B. Myc-LAP1B immunoreactivity is also observed in subnuclear structures (arrows). Bar, 10 μm.

Given the apparent nuclear envelope distribution of LAP1B, co-localization analysis of LAP1B with an endogenous nuclear envelope marker was also carried out to confirm its subcellular distribution. Thus, lamin A/C was used since this protein is well known to associate with LAP1B and is a typical nuclear envelope marker. Localization of endogenous lamin A/C was performed using an anti-lamin A/C antibody and detected with an anti-rabbit Alexa Fluor 594 conjugated secondary antibody. As expected, endogenous lamin A/C was almost exclusively distributed in the nuclear envelope where it co-localizes extensively with Myc-LAP1B (Fig. 29).

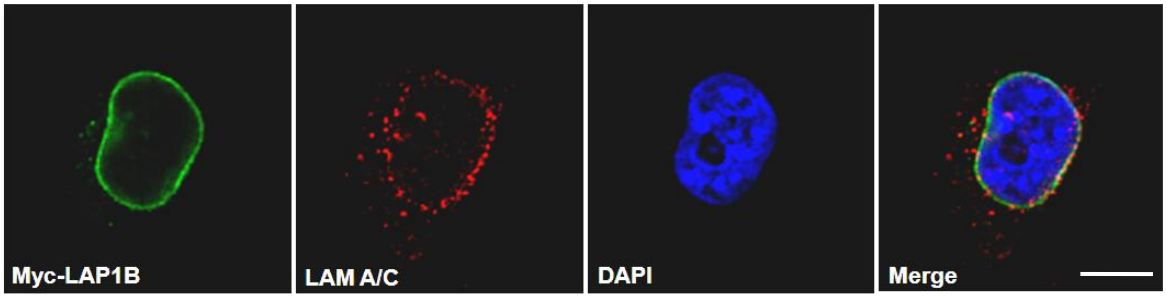

Figure 29. Co-localization of Myc-LAP1B and endogenous lamin A/C. Myc-LAP1B was detected with an anti-mouse FITC conjugated secondary antibody (green). Lamin A/C was detected with an anti-rabbit Alexa Fluor 594 conjugated secondary antibody (red). Nucleic acids were stained using DAPI (blue). The nuclear envelope co-localization of Myc-LAP1B and lamin A/C can be clearly seen in the merge figure. Bar, 10 μm.

Since PP1 isoforms are particularly enriched within the nucleus, we also evaluated the co-localization of LAP1B with and endogenous PP1 isoforms (α and γ). Endogenous PP1α and PP1γ were labeled with specific anti-PP1α or anti-PP1γ antibodies, respectively, and detected with an anti-rabbit Alexa Fluor 594 conjugated secondary antibody. Endogenous PP1γ (Fig. 30A) and PP1α (Fig. 30B) were found mainly in the nucleus but some immunoreactivity in the cytoplasm was also observed. In the nucleus, PP1γ was found within the nucleolar like structures (Fig. 30A), from which PP1α was excluded (Fig. 30B). Co-localization of Myc-LAP1B with PP1γ (Fig. 30A and A') and PP1α (Fig. 30B and B') was observed at several subnuclear structures and at points near the nuclear envelope. The co-localization of Myc-LAP1B and PP1α in specific points (Fig. 30C, arrow) was validated by the overlap between the green fluorescence intensity (FITC conjugated secondary antibody labelling Myc-LAP1B) and the red fluorescence intensity (Alexa Fluor 594 conjugated secondary antibody labelling PP1α), represented in the histogram (Fig. 30C').

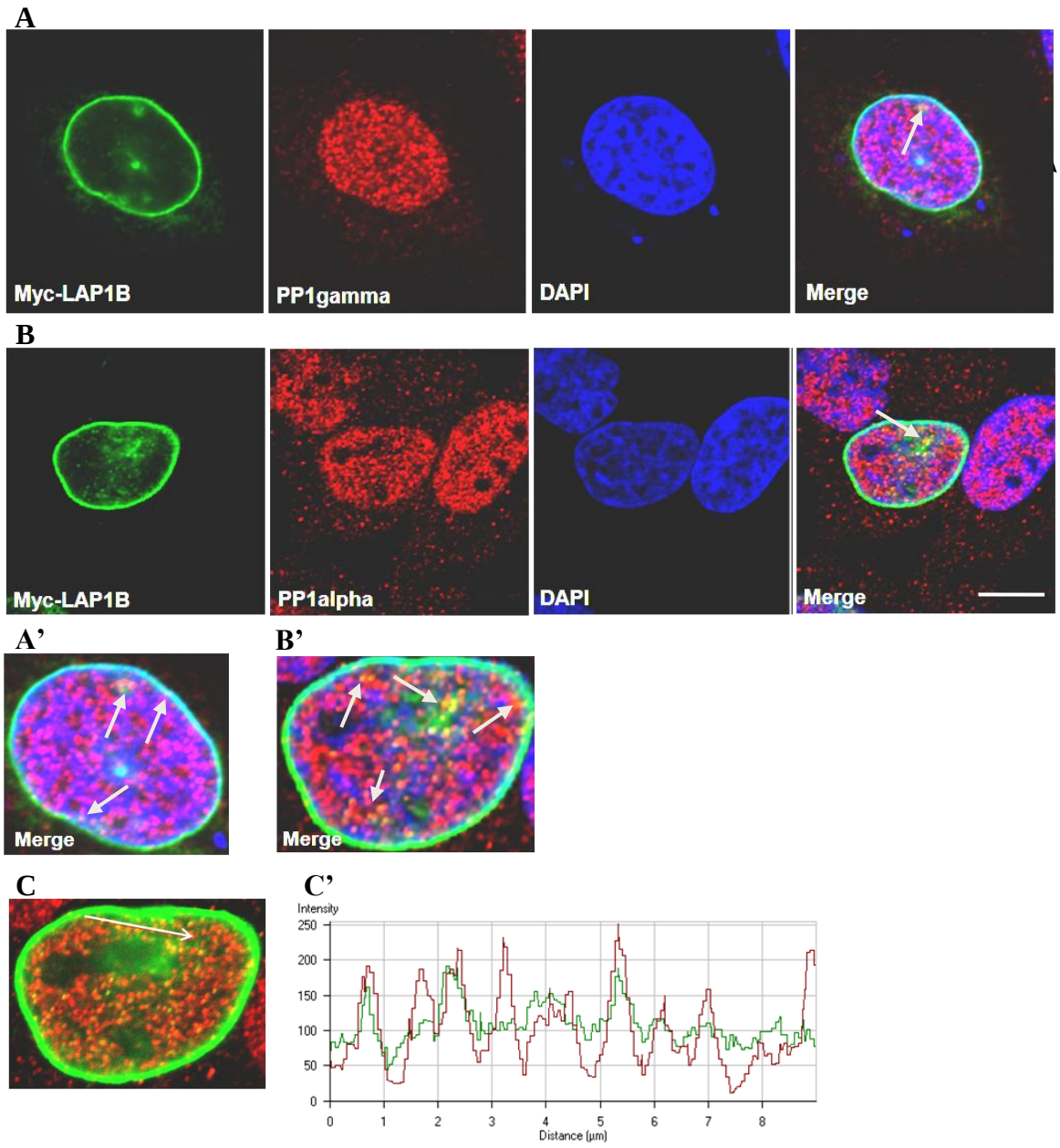

Figure 30. Co-localization of Myc-LAP1B and PP1 in HeLa cells. **A-** Co-localization of Myc-LAP1B with endogenous PP1γ. **B-** Co-localization of Myc-LAP1B with endogenous PP1α. **A'-** Amplified image of A – Merge. **B'-** Amplified image of B - Merge. Expressed Myc-LAP1B was detected with an anti-mouse FITC conjugated secondary antibody (green). Nucleic acids were stained using DAPI (blue). Endogenous PP1γ and PP1α were detected with an anti-rabbit Alexa Fluor 594 conjugated secondary antibody (red). The co-localization of Myc-LAP1B and PP1 isoforms can be observed in the merge figure (yellow/orange, arrows). **C-** Co-localization of Myc-LAP1B with endogenous PP1α in specific points (arrow). **C'-** Histogram representing the green fluorescence intensity (FITC conjugated secondary antibody labelling Myc-LAP1B) and the red fluorescence intensity (Alexa Fluor 594 conjugated secondary antibody labelling PP1α) in a specific distance (arrow from C). Bar, 10 µm.

3.4.4. Discussion

The simultaneous presence of two proteins in the same subcellular compartments is a condition for *in vivo* interaction. However, they might come in contact with each other in the cytoplasm as the protein is translated or in another location. Therefore it is important to determine the subcellular distribution of these proteins and the specific structures with which they are associated. The subcellular distribution and co-localization between PP1 and Myc-LAP1B were evaluated in HeLa cells by immunocytochemistry. Myc-LAP1B exhibited nuclear envelope localization as previously reported (89). To confirm its nuclear envelope distribution, the co-localization of Myc-LAP1B with lamin A/C, a marker for the nuclear envelope, was evaluated. LAP1B binds both lamins A and C and lamin B (83), which are the main components of the nuclear lamina. As expected, co-localization at the nuclear envelope between LAP1B and lamin A/C was clearly observed. Endogenous PP1γ and PP1α were found enriched in the nucleus of HeLa cells. Within the nucleus, whereas PP1γ was found enriched in nucleolar like structures, PP1α was apparently excluded from those structures. Co-localization of endogenous PP1γ and PP1α with Myc-LAP1B was observed at several sites other than the nucleus but, since no specific antibodies for these structures were available, it was not possible to unequivocally identify those structures. Further work will be required to accomplish the identification of these structures. Co-localization of LAP1B and PP1 was also seen at some points near the nuclear envelope, in agreement with putative interaction through the nucleoplasmic portion of LAP1B.

4. Discussion

PP1 is the most widely expressed and abundant protein serine/threonine phosphatase. PP1 is involved in many cellular processes like glycogen metabolism, transcription, protein synthesis, cellular division, meiosis and apoptosis (reviewed in 8). Furthermore, abnormal protein phosphorylation has been associated with several neurodegenerative diseases, such as AD, where PP1 is involved. This versatility of PP1 is only possible by complexing with numerous regulatory subunits, which confer distinct substrate specificity, activity and targeting to a particular subcellular localization (9, 17). For instance, PP1 is enriched in dendritic spines in brain (34) and this observation led to the discovery of spinophilin, which binds PP1 and targets it to the post-synaptic density. The three PP1 isoforms α, β and γ1 are widely expressed in brain and their mRNA is particularly abundant in hippocampus and cerebellum. At the protein level PP1α and PP1γ1 are enriched within the striatum (29).

Given the abundance of PP1 isoforms in brain and the numerous functions that have been associated with PP1 via its binding subunits, a yeast two-hybrid screen of a human brain cDNA library was performed using PP1 isoforms α, γ1 and γ2 and as bait, in order to identify novel PP1 interacting proteins in brain. Among several interesting proteins, LAP1B/TOR1AIP1 was identified as a novel putative PP1 regulator. Overall, fourteen, four and two positive clones encoding for LAP1B were identified using PP1α, PP1γ1 and PP1γ2 and as bait, respectively. We decided to further evaluate LAP1B given that LAP1B binds to TorsinA (67), a protein involved in EOTD. Most cases of EOTD are associated with an in-frame three bp deletion (ΔGAG) in the *DYT1* gene, leading to loss of a single glutamic acid residue at position 302 or 303 (ΔE302/303) within torsinA (44). As other AAA^+ ATPases, torsinA may act as a chaperone, working at several subcellular compartments through interaction with different binding partners, including the transmembrane proteins LAP1B in the NE and LULL1 in the ER (67, 68), KLC1 in the cytoplasm (70) and vimentin (71) and snapin on dense core granules (77). Subcellular studies demonstrated that Wt-torsinA is found in the ER (60, 62) and, upon over-expression, is also found in the NE (64, 65), while mutant torsinA is located mainly in the NE (67). Given that LAP1B is an inner nuclear membrane protein and interacts through its lumenal domain with torsinA, the redistribution of mutant torsinA to the NE suggests that impaired interaction of torsinA with LAP1B may contribute to the development of EOTD (67, 101). Additionally, our results also indicate that LAP1B interacts with PP1, so a new

perspective for the study of EOTD is open, where PP1 and/or abnormal protein phosphorylation might represent a pivotal event.

In order to obtain more information on LAP1B and its putative functions, we performed a bioinformatics analysis of its amino acid sequence. First, all LAP1B clones obtained in the YTH screen were sequenced, and their analysis verified that all were a variant of LAP1B sequence reported in the NCBI database (NM_015602). These clones include 3 more nucleotides (CAG) which result in the inclusion of a single alanine at position 185 of the LAP1B coding sequence. This sequence is identical to that reported by Kondo *et al* (2002) (89). Indeed, the inclusion/exclusion of three nucleotides (CAG) is very common among other proteins and in some reported this subtle alternative splicing may even affect the subcellular localization of such variants (102). Furthermore, expansion of CAG repeats in the coding region characterizes some neurodegenerative diseases, like Huntington's disease. For further study, we chose clone 135 (for the PP1γ1 YTH screen) that encodes for the full-length LAP1B. Bioinformatics analysis revealed that LAP1B possesses three well conserved PP1 binding motifs and a second generic PP1 binding motif named SILK, indicating the strong possibility that LAP1B interacts with PP1. LAP1B also possesses several potential phosphorylation sites for, for example, CK1, CK2, GSK3 and PLK. LAP1B can be both a substrate for PP1 and/or a targeting protein that directs PP1 to a specific subcellular compartment, where PP1 may dephosphorylate another protein. Therefore, we are particularly interested in characterizing the PP1/LAP1B complex.

The PP1/LAP1B interaction was further confirmed using several methodologies. First, by taking advantage of the YTH system, LAP1B and PP1 isoforms were co-transformed in yeast. Results showed that LAP1B interacts with PP1α, PP1γ1 and PP1γ2. These results are in agreement with the fact that positive clones encoding LAP1B were identified in all three YTH screens, using specifically these PP1 isoforms as bait. Furthermore, the LAP1B deletion mutants (cloned into pACT2 vector) indicated that the LAP1B interaction with PP1γ1 occur primarily through BM1. These results are consistent with BM1 being located in the nucleoplasmic portion of LAP1B and PP1 being particularly abundant in the nucleus. As expected, construct BM1/2 also interacts with PP1γ1, since it also possesses BM1. To analyse the PP1/LAP1B interaction *in vitro*, we cloned LAP1B into the pET-28c vector and expressed the recombinant protein in bacteria and performed a blot overlay assay using purified PP1γ1 protein. The results obtained

confirmed the direct interaction between LAP1B and PP1γ1. Using the deletion mutants (also cloned into the pET-28c vector), we also confirmed that PP1γ1 binds BM1/2, in agreement with the yeast-co-transformation results. In order to address the PP1/LAP1B interaction *in vivo*, we performed either co-immunoprecipitation with PP1α or PP1γ antibodies followed by detection with Myc-LAP1B using Myc antibody, or co-immunoprecipitation with the Myc antibody and detection of PP1γ using the PP1γ specific antibody. These experiments showed that PP1 and LAP1B form a complex *in vivo*, thus validating the physiological relevance of the PP1/LAP1B complex. The co-localization of PP1 and Myc-LAP1B were evaluated in a human cell line (HeLa cells). As expected, endogenous PP1γ and PP1α were enriched within the nucleus and Myc-LAP1B was distributed mainly around the nuclear envelope. Co-localization of Myc-LAP1B and PP1γ or PP1α was observed at several locations near the nuclear envelope and in unidentified subnuclear structures. Thus, further work is required to identify the nature of such structures, where PP1 and LAP1B may interact. To evaluate the physiological relevance of the PP1/LAP1B complex, subcellular studies in primary neuronal cultures and co-immunoprecipitation from specific brain regions, particularly from striatum and cerebellum (the more important regions for EOTD) also need to be performed. The validation of a putative PP1/LAP1B/torsinA trimeric complex (Fig. 31) and its relevance for EOTD needs to be fully evaluated.

The functional role of LAP1B is poorly understood but it is known that LAP1B interacts with lamins and chromosomes, which may be important for the maintenance of the nuclear architecture (89). Moreover lamins are phosphorylated during prophase/metaphase and dephosphorylated at telophase when the NE is reassembled, and this may be determined by the association of lamins with other proteins such as LAPs (79) and PP1 (84). LAP1 and LAP2 dissociate from the lamins at the onset of mitosis and associate before the reassembly of the nuclear lamina. Furthermore, LAP1 and LAP2 are phosphorylated during mitosis and hyperphosphorylation of LAP2 inhibits binding to lamin B1 and chromosomes. However, mitotic phosphorylation of LAP1 does not detectably alter the binding to lamins *in vitro* (83). Furthermore, it was proposed that PP1 mediates nuclear lamina reassembly, in part by dephosphorylation of lamin B (85), and AKAP-149 recruits PP1 to the NE upon NE assembly *in vitro* and promotes lamin B dephosphorylation and polymerization (86). Given that LAP1B associates with lamin B

and that AKAP-149/PP1 complex is involved in lamin B dephosphorylation, LAP1B may target PP1 to lamin B. PP1 and LAP1B may be involved in regulating NE reassembly and lamin B association to the NE.

Interestingly, the identification of LAP1B as a PP1 binding protein opens new perspectives for the study of EOTD, where protein phosphorylation may constitute a pivotal regulatory mechanism. Like LAP1B, torsinA also possesses potential sites for phosphorylation. Since PP1 interacts with LAP1B through its nucleoplasmic domain and torsinA interacts with the lumenal domain of LAP1B (Fig. 31), it will be interesting to evaluate the occurrence of a trimeric PP1/LAP1B/torsinA complex and to unravel its functional relevance for EOTD.

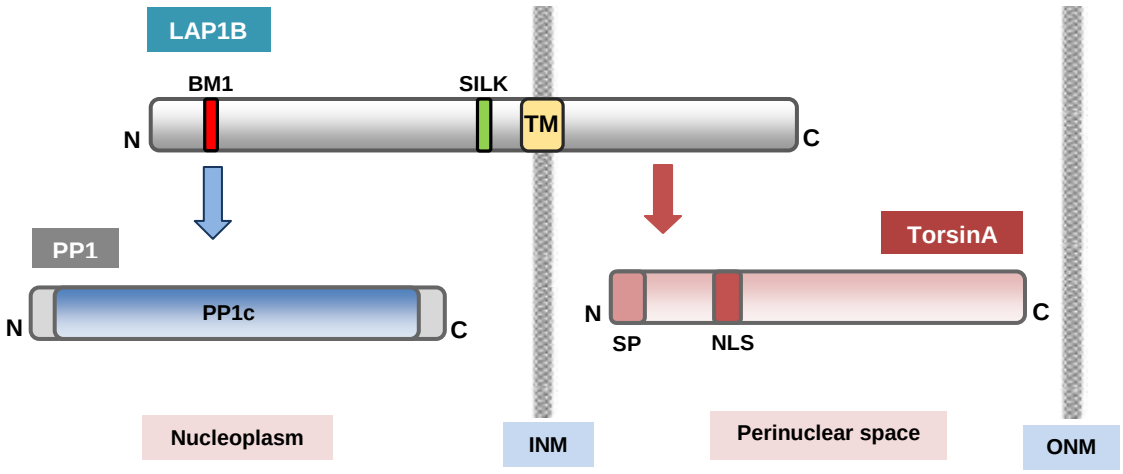

Figure 31. Schematic illustration of the putative PP1/LAP1B/TorsinA tricomplex. LAP1B interacts with the PP1c (PP1 catalytic subunit) in the nucleoplasm through the PP1 binding motif BM1. TorsinA can be found in the perinuclear space where it interacts with the lumenal domain of LAP1B. BM1, PP1 binding motif 1; SILK, a second generic PP1 binding motif; TM, transmembrane domain; SP, signal peptide; NLS, nuclear localization signal, INM, inner nuclear membrane, ONM, outer nuclear membrane.

TorsinA mRNA is widely distributed throughout all brain regions with higher expression in the dopaminergic neurons of the substantia nigra pars compacta (50, 51). The higher expression of torsinA within the substantia nigra pars compacta, which provides dopaminergic innervations to the basal ganglia, implicates a disturbance of dopaminergic function in the pathophysiology of EOTD (50). PP1 isoforms are highly expressed in brain

and PP1γ1 and PP1α are particularly enriched within the striatum. Here PP1 is involved in the action of several neurotransmitters, like dopamine and glutamate, via regulation by DARPP-32. Thus, it is believed that PP1 may play a role in dopaminergic signal transduction (34). Given the high expression levels of PP1 isoforms within the striatum, and the relationship between basal ganglia dopaminergic signalling and EOTD, the hypothesis that PP1 and/or abnormal protein phosphorylation may have a role in EOTD seems worthwhile exploring in the future.

5. References

1. Cohen, P. (1989) The structure and regulation of protein phosphatases. *Annu Rev Biochem,* **58,** 453-508.
2. Delobel, P., Flament, S., Hamdane, M., Mailliot, C., Sambo, A.V., Begard, S., Sergeant, N., Delacourte, A., Vilain, J.P. and Buee, L. (2002) Abnormal Tau phosphorylation of the Alzheimer-type also occurs during mitosis. *J Neurochem,* **83,** 412-20.
3. Planel, E., Yasutake, K., Fujita, S.C. and Ishiguro, K. (2001) Inhibition of protein phosphatase 2A overrides tau protein kinase I/glycogen synthase kinase 3 beta and cyclin-dependent kinase 5 inhibition and results in tau hyperphosphorylation in the hippocampus of starved mouse. *J Biol Chem,* **276,** 34298-306.
4. Bennecib, M., Gong, C.X., Grundke-Iqbal, I. and Iqbal, K. (2000) Role of protein phosphatase-2A and -1 in the regulation of GSK-3, cdk5 and cdc2 and the phosphorylation of tau in rat forebrain. *FEBS Lett,* **485,** 87-93.
5. da Cruz e Silva, E.F., da Cruz e Silva, O.A., Zaia, C.T. and Greengard, P. (1995) Inhibition of protein phosphatase 1 stimulates secretion of Alzheimer amyloid precursor protein. *Mol Med,* **1,** 535-41.
6. Okochi, M., Walter, J., Koyama, A., Nakajo, S., Baba, M., Iwatsubo, T., Meijer, L., Kahle, P.J. and Haass, C. (2000) Constitutive phosphorylation of the Parkinson's disease associated alpha-synuclein. *J Biol Chem,* **275,** 390-7.
7. Lievens, J.C., Woodman, B., Mahal, A. and Bates, G.P. (2002) Abnormal phosphorylation of synapsin I predicts a neuronal transmission impairment in the R6/2 Huntington's disease transgenic mice. *Mol Cell Neurosci,* **20,** 638-48.
8. Ceulemans, H. and Bollen, M. (2004) Functional diversity of protein phosphatase-1, a cellular economizer and reset button. *Physiol Rev,* **84,** 1-39.
9. Bollen, M. (2001) Combinatorial control of protein phosphatase-1. *Trends Biochem Sci,* **26,** 426-31.
10. da Cruz e Silva, O.A., Fardilha, M., Henriques, A.G., Rebelo, S., Vieira, S. and da Cruz e Silva, E.F. (2004) Signal transduction therapeutics: relevance for Alzheimer's disease. *J Mol Neurosci,* **23,** 123-42.
11. Cohen, P.T. (1997) Novel protein serine/threonine phosphatases: variety is the spice of life. *Trends Biochem Sci,* **22,** 245-51.

12. Fardilha, M., Wu, W., Sa, R., Fidalgo, S., Sousa, C., Mota, C., da Cruz e Silva, O.A. and da Cruz e Silva, E.F. (2004) Alternatively spliced protein variants as potential therapeutic targets for male infertility and contraception. *Ann N Y Acad Sci,* **1030,** 468-78.
13. Barford, D., Das, A.K. and Egloff, M.P. (1998) The structure and mechanism of protein phosphatases: insights into catalysis and regulation. *Annu Rev Biophys Biomol Struct,* **27,** 133-64.
14. Cohen, P.T. (2002) Protein phosphatase 1--targeted in many directions. *J Cell Sci,* **115,** 241-56.
15. Lin, Q., Buckler, E.S.t., Muse, S.V. and Walker, J.C. (1999) Molecular evolution of type 1 serine/threonine protein phosphatases. *Mol Phylogenet Evol,* **12,** 57-66.
16. Honkanen, R.E. and Golden, T. (2002) Regulators of serine/threonine protein phosphatases at the dawn of a clinical era? *Curr Med Chem,* **9,** 2055-75.
17. Ceulemans, H., Stalmans, W. and Bollen, M. (2002) Regulator-driven functional diversification of protein phosphatase-1 in eukaryotic evolution. *Bioessays,* **24,** 371-81.
18. Connor, J.H., Kleeman, T., Barik, S., Honkanen, R.E. and Shenolikar, S. (1999) Importance of the beta12-beta13 loop in protein phosphatase-1 catalytic subunit for inhibition by toxins and mammalian protein inhibitors. *J Biol Chem,* **274,** 22366-72.
19. Katayose, Y., Li, M., Al-Murrani, S.W., Shenolikar, S. and Damuni, Z. (2000) Protein phosphatase 2A inhibitors, I(1)(PP2A) and I(2)(PP2A), associate with and modify the substrate specificity of protein phosphatase 1. *J Biol Chem,* **275,** 9209-14.
20. Allen, P.B., Ouimet, C.C. and Greengard, P. (1997) Spinophilin, a novel protein phosphatase 1 binding protein localized to dendritic spines. *Proc Natl Acad Sci U S A,* **94,** 9956-61.
21. Wakula, P., Beullens, M., Ceulemans, H., Stalmans, W. and Bollen, M. (2003) Degeneracy and function of the ubiquitous RVXF motif that mediates binding to protein phosphatase-1. *J Biol Chem,* **278,** 18817-23.

22. Egloff, M.P., Johnson, D.F., Moorhead, G., Cohen, P.T., Cohen, P. and Barford, D. (1997) Structural basis for the recognition of regulatory subunits by the catalytic subunit of protein phosphatase 1. *EMBO J,* **16,** 1876-87.

23. Hendrickx, A., Beullens, M., Ceulemans, H., Den Abt, T., Van Eynde, A., Nicolaescu, E., Lesage, B. and Bollen, M. (2009) Docking motif-guided mapping of the interactome of protein phosphatase-1. *Chem Biol,* **16,** 365-71.

24. Lin, T.H., Tsai, P.C., Liu, H.T., Chen, Y.C., Wang, L.H., Hsieh, F.K. and Huang, H.B. (2005) Characterization of the protein phosphatase 1-binding motifs of inhibitor-2 and DARPP-32 by surface plasmon resonance. *J Biochem,* **138,** 697-700.

25. Browne, G.J., Fardilha, M., Oxenham, S.K., Wu, W., Helps, N.R., da Cruz, E.S.O.A., Cohen, P.T. and da Cruz, E.S.E.F. (2007) SARP, a new alternatively spliced protein phosphatase 1 and DNA interacting protein. *Biochem J,* **402,** 187-96.

26. Sasaki, K., Shima, H., Kitagawa, Y., Irino, S., Sugimura, T. and Nagao, M. (1990) Identification of members of the protein phosphatase 1 gene family in the rat and enhanced expression of protein phosphatase 1 alpha gene in rat hepatocellular carcinomas. *Jpn J Cancer Res,* **81,** 1272-80.

27. Barker, H.M., Craig, S.P., Spurr, N.K. and Cohen, P.T. (1993) Sequence of human protein serine/threonine phosphatase 1 gamma and localization of the gene (PPP1CC) encoding it to chromosome bands 12q24.1-q24.2. *Biochim Biophys Acta,* **1178,** 228-33.

28. Barker, H.M., Brewis, N.D., Street, A.J., Spurr, N.K. and Cohen, P.T. (1994) Three genes for protein phosphatase 1 map to different human chromosomes: sequence, expression and gene localisation of protein serine/threonine phosphatase 1 beta (PPP1CB). *Biochim Biophys Acta,* **1220,** 212-8.

29. da Cruz e Silva, E.F., Fox, C.A., Ouimet, C.C., Gustafson, E., Watson, S.J. and Greengard, P. (1995) Differential expression of protein phosphatase 1 isoforms in mammalian brain. *J Neurosci,* **15,** 3375-89.

30. Trinkle-Mulcahy, L., Sleeman, J.E. and Lamond, A.I. (2001) Dynamic targeting of protein phosphatase 1 within the nuclei of living mammalian cells. *J Cell Sci,* **114,** 4219-28.

31. Andreassen, P.R., Lacroix, F.B., Villa-Moruzzi, E. and Margolis, R.L. (1998) Differential subcellular localization of protein phosphatase-1 alpha, gamma1, and delta isoforms during both interphase and mitosis in mammalian cells. *J Cell Biol,* **141,** 1207-15.

32. Hemmings, H.C., Jr., Greengard, P., Tung, H.Y. and Cohen, P. (1984) DARPP-32, a dopamine-regulated neuronal phosphoprotein, is a potent inhibitor of protein phosphatase-1. *Nature,* **310,** 503-5.

33. Halpain, S., Girault, J.A. and Greengard, P. (1990) Activation of NMDA receptors induces dephosphorylation of DARPP-32 in rat striatal slices. *Nature,* **343,** 369-72.

34. Ouimet, C.C., da Cruz e Silva, E.F. and Greengard, P. (1995) The alpha and gamma 1 isoforms of protein phosphatase 1 are highly and specifically concentrated in dendritic spines. *Proc Natl Acad Sci U S A,* **92,** 3396-400.

35. Bordelon, J.R., Smith, Y., Nairn, A.C., Colbran, R.J., Greengard, P. and Muly, E.C. (2005) Differential localization of protein phosphatase-1alpha, beta and gamma1 isoforms in primate prefrontal cortex. *Cereb Cortex,* **15,** 1928-37.

36. Muly, E.C., Allen, P., Mazloom, M., Aranbayeva, Z., Greenfield, A.T. and Greengard, P. (2004) Subcellular distribution of neurabin immunolabeling in primate prefrontal cortex: comparison with spinophilin. *Cereb Cortex,* **14,** 1398-407.

37. Nakanishi, H., Obaishi, H., Satoh, A., Wada, M., Mandai, K., Satoh, K., Nishioka, H., Matsuura, Y., Mizoguchi, A. and Takai, Y. (1997) Neurabin: a novel neural tissue-specific actin filament-binding protein involved in neurite formation. *J Cell Biol,* **139,** 951-61.

38. Colbran, R.J., Bass, M.A., McNeill, R.B., Bollen, M., Zhao, S., Wadzinski, B.E. and Strack, S. (1997) Association of brain protein phosphatase 1 with cytoskeletal targeting/regulatory subunits. *J Neurochem,* **69,** 920-9.

39. Strack, S., Kini, S., Ebner, F.F., Wadzinski, B.E. and Colbran, R.J. (1999) Differential cellular and subcellular localization of protein phosphatase 1 isoforms in brain. *J Comp Neurol,* **413,** 373-84.

40. Munton, R.P., Vizi, S. and Mansuy, I.M. (2004) The role of protein phosphatase-1 in the modulation of synaptic and structural plasticity. *FEBS Lett,* **567,** 121-8.

41. Terry, R.D., Masliah, E., Salmon, D.P., Butters, N., DeTeresa, R., Hill, R., Hansen, L.A. and Katzman, R. (1991) Physical basis of cognitive alterations in Alzheimer's disease: synapse loss is the major correlate of cognitive impairment. *Ann Neurol,* **30,** 572-80.

42. Liao, H., Li, Y., Brautigan, D.L. and Gundersen, G.G. (1998) Protein phosphatase 1 is targeted to microtubules by the microtubule-associated protein Tau. *J Biol Chem,* **273,** 21901-8.

43. Lindesmith, L., McIlvain, J.M., Jr., Argon, Y. and Sheetz, M.P. (1997) Phosphotransferases associated with the regulation of kinesin motor activity. *J Biol Chem,* **272,** 22929-33.

44. Ozelius, L.J., Hewett, J.W., Page, C.E., Bressman, S.B., Kramer, P.L., Shalish, C., de Leon, D., Brin, M.F., Raymond, D., Corey, D.P. *et al.* (1997) The early-onset torsion dystonia gene (DYT1) encodes an ATP-binding protein. *Nat Genet,* **17,** 40-8.

45. Vale, R.D. (2000) AAA proteins. Lords of the ring. *J Cell Biol,* **150,** F13-9.

46. Ozelius, L.J., Page, C.E., Klein, C., Hewett, J.W., Mineta, M., Leung, J., Shalish, C., Bressman, S.B., de Leon, D., Brin, M.F. *et al.* (1999) The TOR1A (DYT1) gene family and its role in early onset torsion dystonia. *Genomics,* **62,** 377-84.

47. Goodchild, R.E., Kim, C.E. and Dauer, W.T. (2005) Loss of the dystonia-associated protein torsinA selectively disrupts the neuronal nuclear envelope. *Neuron,* **48,** 923-32.

48. Zorzi, G., Zibordi, F., Garavaglia, B. and Nardocci, N. (2009) Early onset primary dystonia. *Eur J Paediatr Neurol*.

49. Muraro, N.I. and Moffat, K.G. (2006) Down-regulation of torp4a, encoding the Drosophila homologue of torsinA, results in increased neuronal degeneration. *J Neurobiol,* **66,** 1338-53.

50. Augood, S.J., Penney, J.B., Jr., Friberg, I.K., Breakefield, X.O., Young, A.B., Ozelius, L.J. and Standaert, D.G. (1998) Expression of the early-onset torsion dystonia gene (DYT1) in human brain. *Ann Neurol,* **43,** 669-73.

51. Augood, S.J., Martin, D.M., Ozelius, L.J., Breakefield, X.O., Penney, J.B., Jr. and Standaert, D.G. (1999) Distribution of the mRNAs encoding torsinA and torsinB in the normal adult human brain. *Ann Neurol,* **46,** 761-9.

52. Konakova, M., Huynh, D.P., Yong, W. and Pulst, S.M. (2001) Cellular distribution of torsin A and torsin B in normal human brain. *Arch Neurol,* **58,** 921-7.

53. Augood, S.J., Keller-McGandy, C.E., Siriani, A., Hewett, J., Ramesh, V., Sapp, E., DiFiglia, M., Breakefield, X.O. and Standaert, D.G. (2003) Distribution and ultrastructural localization of torsinA immunoreactivity in the human brain. *Brain Res,* **986,** 12-21.

54. Shashidharan, P., Kramer, B.C., Walker, R.H., Olanow, C.W. and Brin, M.F. (2000) Immunohistochemical localization and distribution of torsinA in normal human and rat brain. *Brain Res,* **853,** 197-206.

55. Shashidharan, P., Good, P.F., Hsu, A., Perl, D.P., Brin, M.F. and Olanow, C.W. (2000) TorsinA accumulation in Lewy bodies in sporadic Parkinson's disease. *Brain Res,* **877,** 379-81.

56. Shashidharan, P., Sandu, D., Potla, U., Armata, I.A., Walker, R.H., McNaught, K.S., Weisz, D., Sreenath, T., Brin, M.F. and Olanow, C.W. (2005) Transgenic mouse model of early-onset DYT1 dystonia. *Hum Mol Genet,* **14,** 125-33.

57. Torres, G.E., Sweeney, A.L., Beaulieu, J.M., Shashidharan, P. and Caron, M.G. (2004) Effect of torsinA on membrane proteins reveals a loss of function and a dominant-negative phenotype of the dystonia-associated DeltaE-torsinA mutant. *Proc Natl Acad Sci U S A,* **101,** 15650-5.

58. Cao, S., Gelwix, C.C., Caldwell, K.A. and Caldwell, G.A. (2005) Torsin-mediated protection from cellular stress in the dopaminergic neurons of Caenorhabditis elegans. *J Neurosci,* **25,** 3801-12.

59. Neuwald, A.F., Aravind, L., Spouge, J.L. and Koonin, E.V. (1999) AAA+: A class of chaperone-like ATPases associated with the assembly, operation, and disassembly of protein complexes. *Genome Res,* **9,** 27-43.

60. Liu, Z., Zolkiewska, A. and Zolkiewski, M. (2003) Characterization of human torsinA and its dystonia-associated mutant form. *Biochem J,* **374,** 117-22.

61. Granata, A., Schiavo, G. and Warner, T.T. (2009) TorsinA and dystonia: from nuclear envelope to synapse. *J Neurochem,* **109,** 1596-609.

62. Hewett, J., Gonzalez-Agosti, C., Slater, D., Ziefer, P., Li, S., Bergeron, D., Jacoby, D.J., Ozelius, L.J., Ramesh, V. and Breakefield, X.O. (2000) Mutant torsinA,

responsible for early-onset torsion dystonia, forms membrane inclusions in cultured neural cells. *Hum Mol Genet,* **9,** 1403-13.

63. Callan, A.C., Bunning, S., Jones, O.T., High, S. and Swanton, E. (2007) Biosynthesis of the dystonia-associated AAA+ ATPase torsinA at the endoplasmic reticulum. *Biochem J,* **401,** 607-12.
64. Naismith, T.V., Heuser, J.E., Breakefield, X.O. and Hanson, P.I. (2004) TorsinA in the nuclear envelope. *Proc Natl Acad Sci U S A,* **101,** 7612-7.
65. Goodchild, R.E. and Dauer, W.T. (2004) Mislocalization to the nuclear envelope: an effect of the dystonia-causing torsinA mutation. *Proc Natl Acad Sci U S A,* **101,** 847-52.
66. Giles, L.M., Chen, J., Li, L. and Chin, L.S. (2008) Dystonia-associated mutations cause premature degradation of torsinA protein and cell-type-specific mislocalization to the nuclear envelope. *Hum Mol Genet,* **17,** 2712-22.
67. Goodchild, R.E. and Dauer, W.T. (2005) The AAA+ protein torsinA interacts with a conserved domain present in LAP1 and a novel ER protein. *J Cell Biol,* **168,** 855-62.
68. Vander Heyden, A.B., Naismith, T.V., Snapp, E.L., Hodzic, D. and Hanson, P.I. (2009) LULL1 Retargets TorsinA to the Nuclear Envelope Revealing an Activity that Is Impaired by the DYT1 Dystonia Mutation. *Mol Biol Cell*.
69. Gerace, L. (2004) TorsinA and torsion dystonia: Unraveling the architecture of the nuclear envelope. *Proc Natl Acad Sci U S A,* **101,** 8839-40.
70. Kamm, C., Boston, H., Hewett, J., Wilbur, J., Corey, D.P., Hanson, P.I., Ramesh, V. and Breakefield, X.O. (2004) The early onset dystonia protein torsinA interacts with kinesin light chain 1. *J Biol Chem,* **279,** 19882-92.
71. Hewett, J.W., Zeng, J., Niland, B.P., Bragg, D.C. and Breakefield, X.O. (2006) Dystonia-causing mutant torsinA inhibits cell adhesion and neurite extension through interference with cytoskeletal dynamics. *Neurobiol Dis,* **22,** 98-111.
72. Difiglia, M., Pasik, P. and Pasik, T. (1980) Early postnatal development of the monkey neostriatum: a Golgi and ultrastructural study. *J Comp Neurol,* **190,** 303-31.
73. Tepper, J.M. and Trent, F. (1993) In vivo studies of the postnatal development of rat neostriatal neurons. *Prog Brain Res,* **99,** 35-50.

74. Maison, C., Pyrpasopoulou, A., Theodoropoulos, P.A. and Georgatos, S.D. (1997) The inner nuclear membrane protein LAP1 forms a native complex with B-type lamins and partitions with spindle-associated mitotic vesicles. *EMBO J,* **16,** 4839-50.

75. Nery, F.C., Zeng, J., Niland, B.P., Hewett, J., Farley, J., Irimia, D., Li, Y., Wiche, G., Sonnenberg, A. and Breakefield, X.O. (2008) TorsinA binds the KASH domain of nesprins and participates in linkage between nuclear envelope and cytoskeleton. *J Cell Sci,* **121,** 3476-86.

76. Ferrari-Toninelli, G., Paccioretti, S., Francisconi, S., Uberti, D. and Memo, M. (2004) TorsinA negatively controls neurite outgrowth of SH-SY5Y human neuronal cell line. *Brain Res,* **1012,** 75-81.

77. Granata, A., Watson, R., Collinson, L.M., Schiavo, G. and Warner, T.T. (2008) The dystonia-associated protein torsinA modulates synaptic vesicle recycling. *J Biol Chem,* **283,** 7568-79.

78. Misbahuddin, A., Placzek, M.R., Taanman, J.W., Gschmeissner, S., Schiavo, G., Cooper, J.M. and Warner, T.T. (2005) Mutant torsinA, which causes early-onset primary torsion dystonia, is redistributed to membranous structures enriched in vesicular monoamine transporter in cultured human SH-SY5Y cells. *Mov Disord,* **20,** 432-40.

79. Goldman, R.D., Gruenbaum, Y., Moir, R.D., Shumaker, D.K. and Spann, T.P. (2002) Nuclear lamins: building blocks of nuclear architecture. *Genes Dev,* **16,** 533-47.

80. Holmer, L. and Worman, H.J. (2001) Inner nuclear membrane proteins: functions and targeting. *Cell Mol Life Sci,* **58,** 1741-7.

81. Rober, R.A., Weber, K. and Osborn, M. (1989) Differential timing of nuclear lamin A/C expression in the various organs of the mouse embryo and the young animal: a developmental study. *Development,* **105,** 365-78.

82. Furukawa, K. and Hotta, Y. (1993) cDNA cloning of a germ cell specific lamin B3 from mouse spermatocytes and analysis of its function by ectopic expression in somatic cells. *EMBO J,* **12,** 97-106.

83. Foisner, R. and Gerace, L. (1993) Integral membrane proteins of the nuclear envelope interact with lamins and chromosomes, and binding is modulated by mitotic phosphorylation. *Cell,* **73,** 1267-79.

84. Steen, R.L., Martins, S.B., Tasken, K. and Collas, P. (2000) Recruitment of protein phosphatase 1 to the nuclear envelope by A-kinase anchoring protein AKAP149 is a prerequisite for nuclear lamina assembly. *J Cell Biol,* **150,** 1251-62.

85. Thompson, L.J., Bollen, M. and Fields, A.P. (1997) Identification of protein phosphatase 1 as a mitotic lamin phosphatase. *J Biol Chem,* **272,** 29693-7.

86. Steen, R.L., Beullens, M., Landsverk, H.B., Bollen, M. and Collas, P. (2003) AKAP149 is a novel PP1 specifier required to maintain nuclear envelope integrity in G1 phase. *J Cell Sci,* **116,** 2237-46.

87. Senior, A. and Gerace, L. (1988) Integral membrane proteins specific to the inner nuclear membrane and associated with the nuclear lamina. *J Cell Biol,* **107,** 2029-36.

88. Martin, L., Crimaudo, C. and Gerace, L. (1995) cDNA cloning and characterization of lamina-associated polypeptide 1C (LAP1C), an integral protein of the inner nuclear membrane. *J Biol Chem,* **270,** 8822-8.

89. Kondo, Y., Kondoh, J., Hayashi, D., Ban, T., Takagi, M., Kamei, Y., Tsuji, L., Kim, J. and Yoneda, Y. (2002) Molecular cloning of one isotype of human lamina-associated polypeptide 1s and a topological analysis using its deletion mutants. *Biochem Biophys Res Commun,* **294,** 770-8.

90. Yang, L., Guan, T. and Gerace, L. (1997) Integral membrane proteins of the nuclear envelope are dispersed throughout the endoplasmic reticulum during mitosis. *J Cell Biol,* **137,** 1199-210.

91. Bione, S., Maestrini, E., Rivella, S., Mancini, M., Regis, S., Romeo, G. and Toniolo, D. (1994) Identification of a novel X-linked gene responsible for Emery-Dreifuss muscular dystrophy. *Nat Genet,* **8,** 323-7.

92. Taylor, M.R., Slavov, D., Gajewski, A., Vlcek, S., Ku, L., Fain, P.R., Carniel, E., Di Lenarda, A., Sinagra, G., Boucek, M.M. *et al.* (2005) Thymopoietin (lamina-associated polypeptide 2) gene mutation associated with dilated cardiomyopathy. *Hum Mutat,* **26,** 566-74.

93. Waterham, H.R., Koster, J., Mooyer, P., Noort Gv, G., Kelley, R.I., Wilcox, W.R., Wanders, R.J., Hennekam, R.C. and Oosterwijk, J.C. (2003) Autosomal recessive HEM/Greenberg skeletal dysplasia is caused by 3 beta-hydroxysterol delta 14-reductase deficiency due to mutations in the lamin B receptor gene. *Am J Hum Genet,* **72,** 1013-7.

94. Hellemans, J., Preobrazhenska, O., Willaert, A., Debeer, P., Verdonk, P.C., Costa, T., Janssens, K., Menten, B., Van Roy, N., Vermeulen, S.J. *et al.* (2004) Loss-of-function mutations in LEMD3 result in osteopoikilosis, Buschke-Ollendorff syndrome and melorheostosis. *Nat Genet,* **36,** 1213-8.

95. Chien, C.T., Bartel, P.L., Sternglanz, R. and Fields, S. (1991) The two-hybrid system: a method to identify and clone genes for proteins that interact with a protein of interest. *Proc Natl Acad Sci U S A,* **88,** 9578-82.

96. Finley, R.L., Jr. and Brent, R. (1994) Interaction mating reveals binary and ternary connections between Drosophila cell cycle regulators. *Proc Natl Acad Sci U S A,* **91,** 12980-4.

97. Serebriiskii, I.G., Toby, G.G., Finley, R.L., Jr. and Golemis, E.A. (2001) Genomic analysis utilizing the yeast two-hybrid system. *Methods Mol Biol,* **175,** 415-54.

98. Berggard, T., Linse, S. and James, P. (2007) Methods for the detection and analysis of protein-protein interactions. *Proteomics,* **7,** 2833-42.

99. Dalby, B., Cates, S., Harris, A., Ohki, E.C., Tilkins, M.L., Price, P.J. and Ciccarone, V.C. (2004) Advanced transfection with Lipofectamine 2000 reagent: primary neurons, siRNA, and high-throughput applications. *Methods,* **33,** 95-103.

100. Boussif, O., Lezoualc'h, F., Zanta, M.A., Mergny, M.D., Scherman, D., Demeneix, B. and Behr, J.P. (1995) A versatile vector for gene and oligonucleotide transfer into cells in culture and in vivo: polyethylenimine. *Proc Natl Acad Sci U S A,* **92,** 7297-301.

101. Naismith, T.V., Dalal, S. and Hanson, P.I. (2009) Interaction of TorsinA with its major binding partners is impaired by the dystonia associated {Delta}GAG deletion. *J Biol Chem.*

102. Tadokoro, K., Yamazaki-Inoue, M., Tachibana, M., Fujishiro, M., Nagao, K., Toyoda, M., Ozaki, M., Ono, M., Miki, N., Miyashita, T. *et al.* (2005) Frequent occurrence of protein isoforms with or without a single amino acid residue by

subtle alternative splicing: the case of Gln in DRPLA affects subcellular localization of the products. *J Hum Genet,* **50,** 382-94.

Appendix

I. Culture media and solutions

Bacteria media

LB (Luria-Bertani) Medium

To 950 mL of deionised H_2O add:

LB 25 g

Agar 15 g (for plates only)

Shake until the solutes have dissolved. Adjust the volume of the solution to 1 L with deionised H_2O. Sterilize by autoclaving.

SOB Medium

To 950 mL of deionised H_2O add:

SOB Broth 25.5 g

Shake until the solutes have dissolved. Add 10 mL of a 250mM KCl (prepared by dissolving 1.86g of KCl in 100 mL of deionised H_2O). Adjust the pH to 7.0 with 5N NaOH. Just prior to use add 5 mL of a sterile solution of 2M $MgCl_2$ (prepared by dissolving 19 g of $MgCl_2$ in 90 mL of deionised H_2O). Adjust the volume of the solution to 1 L with deionised H_2O and sterilize by autoclaving).

SOC Medium

SOC is identical to SOB except that it contains 20 mM glucose. After the SOB medium has been autoclaved, allow it to cool to 60ºC and add 20 mL of a sterile 1M glucose (this solution is made by dissolving 18 g of glucose in 90 mL of deionised H_2O; after the sugar has dissolved, adjust the volume of the solution to 1 L with deionised H_2O and sterilize by filtration through a 0.22-micron filter).

Antibiotics (1000x)

Ampicilin	100 μg/μL
Kanamycin	30 μg/μL

Competent Cell Solutions

Solution I (1L)

$MnCl_2.4H_2O$	9.9 g
$CaCl_2.2H_2O$	1.5 g
Glycerol	150 g
KHAc 1M	30 mL

Adjust the volume of the solution to 1 L with deionised H_2O. Adjust pH to 5.8, filter through a 0.2 μm filter and store at 4ºC

Solution II (1L)

0.5M MOPS (pH 6.8)	20 mL
RbCl	1.2 g
$CaCl_2.2H_2O$	11g
Glycerol	150 g

Adjust the volume of the solution to 1 L with deionised H_2O. Filter through a 0.2 μm filter and store at 4ºC

DNA electrophoresis solutions

50x TAE Buffer

Tris base	242 g
Glacial acetic acid	57.1 mL
0.5M EDTA (pH 8.0)	100 mL

Loading Buffer (LB)

Bromophenol blue	0.25%
Glycerol	30%

Midiprep Solutions

Cell Resuspension Solution

50 mM Tris-HCl (pH 7.5)
10 mM EDTA
100 µg/mL RNAase A

Cell Lysis Solution

0.2 M NaOH
1% SDS

Neutralization Solution

4.09 M Guanidine hydrochloride (pH 4.8)
759 mM potassium acetate
2.12 M Glacial acetic acid

Column Wash Solution

60 mM potassium acetate
8.3 mM Tris-HCl (pH 7.5)
0.04 mM EDTA
60 % ethanol

Yeast Media

10x Dropout solution (10x DO)

This solution contains all but one or more of the following components:

	10x concentration (mg/L)	SIGMA #
L-Isoleucine	300	I-7383
L-Valine	1500	V-0500
L-Adenine hemisulfate salt	200	A-9126
L-Arginine HCl	200	A-5131
L-Histidine HCl monohydrate	200	H-9511
L-Leucine	1000	L-1512
L-Lysine HCl	300	L-1262
L-Methionine	200	M-9625
L-Phenylalanine	500	P-5030
L-Threonine	2000	T-8625
L-Tryptophan	200	T-0254
L-Tyrosine	300	T-3754
L-Uracil	200	U-0750

10x dropout supplements may be autoclaved and stored for up to 1 year.

Triple Drop Out: DO/-Leu/-Trp/-His
Quadruple Drop Out: DO/-Leu/-Trp/-His/-Ade

YPD medium

To 950 mL of deionised H_2O add:
YPD 50 g
Agar 15 g (for plates only)

Shake until the solutes have dissolved. Adjust the volume to 1 L with deionised H_2O and sterilize by autoclaving. Allow medium to cool to 60ºC and add glucose to 2% (50 mL of a sterile 40% stock solution).

SD synthetic medium

To 800 mL of deionised H_2O add:

Yeast nitrogen base without amino acids (DIFCO) 6.7 g

Agar (for plates only) 15 g

Shake until the solutes have dissolved. Adjust the volume to 850mL with deionised H_2O and sterilize by autoclaving. Allow medium to cool to 60ºC and add glucose to 2% (50 mL of a sterile 40% stock solution) and 100 mL of the appropriate 10x dropout solution.

TE Buffer (pH 7.5)

10 mM Tris-HCl (pH 7.5)

1 mM EDTA (pH 8.0)

SDS-PAGE and Immunoblotting Solutions

LGB (Lower Gel Buffer)

To 900 mL of deionised H2O add:

Tris 181.65 g

SDS 4 g

Mix until the solutes have dissolved. Adjust the pH to 8.9 and adjust the volume to 1 L with deionised H_2O.

UGB (Upper Gel Buffer)

To 900 mL of deionised H2O add:

Tris 75.69 g

Mix until the solute has dissolved. Adjust the pH to 6.8 and adjust the volume to 1 L with deionised H_2O.

30% Acrylamide/0.8% Bisacrylamide

To 70 mL of deionised H2O add:

Acrylamide 29.2 g

Bisacrylamide 0.8 g

Mix until the solutes have dissolved. Adjust the volume to 100 mL with deionised H_2O. Filter through a 0.2 μm filter and store at 4°C.

10% APS (ammonium persulfate)

In 10 mL of deonised H_2O dissolve 1 g of APS.

10% SDS (sodium dodecilsulfate)

In 10 mL of deonised H_2O dissolve 1 g of SDS.

Loading Gel Buffer (4x)

1 M Tris solution (pH 6.8)	2.5 ml (250 mM)
SDS	0.8 g (8%)
Glycerol	4 mL (40%)
β-Mercaptoethanol	2 mL (2%)
Bromophenol blue	1 mg (0.01 %)

Adjust the volume to 10 mL with deionised H_2O. Store in darkness at room temperature.

1 M Tris (pH 6.8) solution

To 150 mL of deonised H_2O add:

Tris base 30.3 g

Adjust the pH to 6.8 and adjust the final volume to 250 mL.

10x Running Buffer

Tris 30.3 g (250 mM)

Glycine 144.2 g (2.5 M)

SDS 10 g (1%)

Dissolve in deionised H_2O, adjust the pH to 8.3 and adjust the volume to 1 L.

1x Transfer buffer

Tris 3.03 g (25 mM)

Glycine 14.41 g (192 mM)

Mix until solutes dissolution. Adjust the pH to 8.3 with HCl and adjust the volume to 800 mL with deionised H_2O. Just prior to use add 200 mL of methanol (20%).

10x TBS (Tris buffered saline)

Tris 12.11 g (10 mM)

NaCl 87.66 g (150 mM)

Adjust the pH to 8.0 with HCl and adjust the volume to 1 L with deionised H_2O.

10x TBST (TBS + Tween)

Tris 12.11 g (10 mM)

NaCl 87.66 g (150 mM)

Tween 20 5 mL (0.05 %)

Adjust the pH to 8.0 with HCl and adjust the volume to 1 L with deionised H_2O.

Coomassie blue staining solutions

Staining solution

Coomassie Brilliant Blue	2 g
Methanol	500 mL
Acetic Acid	100 mL

Adjust the volume to 1 L with deionised H_2O.

Destaining solution

Methanol	250 mL
Acetic Acid	50 mL

Adjust the volume to 1 L with deionised H_2O.

Cell Culture Solutions and Immunocytochemistry

1x PBS

For a final volume of 500 mL, dissolve one pack of BupH Modified Dulbecco's Phosphate Buffered Saline Pack (Pierce) in deionised H_2O. Final composition:

8 mM Sodium Phosphate

2 mM Potassium Phosphate

40 mM NaCl

10 mM KCl

Sterilize by filtering through a 0.2 μm filter and store at 4ºC

1 mg/mL Poly-L-ornithine solution (10x)

To a final volume of 100 mL, dissolve in deionised H_2O 100 mg of poly-L-ornithine (Sigma-Aldrich, Portugal).

4% Paraformaldehyde

For a final volume of 100 mL, add 4 g of paraformaldehyde to 25 mL deionised H_2O. Dissolve by heating the mixture at 58ºC while stirring. Add 1-2 drops of 1 M NaOH to clarify the solution and filter (0.2 μm filter). Add 50 mL of 2X PBS and adjust the volume to 100 mL with deionised H_2O.

Complete MEM + GLUTAMAX (HeLa cells)

For a final volume of 500 mL, add:

Fetal Bovine Serum (FBS) (Gibco BRL, Invitrogen)	50 mL (10% v/v)
Non-Essential aminoacids (1% v/v)	5 mL
Penicillin	100 U/mL
Streptomycin (100 mg/mL)	5 mL

FBS is heat-inactivated for 30 min at 56ºC. For cell maintenance, prior to pH adjustment add 100 U/mL penicillin and 100 mg/mL streptomycin [10 mL Streptomycin/ Penicilin/Amphotericin solution (Gibco BRL, Invitrogen)

MEM + GLUTAMAX Components

Amino Acids:	Concentration (mg/L)
L-Alanyl-Glutamine	406
L-Arginine hydrochloride	126
L-Cystine	24
L-Histidine hydrochloride	42
L-Isoleucine	52
L-Leucine	52
L-Lysine hydrochloride	73
L-Methionine	15
L-Phenylalanine	32
L-Threonine	48
L-Tyrosine	10
L-Valine	46

Vitamins:	
Choline chloride	1
D-Calcium pantothenate	1
Folic Acid	1
Niacinamide	1
Riboflavin	0.1
Thiamine hydrochloride	1
i-Inositol	2
Inorganic Salts:	
Calcium Chloride ($CaCl_2.2H_2O$)	264
Magnesium Sulfate ($MgSO_4.7H_2O$)	200
Potassium Chloride	400
Sodium Bicarbonate	2200
Sodium Chloride	6800
Sodium Phosphate monobasic ($NaH_2PO_4.2H_2O$)	158
Other components:	
D-Glucose	1000
Phenol Red	10

DMEM medium (COS-7 cells)

For a final volume of 1 L, dissolve one pack of DMEM powder (with L-glutamine and 4500 mg glucose/L, Sigma Aldrich) in deionised H_20 and add:

$NaHCO_3$ (Sigma-Aldrich) 3.7 g

Adjust the pH 7.4. Sterilize by filtering through a 0.2 μm filter and store at 4°C.

Complete DMEM (COS-7 cells)

For a final volume of 1 L, when preparing DMEM medium adjust to pH 7.4 and before sterilizing add:

Fetal bovine Serum (FBS) (Gibco BRL, Invitrogen) 100 mL (10% v/v)

Notes: FBS is heat-inactivated for 30 min at 56°C. For cell maintenance, prior to pH adjustment add 100 U/mL penicillin and 100 mg/mL streptomycin (100 mL Streptomycin/Penicilin/Amphotericin solution (Gibco BRL, Invitrogen)).

Polyethylenimine (PEI) solution

For a final volume of 10 mL, add 9 mg of PEI to deionised H_20. Dissolve by vortexing. Sterilize by filtration.

Immunoprecipitation solutions

Lysis Buffer

50 mM Tris-HCl (pH 8)	1 mL
120 mM NaCl	2.4 mL
4% CHAPS	0.8 g

Adjust the volume to 20 mL with deionised H_2O.

Lysis Buffer + Protease inhibitors

Add to 4 mL of Lysis buffer the following quantities for a final volume of 5 mL:

Pepstatin A (1 mg/mL stock solution in DMSO)	23.8 µL
Leupeptin (5 mg/mL stock solution)	0.72 µL
Benzamidine (200 mM stock solution)	180 µL
Aprotinin (2,1 mg/mL stock solution)	43.2 µL
PMSF (10 mM stock solution)	176 µL

Washing solution

50 mM Tris-HCl	2.5 mL
120 mM NaCl	6 mL

Adjust the volume to 50 mL with deionised H_2O.

II. Plasmids

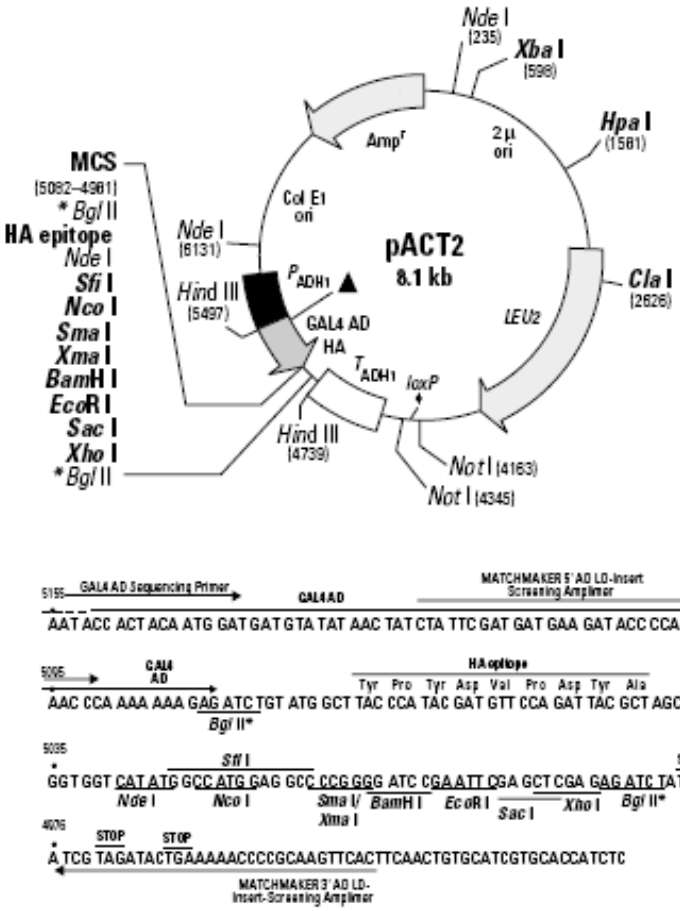

pACT2 (Clontech) map and multiple cloning sites. Unique sites are in bold. pACT2 is used to generate a hybrid containing the GAL4 AD, an epitope tag and a protein encoded by a cDNA in a fusion library. The hybrid protein is expressed at medium levels in yeast host cells from an enhanced, truncated ADH1 promoter and is targeted to the nucleus by the SV40 T-antigen nuclear localization sequence. pACT2 contains the LEU2 gene for selection in Leu$^-$ auxotrophic yeast strains.

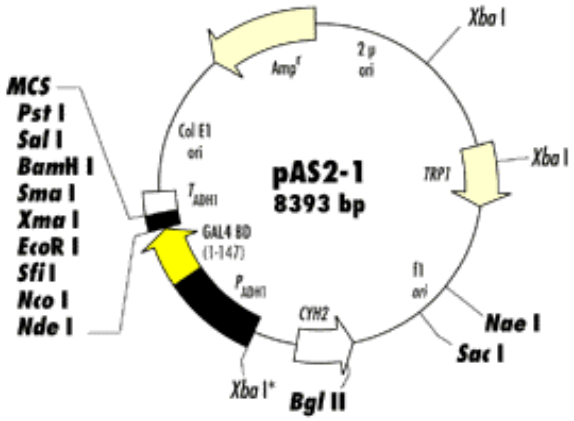

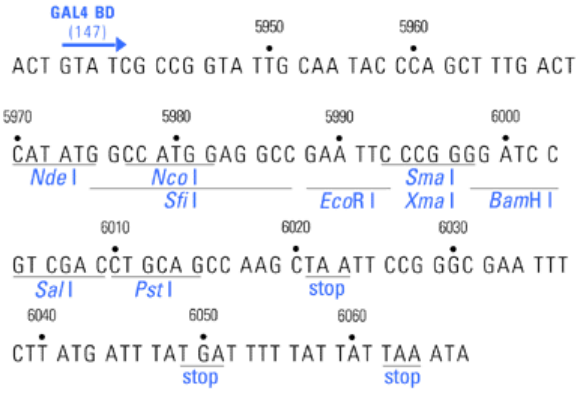

pAS2-1 (Clontech) map and multiple cloning sites. Unique restriction sites are coloured blue. pAS2-1 is a cloning vector used to generate fusions of a bait protein with the GAL4 DNA-BD. The hybrid protein is expressed at high levels in yeast host cells from the full-length ADH1 promoter. The hybrid protein is targeted to the yeast nucleus by nuclear localization sequences. pAS2-1 contains the TRP1 gene for selection in Trp^- auxotrophic yeast strains.

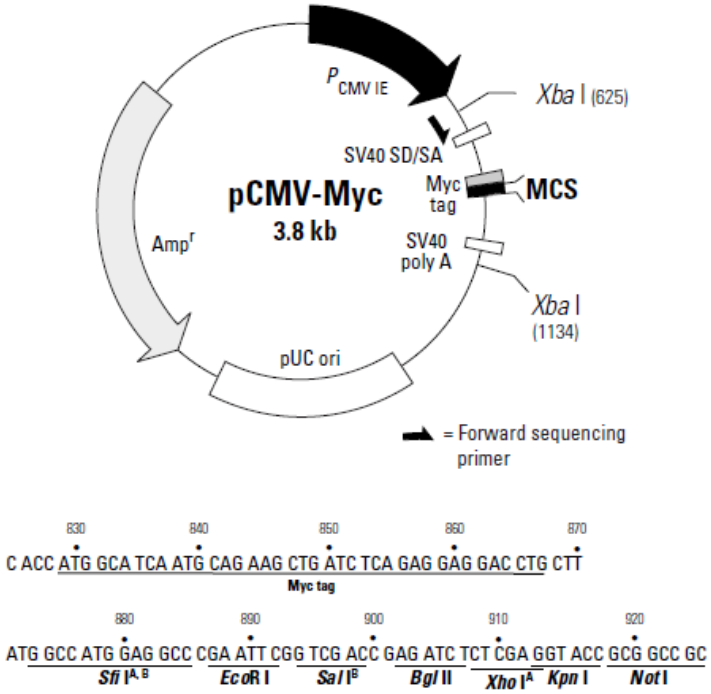

pCMV-Myc (Clontech) restriction map and multiple cloning sites. Unique restriction sites are in bold. pCMV-Myc is a mammalian expression vector with an N-terminal c-Myc epitope tag. This vector possesses the ampicillin resistance gene for selection in *E. coli*.

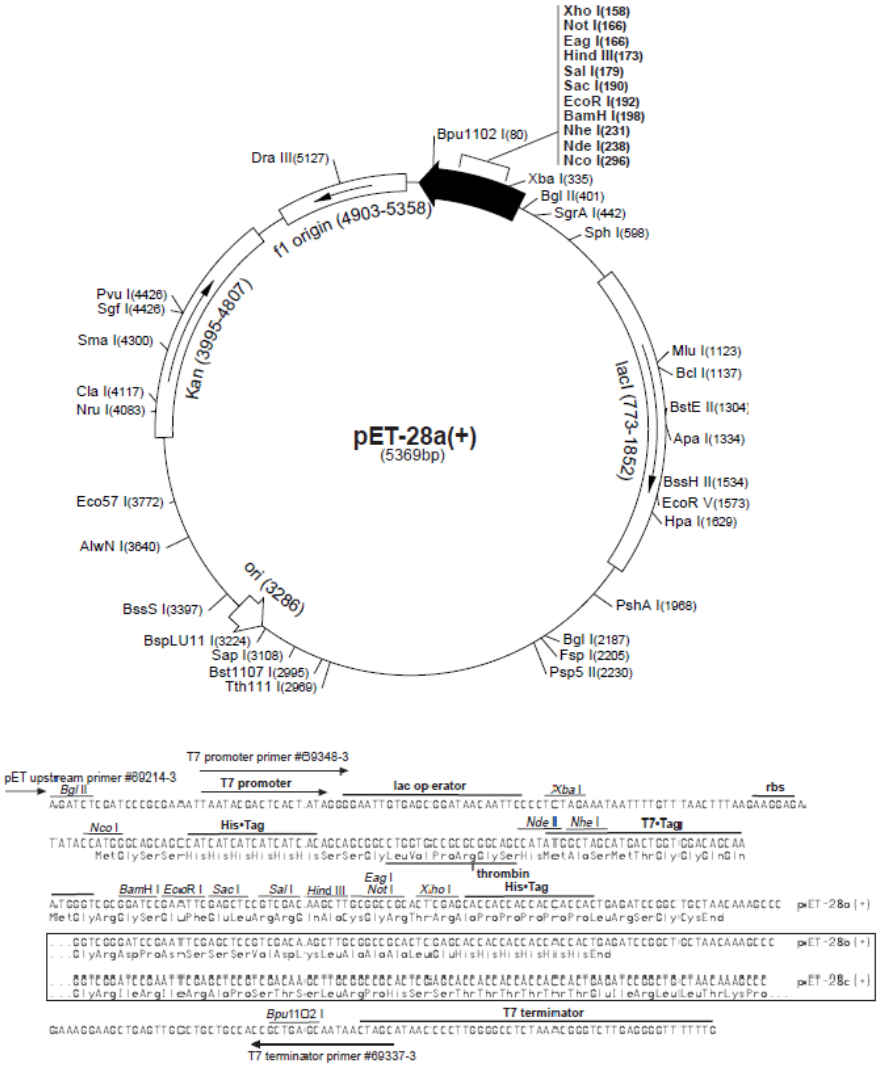

pET-28a-c(+) (Novagen) restriction map and multiple cloning sites. Unique sites are indicated on the circular map. pET-28a-c(+) is a *E. coli* expression vector with an N-terminal His tag/thrombin/T7 tag. This vector possesses the Kanamycin resistance gene.

III. Primers

Primer	Sequence 5' --- 3'	MT °C
Gal4-AD, FW	TACCACTACAATGGATG	48
Amplimer 3, RV	ATCGTAGATACTGAAAAACCCCGCAAGTTCAC	84
T7 promoter	TAATACGACTCACTATAGGG	56
TOR1AIP1 cds, FW	GGAATTCATATGGCGGGCGACGGG	69
TOR1AIP1 cds, RV	CCTCGAGTTATAAGCAGATGCCCCT	60
TOR1AIP1 BM1, RV	CCGCTCGAGTTAGACACTGGTGGCTTC	66
TOR1AIP1 BM2, FW	GGAATTCATATGGACGAGCCGCCAGAA	67
TOR1AIP1 BM2, RV	CCGCTCGAGTTAGGCTACATCTTTGAAGGC	67
TOR1AIP1 BM3, FW	GGAATTCATATGGCCAGATCCAGGGAT	64
TOR1AIP1 681	CATTCCTCTGAAGAGGATG	55
TOR1AIP1 1356	CAAGGTCAAGATGAGAAGCTG	58